Bioethanol from lignocellulose - pretreatment, enzyme immobilization and hydrolysis kinetics

Tsai, Chien Tai

Publication date:
2012

Document Version
Publisher's PDF, also known as Version of record

Bioethanol from lignocellulose - pretreatment, enzyme immobilization and hydrolysis kinetics

Chien-Tai Tsai

PhD thesis

Ceter for Bioprocess Engineering
Department of Chemical and Biochmical Engineering
Technical University of Denmark

Aug/2012

Preface

This research was carried out form May 2008 to August 2012. The first three years was at the Ceter for Bioprocess Engineering, Department of Chemical and Biochmical Engineering, DTU and the last year was completed in Taiwan.

This work is under the superivse of Anne S. Meyer, Head of Ceter for Bioprocess Engineering, Department of Chemical and Biochmical Engineering, DTU as well as Anders Viksø-Nielsen and Katja Salomon Johansen, Novozymes A/S. The project was funded by DTU and The Novozymes BioProcess Academy.

Chien-Tai Tsai
August, 2012

Acknowledgements

I would like to appreciate Anne's instructions and giving me a lot of freedom to try different ideas. Although most ideas did not work, thank to her patience. I also want to thank Gürkan Sin, Ricardo Morales-Rodriguez, Guillaume Balduck, Jonas Eecloo and Stef Vangroenweghe for their help on the part of kinetic modeling. Finally I want to thank for my wife, Ming-Ju, who always support me.

Abstract

Pretreatment and enzymatic hydrolysis are two of the processes involved in the production of cellulosic ethanol. Several pretreatment methods were proposed, however new pretreatment strategies to increase enzymetic hydrolysis efficiency are still under investigation. For enzymatic hydrolysis, the cost of enzyme is still the bottle neck, re-using the enzyme is a possible way to reduce the input of enzyme in the process. In the point view of engineering, the prediction of enzymatic hydrolysis kinetics under different substrate loading, enzyme combination is usful for process design. Therefore, several kinetic models were proposed previously. In view of the connetions between pretreatment and enzymatic hydrolysis. The hypotheses and objective of this PhD study consists of three parts:

(1) Pretreatment of barley straw by 1-ethyl-3-methylimidazolium acetate ([EMIM]Ac), which was done during 2009. Ionic liquid had been reported to be able to dissolve lignocellulose. However, as our knowledge, in all published researches, the concentration of lignocellulose in ionic liquid were low (5~10%). Besides, pretreatment time were long (from 1 hr to 1 day). Based on the hypothesis that the amount of ionic liquid and pretreatment time can be reduced, the influence of substrate concentration, pretreatment time and temperature were investigated and optimized.

Pretreatment of barley straw by [EMIM]Ac, correlative models were constructed using 3 different pretreatment parameters (temperature, time, concentration of barley straw substrate) and sugar recoveries obtained following enzymatic hydrolysis. Elevated pretreatment temperature and longer pretreatment time favoured hydrolysis. However intensive pretreatment at high temperature also causes degradation of cellulose. In addition, [EMIM]Ac pretreated lignocellulose was found to stabilize and protect the enzymes at elevated temperatures. Therefore lower levels of enzymes were required to obtain similar hydrolytic efficiencies. Optimal pretreatment condition was found with the aid of models based on multiple linear regression. Consider the balanced against economic considerations, barley straw can be pretreated under 150°C for 50 min with dry matter of 20% (w/w). Glucose yield can be up to 70% after enzymatic hydrolysis.

(2) Immobilization of β-glucosidase (BG), which was done during 2010. One of the major bottlenecks in production of ethanol from lignocellulose is the required high cellulase enzyme dosages that increase the processing costs. One method to decrease the enzyme dosage is to re-use BG, which hydrolyze the soluble substrate cellobiose. Based on the hypothesis that immobilized BG can be re-used,

how many times the enzyme could be recycled and how coupling with glutaraldehyde affected enzyme recovery after immobilization were investigated.

Glutaraldehyde cross-linked BG aggregates were entrapped in 3.75% calcium alginate. Glutaraldehyde inactivate enzyme activity but also reduce the leakage of enzyme from calcium alginate. Findings showed that more than 60% of enzymatic activity could be maintained under optimized immobilization condition. In order to evaluate stability, the immobilized enzymes were reused for the hydrolysis of Avicel. No significant loss of activity was observed up to 20 th round. Similar glucose yields were obtained following enzymatic hydrolysis of hot water pretreated barley straw by immobilized and free BG. Finally, this is the first time that BG aggregates in a calcium alginate were visualized by confocal laser scanning microscope. The images prove that more BG aggregates were entrapped in the matrix when the enzyme was cross-linked by glutaraldehyde.

(3) Validation and modification of a semimechanistic model, which was done during 2010 ~ 2012. A number of cellulosic hydrolysis kinetic models were proposed. Among the models, a simple and usful mathamatical model proposed by Kadam et al. (2004) has potential for supporting process design. However, like the other models, it was not validated intensivly, especially under high glucose concentration background and high substrate loading. Thus, the role of transglycosylation was not considered in previous reports. Based on the hypothesis that transglycosylation plays an important role under these conditions, the influence of transglycosylation was introduced into the model and evaluated.

The semimechanistic multi-reaction kinetic model consists of homogeneous and heterogeneous reaction proposed by Kadam et al. (2004) was systematically validated and modified under a step by step analysis. The objective is to perform a comprehensive analysis in view of validating and further consolidating the model. A number of dedicated experiments were carried out under a wide range of initial conditions (Avicel versus pretreated barley as substrate, different enzyme loadings, and different product inhibitors such as glucose, cellobiose and xylose) to test the hydrolysis and product inhibition mechanism of the model. Nonlinear least squares methodwas used to identify the model and estimate kinetic parameters based on the experimental data. The analysis showed that transglycosylation reaction at high glucose level play a key role in the model. Therefore with the indroduction of transglycosylation into the model, prediction of cellulose hydrolysis behavior over a broad range of substrate loading is possible. It also revealed that the experimental data used for parameters estimation or different estimation strategies influence the values of parameters and performance of the model. The revised model structure can now be used to support process design and technology improvement efforts at pilot and full-scale studies especially under high cellulose loading.

Dansk Sammmenfatning

Forbehandling og enzymatisk hydrolyse er to af processerne involveret i produktionen af cellulose-baseret ethanol. Adskillige forbehandlings-strategier er foreslået, hvor nye forbehandlings-strategier udvikles til at øge effektiviteten af den enzymatiske hydrolyse. Prisen på enzymer er til stadighed en flaskehals i den enzymatiske hydrolyse, hvor genanvendelse af enzymerne er en mulig strategi for at reducere enzym-tilførslen i processen. Fra proces-ingeniørens synspunkt, er kinetikken bag enzymhydrolysen ved forskellige substrat-tilsætninger og enzym-kombinationer vigtig for proces-design. Derfor er der hidtil foreslået adskillige kinetiske modeller for at visualisere relationen mellem forbehandling og enzymatisk hydrolyse. Hypoteserne og målsætningen for dette PhD-studium er delt i tre dele:

(1) Forbehandling af bygstrå ved 1-ethyl-3-methylimidazoliumacetat ([EMIM]Ac) foretaget i løbet af 2009. Det er rapporteret, at ioniske væsker kan opløse lignocellulose. Dog, som det også blev erfaret, var koncentrationen af lignocellulose i den ioniske væske lav i andres arbejde (5-10 %). Derudover var forbehandlingstiden lang (fra 1 time til 1 dag). Baseret på hypotesen om, at mængden af ionisk væske og forbehandlingstid kan reduceres, blev påvirkningen af substrat-koncentration, forbehandlingstid og tempteratur studeret og optimeret.

Forbehandling af bygstrå ved korrelerende modeller med1-ethyl-3-methylimidazoliumacetat ([EMIM]Ac) blev sat op ved tre forskellige forbehandlings-parametre (temperatur, tid og substrat-koncentration af bygstrå) og udvindingen af sukker fra den efterfølgende enzymatiske hydrolyse. Højere forbehandlingstemperaturer og længere forbehandlingstider er til fordel for den enzymatiske hydrolyse, men hårde forbehandlinger ved høje temperaturer kan forårsage nedbrydning af cellulose. Ved forbehandling af lignocellulose med [EMIM]Ac bliver enzymerne stabiliseret og beskyttet ved højere temperaturer. Derfor var lavere mængder af enzymer nødvendigt for at opnå en tilsvarende effektivitet af den enzymatiske hydrolyse. Optimale forbehandlingsbetingelser blev fundet ved hjælp af modeller baseret på multipel, lineær regression. Med økonomiske aspekter taget i betragtning, skal bygstrå forbehandles ved 150 ˚C i 50 minutter ved en tørstofprocent på 20 % (w/w). Glukose-udbyttet kan nå op til 70 % efter enzymatisk hydrolyse.

(2) Immobilisering af β-glucosidase (BG) foretaget i løbet af 2010. En af de store flaskehalse i produktionen af ethanol fra lignocellulose er den nødvendigt høje cellulase dosering, der medfører øget procesomkostning. En strategi til at sænke enzymforbruget er at genbruge BG, der hydrolyserer den

opløste cellobiose. Baseret på hypotesen om, at immobiliseret BG kan blive genbrugt, blev antallet af cykler enzymet kan blive genbrugt og hvordan koblingen med glutaraldehyd påvirker udvindingen af enzym efter immobiliering studeret.

Glutaraldehyd krydsbundet med BG aggregater blev bundet i 3,75 % calcium alginat. Glutaraldehyd reducerer enzymaktiviteten, men reducerer også tabet af enzym fra calcium alginat. Det er fundet, at mere end 60 % af enzymaktiviteten blev bibeholdt under optimale forhold for immobilisering. For at evaluere stabiliteten blev de immobiliserede enzymer genbrugt til hydrolyse af Avicel. Der blev ikke fundet signifikant tab af aktivitet indtil 20. cyklus. Lignende glukose-udbytter blev opnået ved enzymatisk hydrolyse med immobiliseret og fri BG af bygstrå forbehandlet ved kogning. Dette er første gang, at BG aggregater i calcium alginat er blevet visualiseret ved 'confocal laser scanning' mikroskopi. Billedet viste, at BG aggregater blev bundet i matricen, når enzymet blev krydsbundet med glutaraldehyd.

(3) Validering og modifikation af en semi-mekanistisk model, foretaget i løbet af 2010 og 2012. Flere kinetiske modeller af cellulose-hydrolysen er blevet foreslået. Imellem disse har en simpel og brugbar matematisk model foreslået af Kadam et al. (2004) vist potentiale for at afhjælpe ved procesdesign. Men som i andre modeller, er modellen ikke blevet valideret tilstrækkeligt. Dette gælder især med høj baggrund af glukose og høj substrat-koncentration. Derfor er der ikke taget højde for vigtigheden af transglycosuleringen i tidligere afrapporteringer. Baseret på hypotesen om, at transglucosyleringen spiller en vigtig rolle under disse forhold, blev transglycosyleringen introduceret i modellen og denne evalueret.

Den semi-mekanistiske multireaktion kinetiske model, der består af en homogen og en heterogen reaktion foreslået af Kadam et al. (2004), blev systematisk valideret og modificeret under en trinvis analyse. Målet var at udføre en dækkende analyse med henblik på validering og videre styrkelse af modellen. Et antal eksperimenter blev udført inden for vide rammer af start-betingelserne (Avicel overfor forbehandlet bygstrå som substrat, forskellige enzymkoncentrationer og forskellige inhiberende produkter såsom glukose, cellobiose og xylose) for at teste modellen med hensyn til selve hydrolysen og mekanismen omkring produktinhibering. 'Nonlinear least squares' på de eksperimentelle data blev brugt til identifikation af modellen og til at estimere de kinetiske parametre. Analysen viste, at transglykosylerings-reaktionen ved højt glukose-niveau spiller en vigtig rolle i modellen. Med introduktionen af transglykosyleringen i modellen, blev det gjort muligt at forudsigelse cellulose-hydrolysen over et større spektrum med hensyn til substrat-koncentration. Det blev også vist, at de eksperimentelle data anvendt til estimering af parametrene og de forskellige estimerings-strategier påvirker parameter-værdierne og modellens egenskaber. Den reviderede modelstruktur kan nu anvendes til at understøtte procesdesign og foreslåede, tekniske forbedringer i pilot og fuld-skala studier, især ved høj cellulose-koncentrationer.

Table of Contents

Preface……....1
Acknowledgements…….2
Abstract……....3
Dasnk Sammmenfatning…….5
Table of Contents……..……..7
List of Figures……..……...9
List of Tables……..…….....……..10
List of Publications……..……10
Hypotheses……..……...11
Aim……..……12
Chapter 1 Introduction……..……13
Chapter 2 Lignocellulosic bioethanol: Materials and processes…….…..……16
2.1 Structure and composition of lignocellulose……..…….16
2.1.1 Lignocellulose……..…….16
2.1.2 Cellulose……..……...16
2.1.3 Hemicellulose……..……..16
2.1.4 Lignin……..…....16
2.2 Overview of production process of lignocellulosic bioethanol……..…….19
2.3 Pretreatment……..……...20
2.4 Enzymatic hydrolysis……..…….21
2.5 References……..……..25
Chapter 3 Determination of optimal conditions for barley straw pretreatment by ionic liquid 1-ethyl-3-methylimidazolium acetate……...….28
3.1 Key point of this research……...…….28
3.2 Conclusion……...……30
Chapter 4 Enzymatic Cellulose Hydrolysis: Reusability and Visualization of Crosslinked β-glucosidase Immobilized in Calcium Alginate…….56
4.1 Key point of this research…….56
4.2 Conclusion……...57
Chapter 5 A Dynamic Model for Cellulosic Biomass Hydrolysis: Validation of Hydrolysis and Product Inhibition Mechanisms……..81

5.1 Key point of this research……81
5.2 Conclusion……...81
5.3 Reference……82
Appendix 5.1. Evaluation of model for cellobiose-to-glucose reaction……..……120
Appendix 5.2. Evaluation of Model 1 (Strategy 1)……...122
Appendix 5.3. Evaluation of Model 1 (Strategy 2)……...127
Appendix 5.4. Evaluation of Model 2 (Gcr,tetra = 75 g/L)……..132
Appendix 5.5. Evaluation of Model 2 (Gcr,tetra = 80 g/L)……..137
Appendix 5.6. Evaluation of Model 3 (Gcr,tetra = 75 g/L)……..142
Appendix 5.7. Evaluation of Model 3 (Gcr,tetra = 80 g/L)……..147
Appendix 5.8. Comparison of hydrolysis kinetics of Avicel by N188 and Xbg……..…152
Appendix 5.9.Transglycosylation reaction induced by Celluclast, N188 and Xbg…….153
Chapter 6 Conclusions and Future works……...154

List of Figures

Figure 1.1 Total primary energy supply in the world from 1971 to 2008……14
Figure 1.2 TPES fuel shares in 1973 and 2008……14
Figure 2.1 Secondary cell wall structures……17
Figure 2.2 Compositions and structures of cellulose and hemicellulose……18
Figure 2.3 Lignin precursors.....18
Figure 2.4 Typical production processes of bioethanol from lignocellulosic biomass.....19
Figure 2.5 Effect of pretreatment on the structure of biomass……20
Figure 2.6 Effects of temperature and final pH on pretreatment of lignocellulose……21
Figure 2.7 Overview of enzymatic hydrolysis of cellulose……22
Figure 2.8 Reaction scheme for modeling cellulose hydrolysis……24
Figure 3.1 Crystal structure of cellulose……28
Figure 3.2 1-ethyl-3-methylimidazolium acetate……29
Figure 3.3 Experimental procedures of IL pretreatment.....29
Figure 3.4 Appearance of barley straw after IL pretreatment under different temperature, substrate concentration and time.....31
Figure 3.5 Appearance of barley straw after IL pretreatment under 150°C with different substrate concentration and time.....32
Figure 3.6 Appearance of Avicel after IL pretreatment (10% substrate, 45 min)……32
Figure 3.7 Appearance of glucose after IL pretreatment (0.54 g glucose + 0.96 g IL, 1 hr)……33
Figure 3.8 Mass balance of barley straw preated under 150°C, 20% dry matter for 50 min……33
Figure 4.1 Experimental procedure of enzyme immobilization.....58
Figure 4.2 Loss BG activity due to crosslinking (3 replication) and leakage.....59
Figure 4.3 Leakage of BG from calcium alginate at different time intervals……60
Figure 4.4 Loss BG activity due to crosslinking and leakage.....61
Figure 4.5 Leakage of BG from calcium alginate at different time intervals……61
Figure 6.1 Process of dissolution of biomass by ILs without any mechanical force……155
Figure 6.2 Process of dissolution of biomass by ILs with mechanical shear force……155
Figure 6.3 Extruder……156
Figure 6.4 Illustration of producing fiber-shaped immobilized enzyme……157
Figure 6.5 Collision probabilities between cellobiose and immobilized BG in calcium alginate with low or high BG densities……158

Figure 6.6 Application of immobilized BG in the reactors…….159

List of Tables

Table 4.1 Comparison of selected commercialized materials for enzyme immobilization…….56
Table 4.2 Conditions of crosslinking at lower BG and glutaraldehyde concentration.....59
Table 4.3 Conditions of crosslinking at higher BG and glutaraldehyde concentration.....60

List of Publications

1. **Determination of optimal conditions for barley straw pretreatment by ionic liquid 1-ethyl-3-methylimidazolium acetate**
   Chien-Tai Tsai and Anne S. Meyer.....34

2. **Enzymatic Cellulose Hydrolysis: Reusability and Visualization of Crosslinked β-Glucosidase Immobilized in Calcium Alginate**
   Chien-Tai Tsai and Anne S. Meyer.....62

3. **A Dynamic Model for Cellulosic Biomass Hydrolysis: a Comprehensive Analysis and Validation of Hydrolysis and Product Inhibition Mechanisms**
   Chien-Tai Tsai, Ricardo Morales-Rodriguez, Gürkan Sin and Anne S. Meyer 83

Hypotheses

Some kinds of ionic liquids (ILs) were reported to be able to interact with the hydroxyl groups and result in the dissolution of crystallized cellulose. This boosts the enzymatic hydrolysis of ILs pretreated cellulose and lignocellulose. 1-ethyl-3-methylimidazolium acetate ([EMIM]Ac), which is more environment friendly than other ILs, is a good choice for the pretreatment medium. In most published reports, pretreatment period were more than 1 hr or up to one day. In addition, dry matters (DM) of substrate were 5-10% (dry matter), meaning that large amount of IL was consumed.

It has been revealed that calcium alginate is able to immobilized glutaraldehyde crosslinked β-glucosidase. However, the performance of recycled enzyme was not intensively investigated; especially the reusability after many recycles. Therefore only little information for industrial application is available.

A semimechanistic model based on adsorption model and modified M-M models was proposed by Kadam et al. (2004). Similar model was modified by introducing the effects of lignin and validated by Zheng et al. (2009). Although previous reports revealed precise prediction of hydrolysis of lignocellulose could be achieved, the model was not intensively validated, especially at higher glucose and substrate concentration. The significance and meaning of the derived parameters were not well discussed neither.

The hypotheses to be tested in this research are:

1. Barley straw can be pretreated by [IMEM]Ac under high dry matter, to say above 15%.
2. Pretreatment time of barley straw by [IMEM]Ac can be less than 1 hr.
3. Lignin can be extracted by [IMEM]Ac. Compact cellulose structure can be disrupted. Thus, glucose yield would be increased.
4. Immobilized β-glucosidase aggregation can be re-used more than 10 times without significant loss of activity.
5. Transglycosylation has significant influence on hydrolysis kinetics under high glucose level and substrate loading. It should be introduced into the model proposed by Kadam.
6. Parameters derived from the semimechanistic model proposed Kadam or it variations proposed in this research are not universal, meaning that the values vary according to different substrate, modeling strategy and enzyme source.

Aim

The aim of this PhD project was to investigate some important processes in producing bioethanol, including pretreatment and enzymatic hydrolysis. More specifically, focus on IL pretreatment, enzyme immobilization and validation/construction of hydrolysis kinetic model.

Chapter 1

Introduction

In the past three decades, the demands of energy almost doubled (Figure 1.1). In 2009, the total primary energy supply (TPES) in the world was 12150 Mtoe (Figure 1.2). Among all the sources of energies, oil is the most important and accounted for 32.8% of the TPES (IEA 2011). However, the uncertainty of supply and security due to international affairs, as well as prospective of fossil source depletion in the future had been forcing many countries to look for alternative sources. Bioethanol produced from plant, is one of the choices. The shares of bioethanol in United States and Brazil in the global production were 50% (mainly from corn) and 39% (mainly from sugar cane juice) respectively. The share of OECD-Europe was only 5% (IEA 2009; Gnansounou 2010). However, bioethanol produced from food had been criticized for raising the price of crops. Therefore lignocellulose, which abounds with cellulose and hemicellulose, is another attractive source of fermentable sugars for producing bioethanol. Lignocelluloses are mainly from agriculture wastes or forest wood residues. This is why it is commonly accepted that the impact on the environment of second generation bioethanol from lignocellulose is smaller than those so called "first generation bioethanol" form crops. Although there are also some negative opinions against second generation of bioethanol, however it is believed the disadvantages can be overcome in the future.

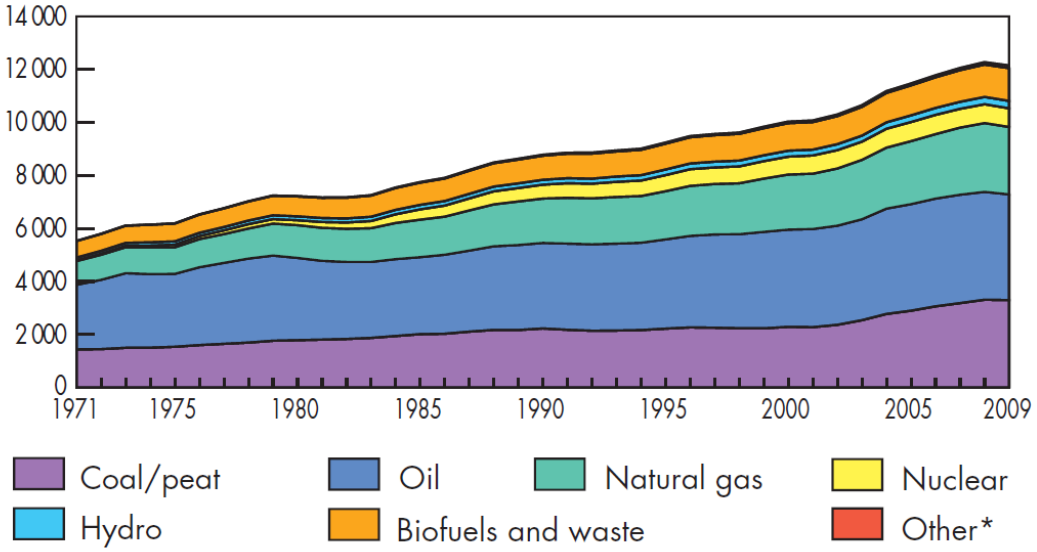

Figure 1.1 Total primary energy supply in the world from 1971 to 2009 (Unit: Mtoe). Toe: tonne of oil equivalent, the amount of energy released by burning one tonne of crude oil; approximately 42 GJ (1 GJ = 10^9 Joule). (From IEA 2011)

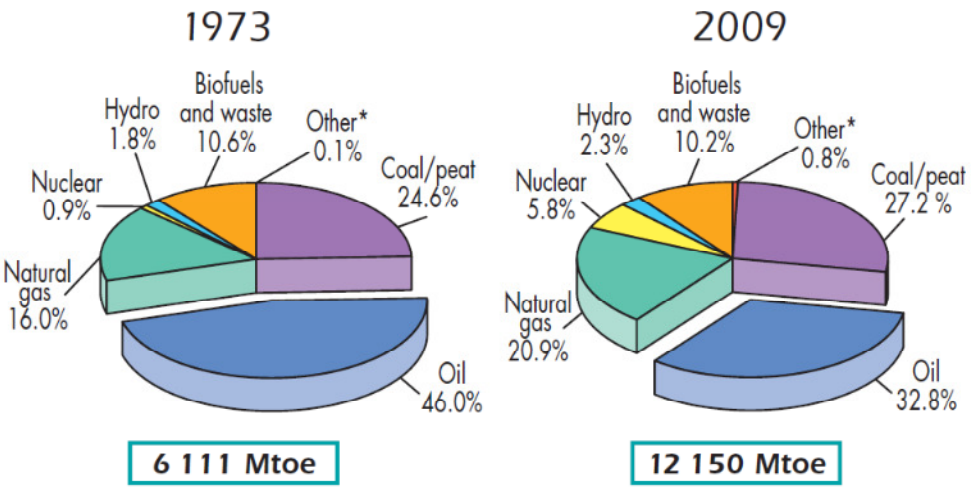

Figure 1.2 TPES fuel shares in 1973 and 2009. (From IEA 2011)

Reference

Gnansounou, E. (2010) Production and use of lignocellulosic bioethanol in Europe: Current situation and perspectives. Bioresource Technology 101, 4842-4850

IEA (2009) Medium-Term Oil market Report. OECD/IEA.

IEA (2011) Key World Energy Statistics 2010. OECD/IEA.

Chapter 2

Lignocellulosic bioethanol: Materials and processes

2.1 Structure and composition of lignocellulose

2.1.1 Lignocellulose

Most lignocellulose exists in plant cell walls. In general, the plant cell walls are subdivided as primary and secondary walls. The compositions vary among these layers. Primary cell walls are composed of cellulose microfibrils (9-25%), hemicelluloses (25-50%), pectins (10-35%) and proteins (10%) (Esau 1977; Goodwin 1983; Salisbury 1992). Cellulose forms the framework and hemicelluloses cross-link the polymers (Keegstra, 1973). Secondary cell walls contain cellulose (40-80%), hemicellulose (10-40%) and lignin (5-25%) (Salisbury 1992; Bidlack 1990). Cellulose is hydrogen-bonded to hemicellulose whereas ester and ether bonds connect hemicellulose to lignin in secondary cell wall. The interactions and arrangement of these components make the cell wall very compact and rigid, like steels are embedded in concrete (Figure 2.1).

2.1.2 Cellulose

Cellulose is composed of D-glucose, linked by β-1,4 glycosidic bonds. Each subunit rotates 180º with respect to their neighbors. This causes cellulose to be highly symmetrical and easy to form hydrogen bonds and Van der Waals forces with adjacent cellulose (Zhang 2004). This structure is called crystalline structure. Those without forming organized crystalline structures are called amorphous structures. The bounded cellulose strains in parallel are called cellulose microfibrils (Figure 2.2). The role of cellulose microfibrils in cell wall serves like steel in the building.

2.1.3 Hemicellulose

Hemicelluloses are complex carbohydrate polymers structures consists of different sugars like xylose and arabinose (pentose), mannose, glucose and galactose (hexose), and sugar acids (Figure 2.2). The main component in hardwood and agricultural plants is xylan, while in soft woods is glucomannan (Fengel 1984; Saha 2003). Hemicellulose is a connection between lignin and cellulose fibers. Compare with cellulose and lignin, hemicellulose is more thermal-chemically sensitive (Levan 1990; Winandy 1995). During pretreatment, firstly the side groups of hemicellulose react and then the linear backbone (Sweet 1999). Hemicellulose dissolves into water from around 150ºC (Garrote 1999) or 180ºC (Bobleter 1994) under neutral conditions. But the extent of solubilization also depends on water content and pH (Fengel 1984).

2.1.4 Lignin

Lignin is an amorphous polymer consisting of three different phenylpropane units, p-coumaryl, coniferyl and sinapyl alcohol (Hendriks 2009) (Figure 2.3). Typical structure of lignin polymer structure is shown in Figure 2.1. It binds cellulose and hemicellulose tightly, makes the cell wall compact and rigid. That is one of the reason that biomass must be pretreated to open its complex structure before enzymatic hydrolysis. Lignin normally starts to dissolve into water around 180ºC under neutral conditions (Bobleter 1994). The solubility of the lignin in different pH depends on the compositions of precursor (Grabber 2005).

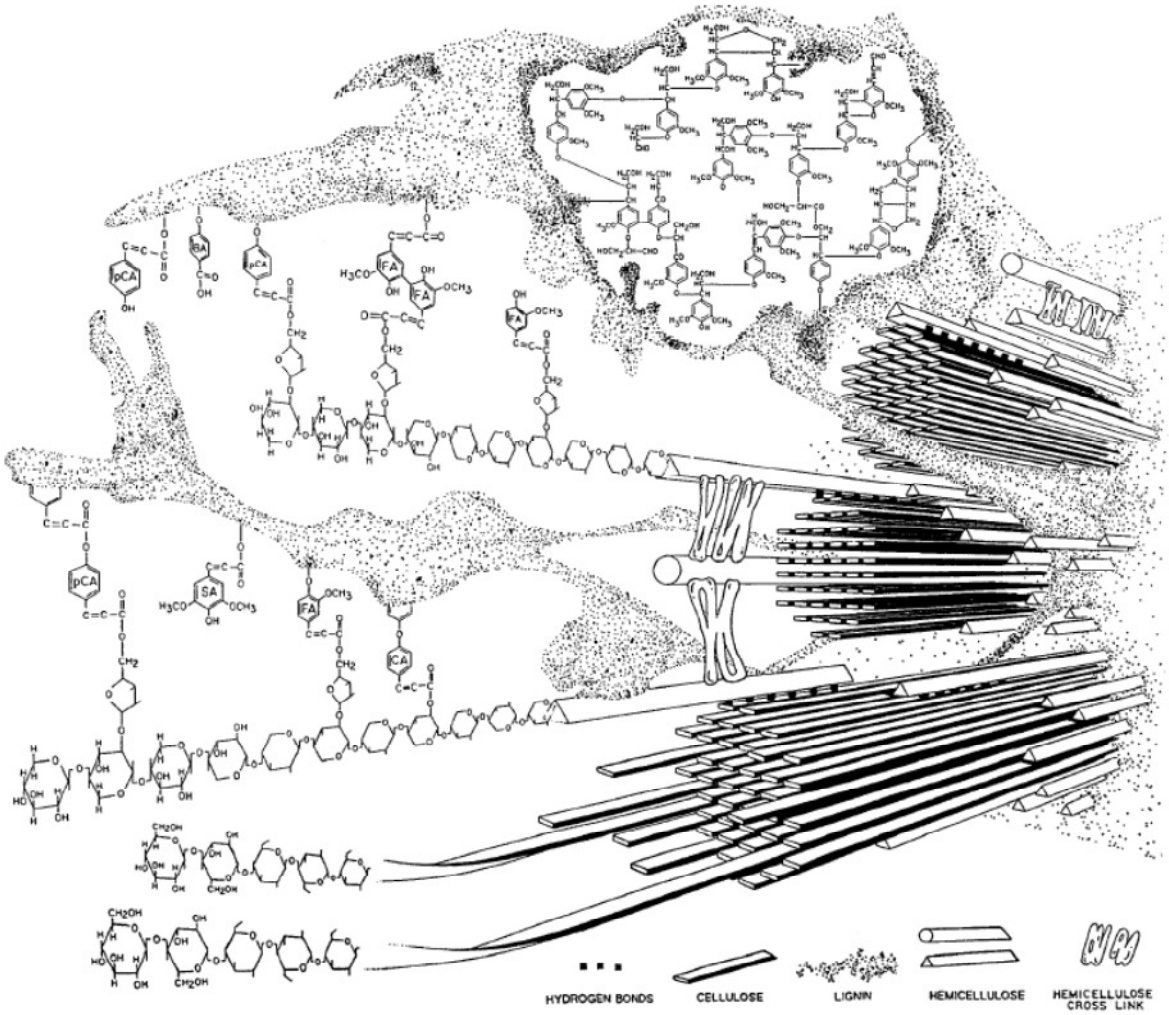

Figure 2.1 Secondary cell wall structures. (From Bidlack 1992)

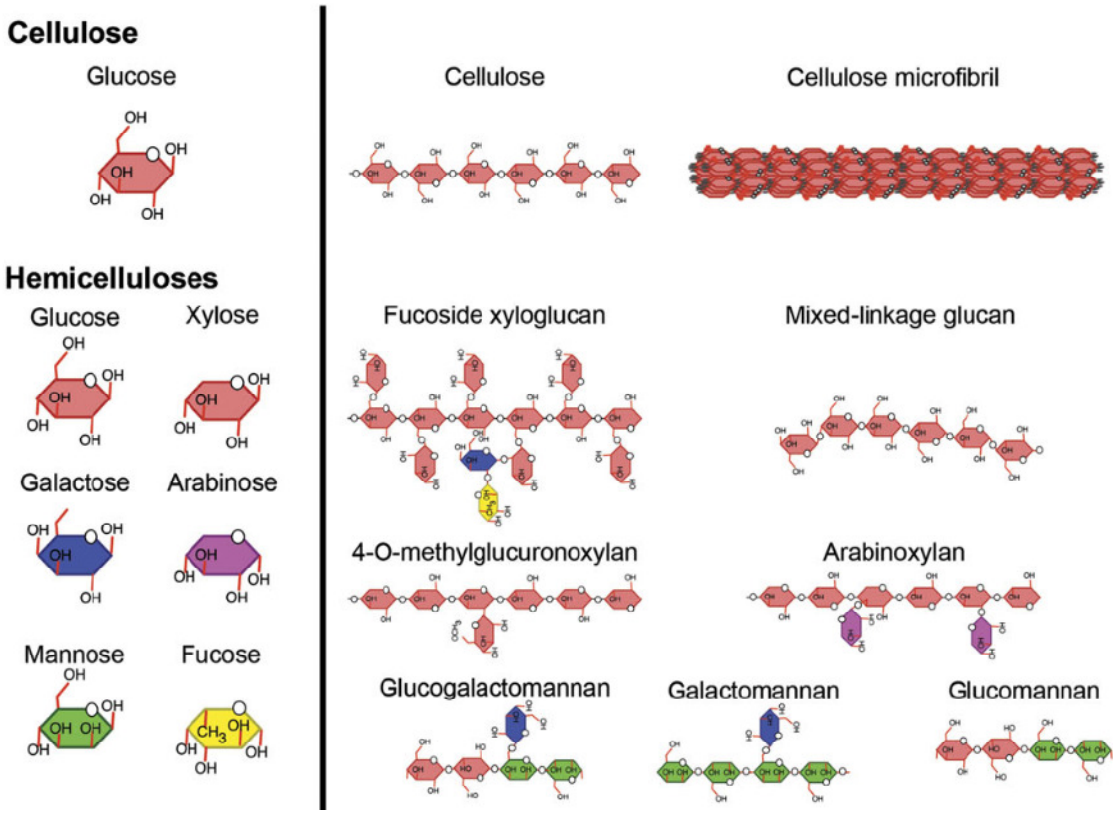

Figure 2.2 Compositions and structures of cellulose and hemicellulose. Left panel: monomers. Right panel: polymers. (From Sarker 2009)

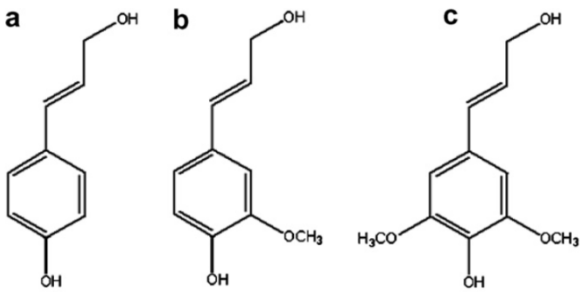

Figure 2.3 Lignin precursors: (a) p-coumaryl alcohol, (b) coniferyl alcohol and (c) sinapyl alcohol. (From Carrott 2007)

2.2 Overview of production process of lignocellulosic bioethanol

The principle of producing lignocellulosic bioethanol is releasing glucose form lignocellulose and then metabolizing the glucose to ethanol by fermentation. The process mainly consists of four steps, (1) Pretreatment - breaking down the structure of the lignocellulose; (2) Enzymatic hydrolysis - releasing glucose from lignocellulose by enzymes; (3) Fermentation - metabolizing the glucose to ethanol by microorganisms; (4) Distillation - separating the ethanol from ethanol broth. Two typical industrial processes are shown in Figure 2.4. In conventional process, hydrolysis and fermentation take place in different steps. However the efficiencies of enzymes are reduced by product inhibition. To overcome this problem, simultaneous saccharification and co-fermentation process (SSCF) was developed, in which hydrolysis and fermentation take place in the same reactor.

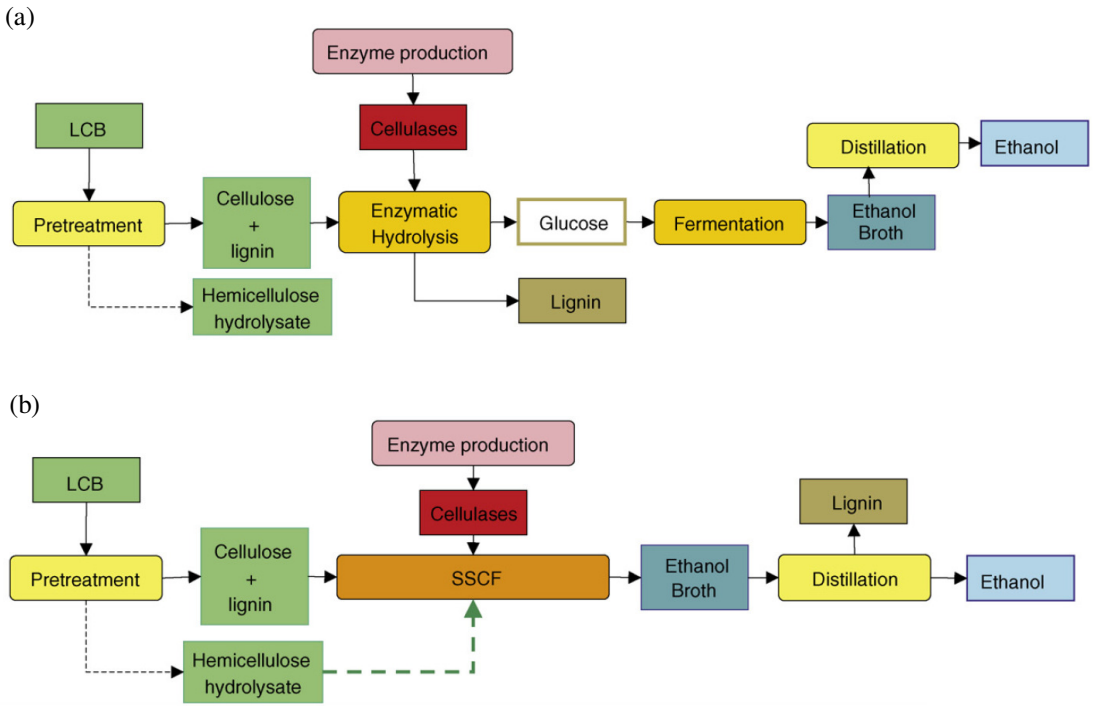

Figure 2.4. Typical production processes of bioethanol from lignocellulosic biomass. (a) Conventional process. Hydrolysis and fermentation take place in different step. (b) Simultaneous saccharification and co-fermentation process (SSCF). Hydrolysis and fermentation take place in the same reactor. (From Margeot 2009)

2.3 Pretreatment

Due to the compact structure of lignocellulose, it is difficult for enzyme to penetrate into the fiber. In addition, the crystalline structure is unfavorable for enzymatic hydrolysis. Thus specific pretreatments are required to overcome the barriers, increase surface area and make it is more accessible for enzyme molecules (Figure 2.5). An ideal pretreatment can increase the digestibility of cellulose and hemicellulose, remove lignin and avoid producing inhibitors for enzyme or microorganisms. However, the pretreatment process is energy intensive, therefore the cost is still the limitation and challenge for most pretreatments.

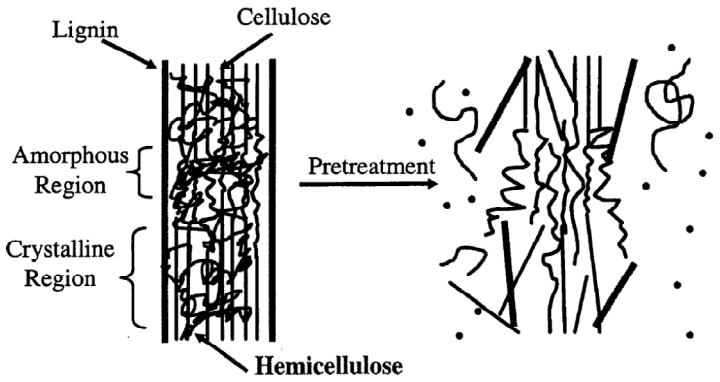

Figure 2.5 Effect of pretreatment on the structure of biomass. (From Mosier 2005)

Numerous pretreatment methods were developed and intensively investigated in the last years. In general, they can be classified into "Physical pretreatment" (*e.g.* milling and irradiation), "Chemical pretreatment" (eg. dilute acid hydrolysis, alkali treatment and ionic liquid), "Physico-chemical pretreatment" (eg. steam explosion and ammonia fiber explosion) and "Biological pretreatment". Each strategy has its own advantages and disadvantages. Some pretreatment remove hemicellulose (at low pH), while the others remove lignin (at high pH) as shown in Figure 2.6 (Pedersen 2010). The performance also depends on the compositions and structures of the biomass. (For more details and comparison of these pretreatment, refer to Laxman 2009; Sanchez 2008; Taherzadeh 2007; Mosier 2005).

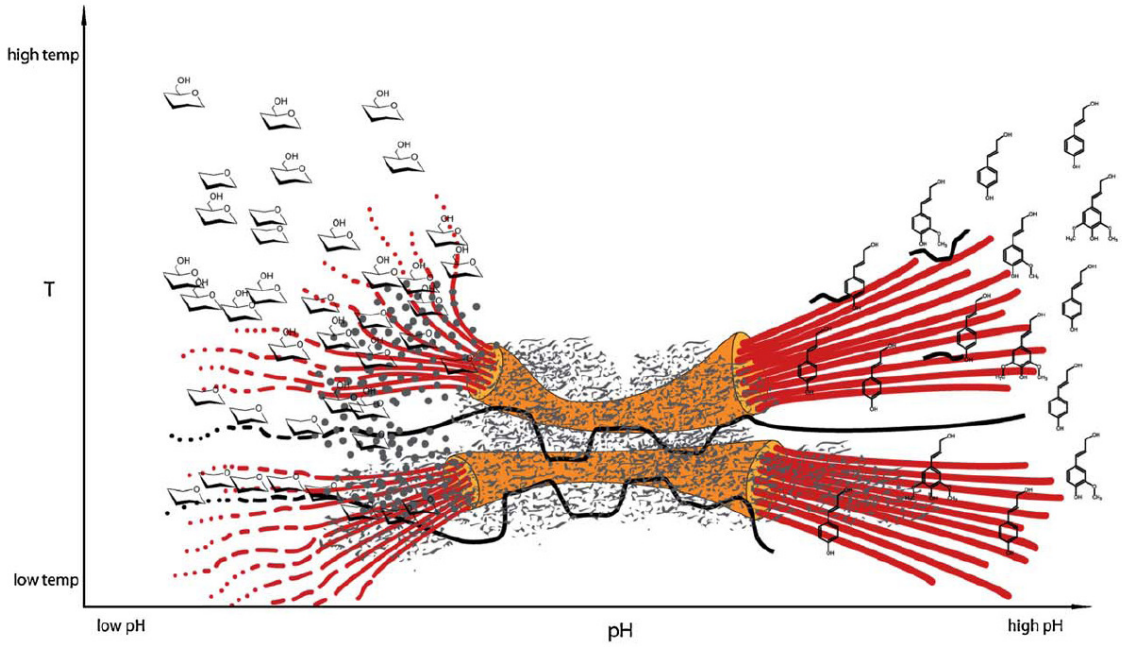

Figure 2.6 Effects of temperature and final pH on pretreatment of lignocellulose. Gray 'veil' indicates lignin sheath; orange and red tubes illustrate cellulosic fibrils and microfibrils, respectively; black curved lines illustrate hemicellulose (xylan); the gray dots on the cellulose microfibrils in the low pH region illustrate redeposited lignin. (From Pedersen 2010)

2.4 Enzymatic hydrolysis

2.4.1 Enzyme system

The enzymatic hydrolysis reactions (Figure 2.7) involve three groups of enzyme: endo-1,4-β-D-glucanase (EG) (EC 3.2.1.4), exo-1,4-β-D-glucanases (or cellobiohydrolase, CBH) (EC 3.2.1.91) and β-glucosidase (BG) (EC 3.2.1.21). The EG cuts the cellulose from inside randomly and CBH hydrolyzes the cellulose from the end and releases mainly cellobiose. Finally BG hydrolyze cellobiose into glucose (Zhang 2004). In *Trichoderma reesei*, the most widely used cellulase filamentous fungus producer, at least two CBH, five EG and two BG have been characterized (Foreman 2003; Jørgensen 2007; Rosgaard 2007).

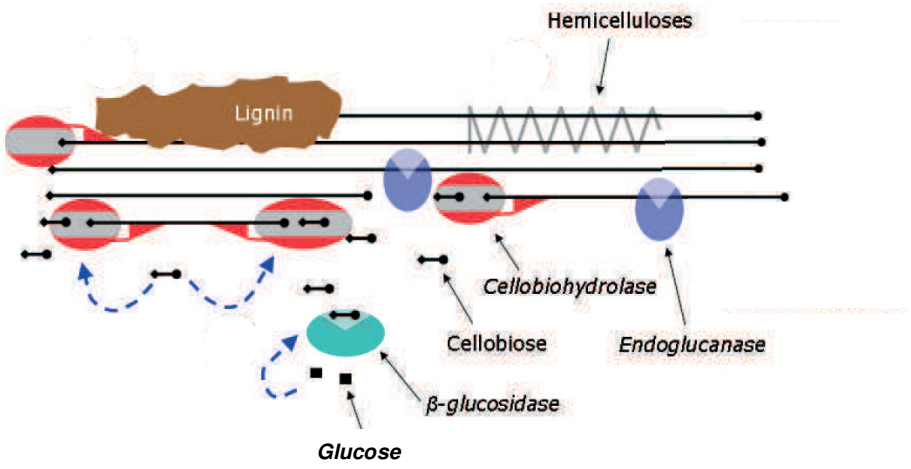

Figure 2.7 Overview of enzymatic hydrolysis of cellulose. The EG cuts the cellulose from inside randomly and CBH hydrolyzes the cellulose from the end and releases mainly cellobiose. Finally BG hydrolyzes cellobiose into glucose. Dashed arrows indicate the product inhibition of CBH and BG by cellobiose and glucose respectively. (Modified from Jørgensen 2007)

2.4.2 Hydrolysis kinetics and modeling

The mechanism of converting insoluble cellulose into soluble glucose by the action of cellulase enzymes has not yet been completely understood due to the complexity of the involved phenomena (such as, adsorption, desorption, enzyme deactivation, accessible area, crystallinity, degree of polymerization, lignin content, enzyme synergism, etc.), which can affect the reaction kinetics. A number of mathematical models for enzymatic hydrolysis have been proposed in the literatures. Zhang (2004) classified the models as (i) nonmechanistic; (ii) semimechanistic; (iii) functionally bsed and (iv) structurally based. Bansal (2009) made a review where a collection of diverse mathematical models for enzymatic hydrolysis was presented. The models were classified as follows: (i) empirical models; (ii) Michaelis-Menten based models; (iii) adsorption in cellulose hydrolysis models and (iv) models on soluble cello-oligosaccharides.

Nonmechanistic (or empirical) models are based on data correlation. This way dose not enhance understanding of the reactions, nor applicable for conditions outside the range from which they are developed. However they help understanding the interactions between different properties. An example

shown in eq 2.1 is the conversion of cellulose (X) measured after 8 hr in relation to surface area (SSA), crystallinity index (CrI), and residual lignin content (L) (Gharpuray 1983):

$$X = 2.044(SSA)^{0.998}(100 - CrI)^{0.257}(L)^{-0.388} \qquad \text{(eq 2.1)}$$

Semimechanistic model are based on adsorption model and somtimes with modified M-M models. Kadam (2004) proposed a model in relation to substrate and product concentration and their effects on product inhibition (Figure 2.8). Langmuir isotherm was used to describe enzyme adsorption to the substrate. For certain extent, this model also count on data correlation but we can understand more about the features of the substrate. Semimechanistic models are believed to be more useful for reactor and process design (Zhang 2004; Zheng 2009). The mathamatical description in Kadam's research are expressed in eq 2.2-2.9:

Enzyme Adsorption

Langmuir isotherm $$E_{iB} = \frac{E_{i\max} K_{iad} E_{iF} S}{1 + K_{iad} E_{iF}} \qquad \text{(eq 2.2)}$$

Cellulose-to-Cellobiose Reaction with Competitive Glucose, Cellobiose and Xylose Inhibition.

$$r_1 = \frac{k_{1r} E_{1B} R_S S}{1 + \frac{G_2}{K_{1IG2}} + \frac{G}{K_{1IG}} + \frac{X}{K_{1IX}}} \qquad \text{(eq 2.3)}$$

Cellulose-to-Glucose Reaction with Competitive Glucose, Cellobiose and Xylose Inhibition.

$$r_2 = \frac{k_{2r} (E_{1B} + E_{2B}) R_S S}{1 + \frac{G_2}{K_{2IG2}} + \frac{G}{K_{2IG}} + \frac{X}{K_{2IX}}} \qquad \text{(eq 2.4)}$$

Cellobiose-to-Glucose Reaction with Competitive Glucose and Xylose Inhibition Reaction.

$$r_3 = \frac{k_{3r} E_{2F} G_2}{K_{3M}(1 + \frac{G}{K_{3IG}} + \frac{X}{K_{3IX}}) + G_2} \qquad \text{(eq 2.5)}$$

Mass Balances

Cellulose: $$\frac{dS}{dt} = -r_1 - r_2 \qquad \text{(eq 2.6)}$$

Cellobiose: $\frac{dG_2}{dt} = 1.056 r_1 - r_3$ (eq 2.7)

Glucose: $\frac{dG}{dt} = 1.111 r_2 + 1.053 r_3$ (eq 2.8)

Enzyme: $E_{Ti} = E_{Fi} + E_{Bi}$ (eq 2.9)

where

E_{Ti} total enzyme concentration (g-protein/L) (i = 1 for CBH + EG; i = 2 for BG)

E_{Bi} bound enzyme concentration (i = 1 for cellulase; i = 2 for BG)

E_{Fi} concentration of free enzyme in solution (i = 1 for cellulase; i = 2 for BG)

G_i glucose (i = 1), cellobiose (i = 2) (g/L)

K_{iad} dissociation constant for enzyme adsorption/desorption reaction (L/g-protein) (i = 1 for CBH + EG; i = 2 for BG)

K_{3M} substrate (cellobiose) saturation constants (g/L)

K_{iIG2} inhibition constant cellobiose (g/L) (i = 1 for r_1; i = 2 for r_2)

K_{iIG} inhibition constant glucose (g/L) (i = 1 for r_1; i = 2 for r_2; i = 3 for r_3)

K_{iIX} inhibition constant xylose (g/L) (i = 1 for r_1; i = 2 for r_2; i = 3 for r_3)

k_{ir} reaction rate constant (i = 1 and 2, L/ g•h ; i = 3, h^{-1})

r_i reaction rate (g/L•h) (i = 1 for cellulose to cellobiose; i = 2 for cellulose to glucose; i = 3 for cellobiose to glucose)

R_S substrate reactivity

S substrate concentration (g/L) (siffix with "0" means initial substrate concentration)

X xylose concentration (g/L)

α dimensionless constant for substrate reactivity

Although functionally and structurally models can help understanding more about the level of substrate structure and multiple enzyme activities, little information for reactor or process design can be provided (Zhang 2004; Zheng 2009). Therefore semimechanistic model is the focus of this research.

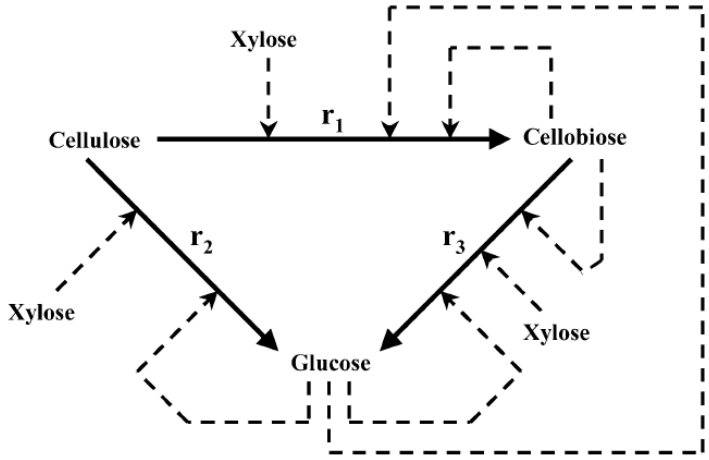

Figure 2.8 Reaction scheme for modeling cellulose hydrolysis. Enzymes involved in r_1: endo-1,4-β-D-glucanase (EG) and cellobiohydrolase (CBH). Enzymes involved in r_2: EG and CBH. Enzymes involved in r_3: β-glucosidase (BG) (Kadam 2004)

2.5 Reference

Bansal, P., Hall, M., Realff, M.J., Lee, J.H., and Bommarius, A.S. (2009) Modeling cellulase kinetics on lignocellulosic substrates. Biotechnology Advances 27, 833-848.

Bidlack, J.E. (1990) Cell-Wall Components and Lignin Biosynthesis in Forages. Ph.D. Dissertation, Iowa State Univ., Ames, IA.

Bidlack, J., Malone, M. and Benson, R. (1992) Molecular Structure and Component Integration of Secondary Cell Walls in Plants, Proceedings of the Oklahoma Academy of Science 72, 51-56.

Bobleter, O. (1994) Hydrothermal degradation of polymers derived from plants. Progress in Polymer Science 19, 797-841.

Esau, K. (1977) Cell Wall. In Plant Anatomy, John Wiley & Sons, New York, NY (1977), 43-60.

Fengel, D. and Wegener, G. (1984) Wood: Chemistry, Ultrastructure, Reactions. De Gruyter, Berlin.

Foreman, P.K., Brown, D., Dankmeyer, L., Dean, R., Diener, S., Dunn-Coleman, N.S., Goedegebuur, F., Houfek, T.D., England, G.J., Kelley, A.S., Meerman, H.J., Mitchell, T., Mitchinson, C., Olivares, H.A., Teunissen, P.J.M., Yao, J., and Ward, M. (2003) Transcriptional Regulation of Biomass-degrading Enzymes in the Filamentous Fungus *Trichoderma reesei*, The Journal of Biological Chemistry 278 (34) 22, 31988-31997.

Garrote, G., Dominguez, H. and Parajo, J.C. (1999) Hydrothermal processing of lignocellulosic materials. Holz Roh Werkst. 57, 191-202.

Gharpuray, M.M., Lee YH and Fan L.T. (1983) Structural modification of lignocellulosic by pretreatments to enhance enzymatic hydrolysis. Biotechnology and Bioengineering 25,157-172.

Goodwin, T.W. and Mercer, E.I. (1983) The Plant Cell Wall. In Introduction to Plant Biochemistry, Pergamon Press, New York, NY, 55-91.

Grabber, J.H. (2005) How do lignin composition, structure, and cross-linking affect degradability? A review of cell wall model studies. Crop Science 45, 820-831.

Hendriks, A.T.W.M. and Zeeman, G. (2009) Pretreatment to enhance the digestibility of lignocellulosic biomass. Bioresource Technology 100, 10-18

Jorgensen, H., Vibe-Pedersen, J., Larsen, J., and Felby, C. (2007) Liquefaction of Lignocellulose at High-Solids Concentrations. Biotechnology and Bioengineering 96 (5), 862-870.

Kadam, K.L., Rydholm, E.C., and McMillan, J.D. (2004) Development and Validation of a Kinetic Model for Enzymatic Saccharification of Lignocellulosic Biomass. Biotechnology Progress 20, 698-705

Keegstra, K., Talmadge, K.W., Bauer, W.D. and Albersheim, P. (1973) The Structure of Plant Cell Walls. III. A Model of the Walls of Suspension-Cultured Sycamore Cells Based on the Interconnections of the Macromolecular Components. Plant Physiology 51, 188-196.

Levan, S.L., Ross, R.J. and Winandy, J.E. (1990) Effects of fire retardant chemicals on bending properties of wood at elevated temperatures. Research Paper FPL-RP498. Madison, WI: U.S. Department of agriculture, Forest service, Forest Products Laboratory, 24.

Margeot, A., Hahn-Hagerdal, B., Edlund, M., Slade, R. and Monot, F. (2009) New improvements for lignocellulosic ethanol, Current Opinion in Biotechnology 20:1-9.

Mosier, N., Wyman, C., Dale, B., Elander, R. and Lee, Y.Y., Holtzapple, M., and Ladisch, M. (2005) Features of promising technologies for pretreatment of lignocellulosic biomass. Bioresource Technology 96, 673-686.

Pedersen, M. and Meyer, A.S. (2010) Lignocellulose pretreatment Severity- relating pH to biomatrix Opening. New Biotechnology 27 (6), 739-750.

Rosgaard, L., Pedersen, S., Langston, J., Akerhielm, D., Cherry, J.R. and Meyer, A.S. (2007) Evaluation of Minimal *Trichoderma reesei* Cellulase Mixtures on Differently Pretreated Barley Straw Substrates. Biotechnology Progress 23, 1270-1276.

Saha, B.C. (2003) Hemicellulose bioconversion. Journal of Industrial Microbiology and Biotechnology 30, 279-291.

Salisbury, F.B. and Ross, C.W. (1992) Plant Physiology and Plant Cells. In Plant Physiology, Wadsworth, Inc., Belmont, CA, 3-26.

Sarkar, P., Bosneaga, E. and Auer, M. (2009) Plant cell walls throughout evolution: towards a molecular understanding of their design principles. Journal of Experimental Botany 60 (13), 3615-3635.

Suhas, P.J.M., Carrott, M.M.L. and Ribeiro Carrott (2007) Lignin- from natural adsorbent to activated carbon: A review. Bioresource Technology 98, 2301-2312.

Sweet, M.S. and Winandy, J.E. (1999) Influence of degree of polymerization of cellulose and hemicellulose on strength loss in fire-retardant-treated southern pine. Holzforschung 53 (3), 311-317.

Winandy, J.E. (1995) Effects of fire retardant treatments after 19 months of exposure at 150°F (66°C). Research Note FPL-RN-0264. U.S. Department of agriculture, Forest Service, Forest Products Laboratory, Madison, WI., p3.

Zhang, Y.H.P. and Lynd, L.R. (2004) Toward an Aggregated Understanding of Enzymatic Hydrolysis of Cellulose: Noncomplexed Cellulase Systems. Biotechnology and Bioengineering 88 (7), 797-824.

Zheng, Y., Pan, A., Zhang, R., and Jenkins, B.M. (2009) Kinetic Modeling for Enzymatic Hydrolysis of Pretreated Creeping Wild Ryegrass. Biotechnology and Bioengineering 102 (6) 1558-1569.

Chapter 3

Determination of optimal conditions for barley straw pretreatment by ionic liquid 1-ethyl-3-methylimidazolium acetate

The recalcitrant nature of biomass leads to very low hydrolysis efficiency for the raw material. This can be attributed to the crystal structure of cellulose, which forms as a result of its intra- and intermolecular hydrogen bonding (Figure 3.1). Lignin and hemicellulose also make the structure compact, forming a physical hindrance (Figure 2.1). Therefore, a pretreatment step must be carried out to disrupt the compact structure. Some ionic liquids (ILs), which have strong ionic strength, can interact with the hydroxyl groups result in the dissolution of crystallized cellulose. When cellulose is regenerated in anti-solvent like water or ethanol, the hydrogen bonds form randomly. New structure is more accessible to enzyme molecules. Thus, this increases the hydrolysis efficiency.

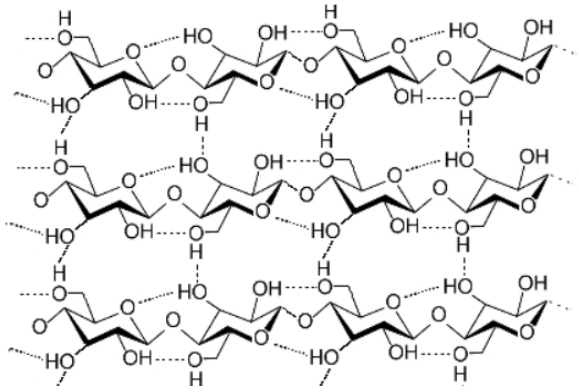

Figure 3.1 Crystal structure of cellulose. Dash lines indicate hydrogen bonds.

3.1 Key point of this research

Barley straw was pretreated by ionic liquid (IL) 1-ethyl-3-methylimidazolium acetate ([EMIM]Ac, Figure 3.2). Optimal pretreatment conditions with three different parameters (temperature, time, concentration of barley straw substrate) versus sugar recoveries obtained following enzymatic hydrolysis was estimated by multiple linear regression statistical using MODDE software. The influence of [IMEM]Ac on the chemical structure of cellulose and glucose under high temperature were also investigated by an indirect method. Figure 3.3 illustrates the structure of this research.

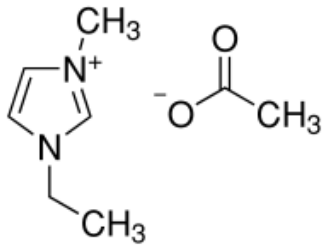

Figure 3.2 1-ethyl-3-methylimidazolium acetate.

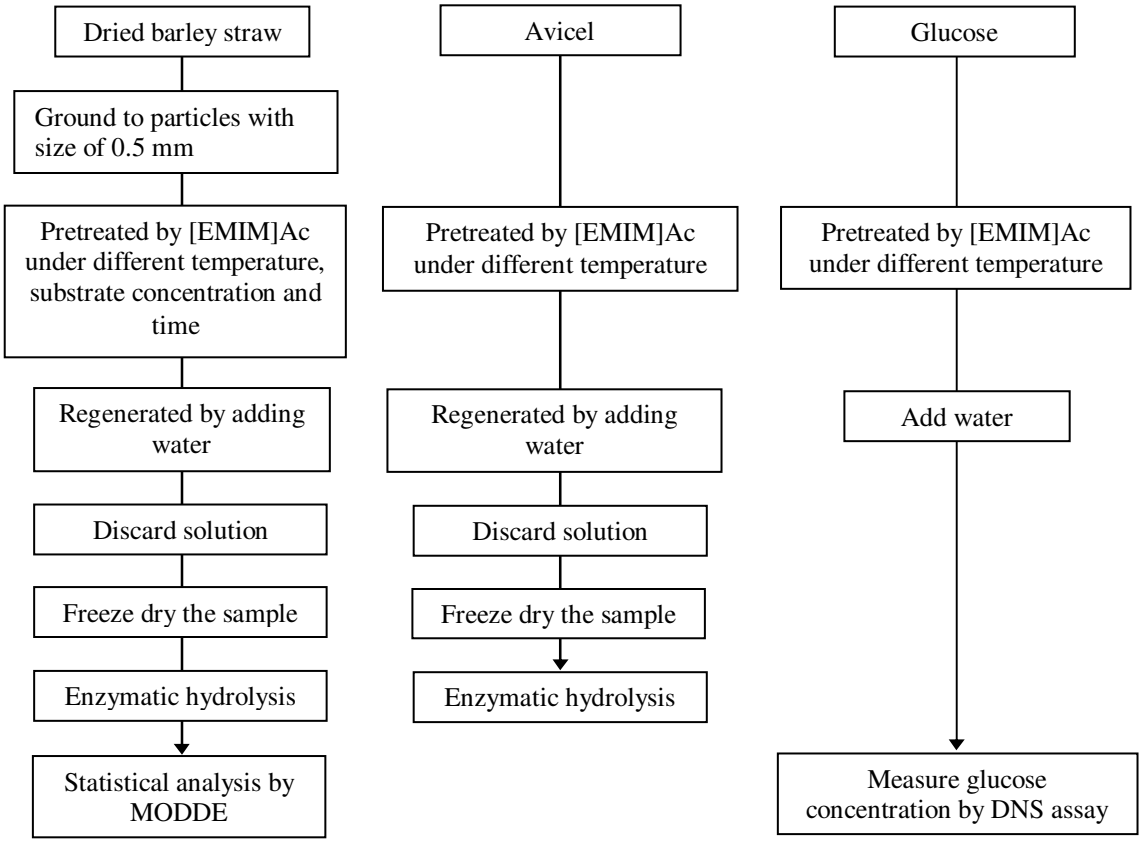

Figure 3.3 Experimental procedures of IL pretreatment. Avicel and glucose were used to investigate the effect of high temperature on the substrate.

3.2 Conclusion

Elevated pretreatment temperatures and longer pretreatment times favoured hydrolysis. Different appearances after pretreatment are shown in Figure 3.4, 3.5 (barley straw), 3.6 (Avicel) and 3.7 (glucose). However intensive pretreatment at 150°C also causes degradation of cellulose and glucose. Functional groups on cellulose may also change, causing the darkened color of the regenerated cellulose. However, direct observation with the aids of advanced spectroscopy like IR and NMR is need for further investigation in the future. According to statistical analysis, optimal pretreatment conditions for glucose and xylose were found to be around 55-60 minutes and barley straw concentration of 8-10%. However considered the amount of consumed ionic liquid, barley straw concentration can be upto 20%. The mass balance of barley straw preated under 150°C, 20% dry matter for 50 min is shown in Figure 3.8.

[EMIM]Ac pretreated substrate was found to stabilize the enzymes at elevated temperatures. Compared with hot water extraction pretreatment developed by Inbicon (Denmark), for IL pretreated barley straw, lower levels of enzymes were required to obtain similar hydrolytic efficiencies. The initial hydrolysis rate of IL pretreated barley straw is higher than that pretreated by hot water extraction, however after 72 hours there is no significant difference between their final glucose yields. It shows product inhibition is still the bottleneck. IL pretreatment only change the enzymatic hydrolysis kinetics.

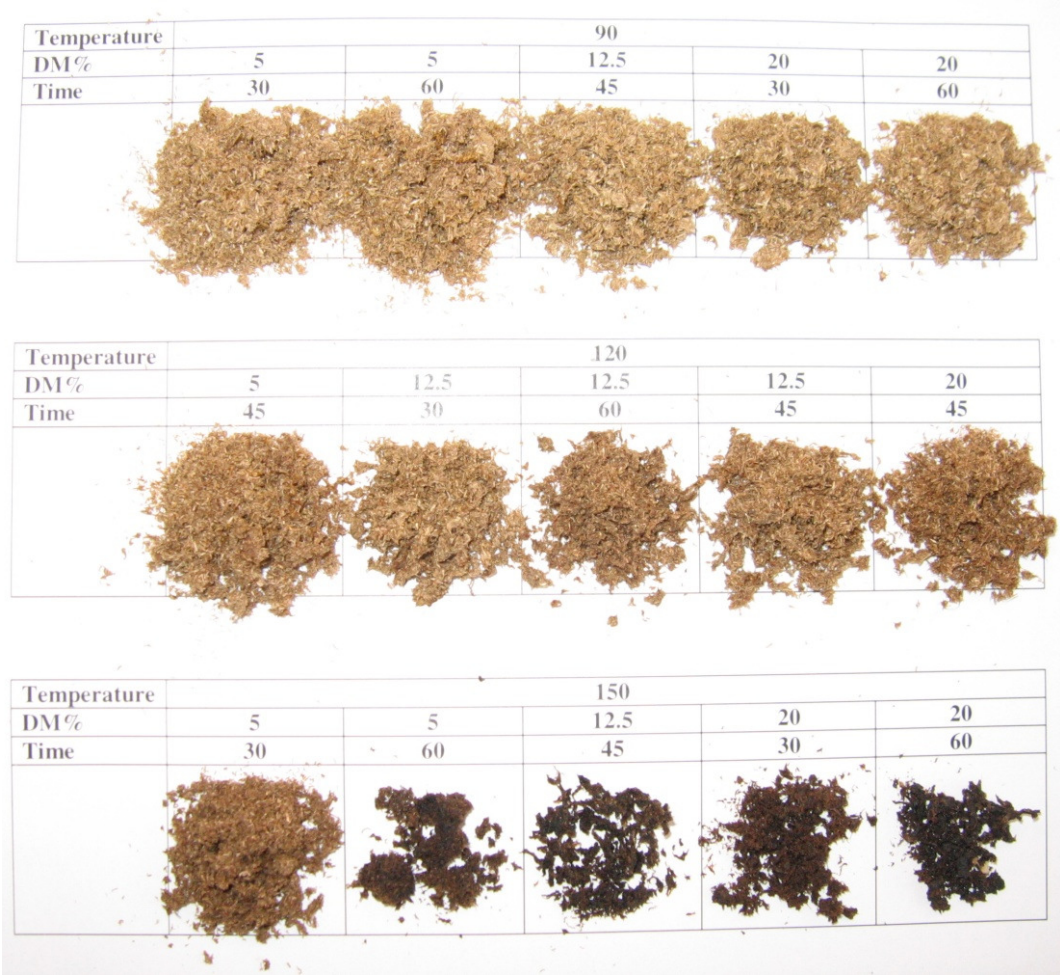

Figure 3.4 Appearance of barley straw after [EMIM]Ac pretreatment under different temperature, substrate concentration and time. Substrates were regenerated by water and then freeze dried. Values of pretreatment temperature, substrate concentration (dry matter, DM%) and time are shown in the figure.

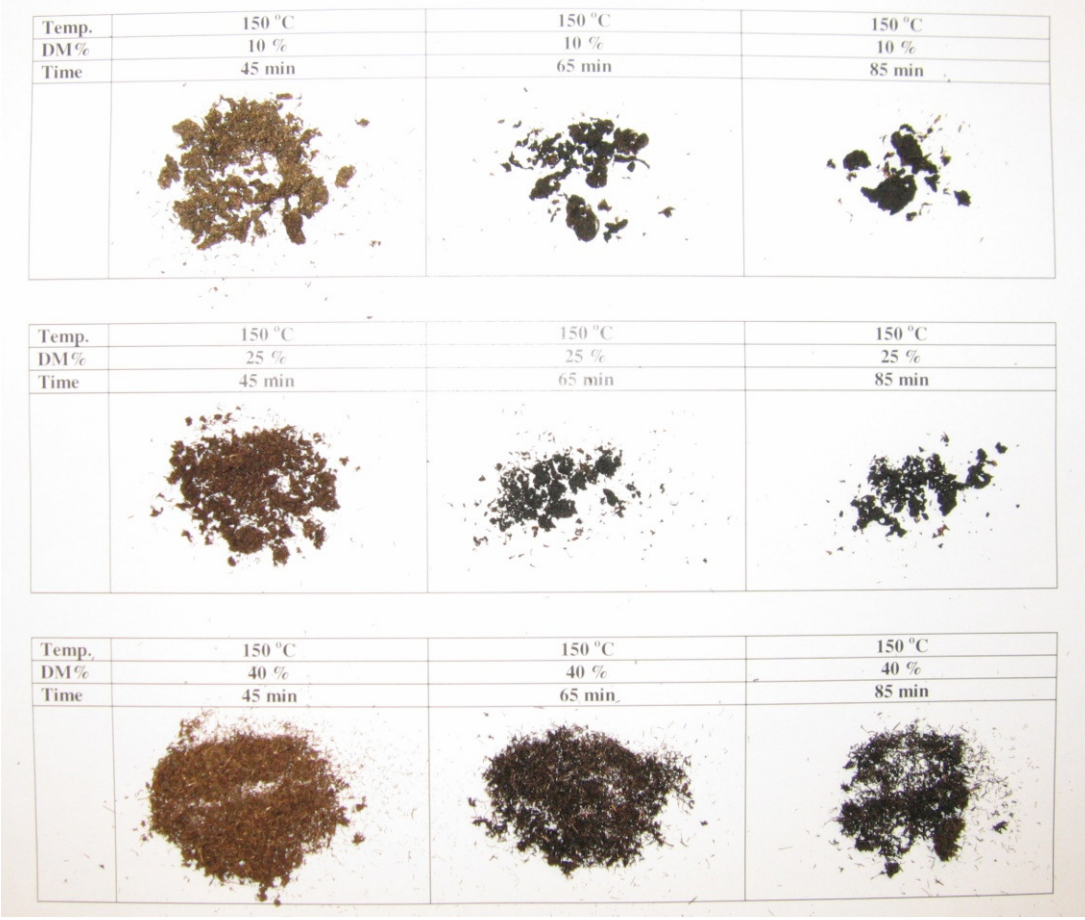

Figure 3.5 Appearance of barley straw after [EMIM]Ac pretreatment under 150°C with different substrate concentration and time. Substrates were regenerated by water and then freeze dried. Values of pretreatment temperature, substrate concentration (dry matter, DM%) and time are shown in the figure.

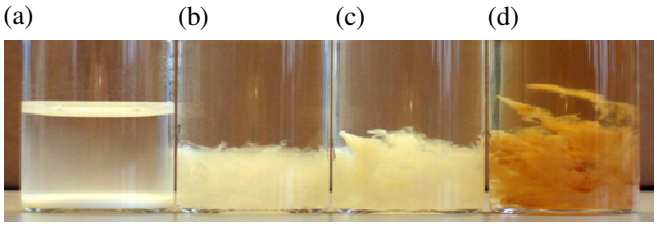

Figure 3.6 Appearance of Avicel after [EMIM]Ac pretreatment (10% substrate, 45 min). Substrates were regenerated by water. (a) no pretreatment, (b) 90°C, (c) 120°C and (d) 150°C.

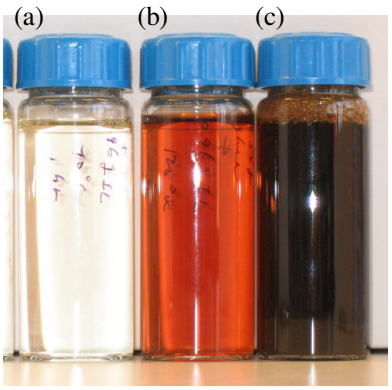

Figure 3.7 Appearance of glucose after [EMIM]Ac pretreatment (0.54 g glucose + 0.96 g [EMIM]Ac, 1 hr). After pretreatment 20 mL water were added. (a) 90°C, (b) 120°C and (c) 150°C.

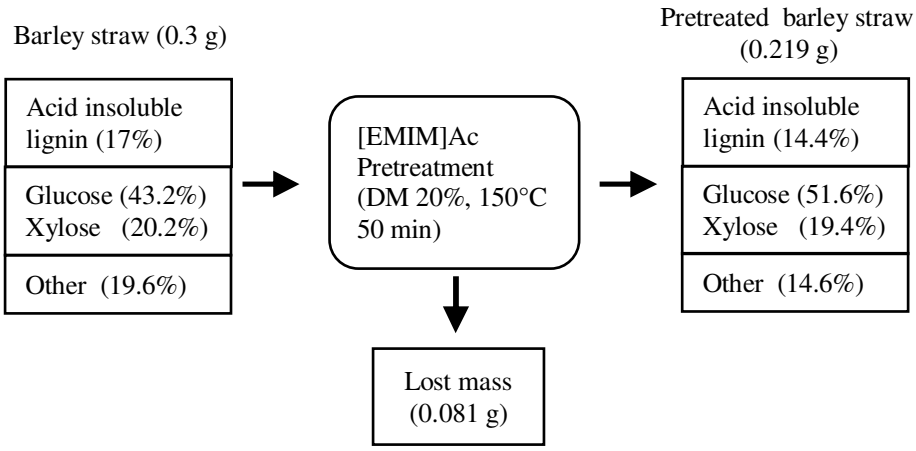

Figure 3.8 Mass balance of barley straw preated under 150°C, 20% DM for 50 min.

Determination of optimal conditions for barley straw pretreatment by ionic liquid 1-ethyl-3-methylimidazolium acetate

Chien Tai Tsai[a]
Email: aaron0115@gmail.com

Anne S. Meyer*[a]
* Corresponding author
Email: am@kt.dtu.dk
Tel: (+45) 4525 2909

[a] Center for Bioprocess Engineering, Dept. of Chemical and Biochemical Engineering, Technical University of Denmark, DK-2800 Kgs. Lyngby, Denmark

[b] Novozymes A/S, Biofuels R&D, Krogshoejvej 36. 2880 Bagsvaerd Denmark

Abstract

Backgrounds

Pretreatment of lignocellulosic biomass can improve the efficiency of hydrolytic enzymes acting on the substrate, thereby resulting in a more economical process. Interest in employing ionic liquids in alternative pretreatment methods has been growing steadily following the discovery that ionic liquids can be excellent media for dissolution of these substrates.

Methods

In order to optimize the pretreatment of barley straw using the relatively benign ionic liquid, 1-ethyl-3-methylimidazolium acetate ([EMIM]Ac), correlative models were constructed using 3 different pretreatment parameters (i.e. temperature, time, concentration of barley straw substrate) and sugar recoveries obtained following enzymatic hydrolysis.

Results

Elevated pretreatment temperatures and longer pretreatment times favoured hydrolysis. However intensive pretreatment at high temperature also causes degradation of cellulose. In addition, [EMIM]Ac pretreated

lignocellulose was found to stabilize and protect the enzymes at elevated temperatures. As such, lower levels of enzymes were required to obtain similar hydrolytic efficiencies. This is significant as the need for reduced enzyme dosages could improve the feasibility of lignocellulosic pretreatment using ionic liquid media.

Conclusions

Optimal pretreatment condition was found with the aid of models based on multiple linear regression. Consider the balanced against economic considerations, barley straw can be pretreated under 150°C for 50 min with concentrations of 20% (w/w). Glucose yield can be up to 70% after enzymatic hydrolysis.

Keywords

Bioethanol, Enzymatic hydrolysis, Pretreatment, Ionic liquid, Barley straw, Lignocellulose

Background

Given the ambitious targets set in both the US and Europe aimed at increasing usage of renewable fuels in the transport sector, there is a significant focus on ethanol production from cellulosic biomass as a renewable, environmentally friendly alternative to fossil fuels [1, 2]. Successful production of ethanol from cellulosic biomass requires, among other things, efficient generation of glucose rich hydrolysate from the biomass feedstock.

Lignocellulose form plant biomass is composed mainly of cellulose, hemicellulose and lignin. Cellulose is a polysaccharide composed of D-glucose monomers those can be converted to ethanol by fermentation. Before utilizing these monomers in fermentation processes, cellulose must first be hydrolyzed to release D-glucose. However, the recalcitrant nature of biomass generally leads to very low hydrolysis efficiency for the raw material. This low efficiency may be attributed to the crystal structure of cellulose, which forms as a result of its intra- and intermolecular hydrogen bonding [3]. More specifically, the small compact porous structure of cellulose impedes accessibility of hydrolytic enzymes to potential sites of action [4]. Lignin can also act as a binder with respect to cellulose fiber, forming a physical hindrance. A further limitation attributed to lignin includes its ability to non-specifically bind enzymes, thereby decreasing overall hydrolysis efficiency [5, 6]. Accordingly, a pretreatment step must be carried out to disrupt the crystal structure of cellulose and to remove lignin. In order to accomplish this task, an additional input of energy is needed. From an economic point of view, the less energy required the better [7]. Simultaneous extraction of valuable by-products such as lignin could further add to the efficiency and profitability of the process [8]. Hence, more effective pretreatment methods are continuously under investigation in order to achieve these goals.

Recently, ionic liquids (ILs) were reportedly used in an alternative pretreatment process. ILs are organic salts that exist in their liquid state at low temperatures (<100°C). They are chemically and thermally stable, non-flammable and have very low vapour pressures [9]. With regards to biomass pretreatment, the most important attribute of select ILs is their ability to compete with cellulose for hydrogen bonding opportunities, thereby reducing crystallinity and disrupting its original three-dimensional structure [10-12]. The implication of this is that lignocellulose is soluble in some ILs. Finally, dissolved cellulose can be regenerated through the addition of an anti-solvent such as water, ethanol or acetone to the system [13-15]. These unique properties have aroused the interest of the bioethanol industry in recent years.

An ideal IL for lignocellulose pretreatment should have the following characteristics: (1) Low melting point (ideally below room temperature), (2) non-degradative towards cellulose, (3) allows simple regeneration of dissolved cellulose, (4) easily recoverable, (5) non-corrosive and non-toxic, (6) low viscosity, and (7) exhibits a high solubility for lignocellulose. At present, the IL 1-butyl-3-methylimidazolium-chloride ([BMIM]Cl) is one of the most widely used within both research and industry. However, it is corrosive, toxic and has a melting point around 70°C. As such, scientists continue to search for more suitable IL candidates. Zavrel (2009) [14] screened numerous ILs, showing 1-allyl-3-methylimidazolium-chloride ([AMIM]Cl) and 1-ethyl-3-methylimidazolium acetate ([EMIM]Ac) to be good potential alternatives for lignocellulosic dissolution. Although the former was found to be more efficient at dissolving lignocellulose, the latter was neither corrosive nor toxic and had a melting point of -20°C. Furthermore, [EMIM]Ac could also dissolve pure cellulose powder under mild conditions [14]. In fact, enzymatic hydrolysis of pure cellulose (Avicel) was found to be similar after a 48 h pretreatment period with either [EMIM]Ac or [BMIM]Cl [12]. Zhao (2009) [12] also showed that cellulose (Avicel) pretreated with [EMIM]Ac could be hydrolyzed at 60°C with higher sugar recoveries than at 50°C. Nguyen (2010) [16] showed [EMIM]Ac can be recycled 5 times through distillation without decreasing pretreatment efficiency. Overall, these results suggest that [EMIM]Ac might be a promising solvent for pretreatment of lignocellulosic biomass.

On an industrial level, it is important to reduce consumption of ILs, to use lower temperatures and shorten pretreatment periods, all while maintaining high enzymatic hydrolysis efficiency. Until now, most studies on IL pretreatment methods have considered either pure cellulose substrate under mild pretreatment conditions, or else lignocellulose substrate pretreated over extended periods (i.e. from 1 hr to 1 day). Although useful in facilitating the understanding of pretreatment phenomena, working with cellulose can be of limited value with regards to industrial applications because it is only a model substrate. Moreover, extensive lignocellulosic pretreatment periods are impractical in industry and can have a negative economic impact on the overall process. Lastly, most studies to date employ excessive amounts of IL during the pretreatment step (i.e. only 5~10% substrate), which is also not economically feasible. As

such, the aim of this investigation was to optimize IL pretreatment through the use of statistical modelling in order to minimize the amount of IL media required, shorten the pretreatment time, and lower the pretreatment temperature associated with efficient enzymatic hydrolysis. Furthermore, this IL pretreatment process was also compared with a more conventional hot-water-extraction (HW) process in order to facilitate greater understanding of this emerging pretreatment technology. Overall, results detailed in this study provide an important connection between lab scale and future industrial process development.

Results and discussion

Effects of IL pretreatment on physical and chemical properties of lignocellulose

Barley straw was subject to IL pretreatment at temperatures ranging from 90 to 150°C. Visual inspection revealed that barley straw heated to 150°C appeared darker than substrates pretreated at lower temperatures, suggesting that rigorous chemical reactions occurred at higher temperature. The volume of the lignocellulosic material also shrunk considerably after oven drying at 105°C, indicating that the organized fibrous material was destroyed by the pretreatment process. Indeed, it seemed that there were no fibres rigid enough to support the original structure, which is also consistent with previous findings using confocal and scanning electron microscope [17]. Mass recovery of lignocellulosic substrates decreased when subject to higher temperatures and longer pretreatment times (Figure 1). It is apparently an energy dependent process. In contrast, the effect of substrate concentration was found to be less significant for pretreatment times of less than 60 minutes. Overall, decreased mass is due to that some dissolved components cannot be precipitated out or recovered by following regeneration.

It was proposed that [EMIM]Ac is capable of delignifying lignocellulose [18, 19] and causing degradation of cellulose. In order to verify whether degraded fragments or monomers of cellulose or hemicellulose were dissolved in IL media, after regeneration, the IL-water supernatant solutions were analyzed via the 3,5-dinitrosalicylic acid (DNS) reducing sugar method, but no reducing sugars were detected. However, with the recovery of glucose, xylose and acid insoluble lignin following IL pretreatment at less than 88%, 78% and 62%, respectively (Table 1). It is apparent that some cellulose and/or hemicellulose decomposed into monoer or oligomers and released into liquid phase. This is inconsistent with previous discovery of DNS analysis. In an effort to understand this discrepancy, Avicel was employed as a model cellulose substrate in investigations of this pretreatment phenomenon. Avicel was pretreated by IL under 90, 120 and 150°C. Mass recoveries were compared after regeneration. Figure 2 reveals that at 90°C and 120°C, no significant loss of cellulose mass. As for appearance, the color did not change significantly after pretreatment. As such, β(1→4)-glycosidic bonds subject to these conditions were presumed stable. In contrast, after pretreatment at 150°C, more than 10% of Avicel could not be

regenerated by precipitation. The color of cellulose became brownish. Given that Avicel is pure cellulose, we can conclude that certain amount of cellulose was degraded. This is consistent with the observation of Sun (2009) [18], which was observed by ^{13}C NMR. However, still no reducing sugars could be detected in liquid phase via the DNS reducing sugar method. The DNS reducing sugar method is based on a redox reaction, whereby free carbonyl groups (i.e. aldehydes, ketones) in monomer or oligomer sugars are oxidized with subsequent reduction of DNS. Negative results from this assay could be due to the alterations in the chemical structures of released sugars during harsh pretreatment, therefore provided false negative results. To confirm this hypothesis, glucose powder was subject to IL pretreatment at different temperatures. It shows that after pretreatment at 150°C, less than 20% of the glucose was detectable via the DNS reducing sugar method (Figure 3). Thus, based on investigations of pretreatment of barley straw, Avicel and glucose, we may conclude that ILs could induce chemical reactions involving reducing sugars at high temperatures.

As with lignin, since the recovery of lignin is less than 62% (Table 1), it reveals some lignin was stripped form barley straw. This is in accordance with Sun (2009) [18] who proved the delignification effect by utilizing an anti-solvent consists of water : acetone (1:1, v/v) to partially precipitate [EMIM]Ac-dissolving lignin. Due to that [EMIM]Ac itself has a high absorbance within the UV range, this makes the quantitative analysis of dissolved lignin in IL-water solutions rather difficult to assess. In the future, analytical methods need to be further developed in order to understand the chemical reaction mechanism. Kim (2011) [19] proposed the mechanism of delignification is partial fragmentation of lignin through the interaction between $[EMIM]^+$ cation and interunint linkages of lignin. In overall, [EMIM]Ac only partially delignify the lignocellulose. Several rounds of pretreatment is necessary to remove lignin completely.

Also noteworthy is that glucose recovery following pretreatment was higher than for xylose (Table 1). In plant cell wall, most cellulose are crystalline polymers surrounded by amorphous hemicellulose and lignin [20]. It is easier for IL molecules to attack the chemical bonds of hemicelluloses, which surround outside. Meaning that hemicellulose were exposed to IL (pretreated) longer than cellulose, effectively lowering xylose recoveries. Avicel was completely dissolved in [EMIM]Ac under mild conditions (*e.g.* 90°C, 60 minutes, 12.5% substrate concentration) while barley straw was found to only partially dissolve, appearing as a solid-jellylike material even at 150°C. This suggests that lignin interacts with cellulose and hemicellulose, forming a barrier and interfering with the dissolution process. Therefore, higher energy is needed to disrupt the compact structure.

Effects of pretreatment conditions on enzymatic hydrolysis

Pretreatment parameters investigated in this study include temperature, time and substrate concentration (%w/w). Sugar recoveries obtained from hydrolysis of cellulose (Avicel, Figure 2) and barley straw

(Figure 4), respectively, are dependent on pretreatment temperature, especially for barley straw; however, the phenomena of these two substrates were different. For Avicel pretreated at 90°C, 120°C and 150°C, all enzymatic hydrolysis reactions were almost complete after 48 hours, which was similar to a previous report by Zhao (2009) [12]. Glucose recovery was highest at 90°C while pretreated at 150°C yielded the lowest levels of glucose. This was attributed to the degradation reaction mentioned in previous section. In contrast, the optimal pretreatment temperature for barley straw was 150°C, the sugar recoveries were more than twice of those under 90°C. Sugar recoveries at 120°C were also rather low. Diverging results between Avicel and barley straw is due to the complex structure of lignocellulose. With respect to Avicel, the IL could directly "attack" the hydrogen or other bonds from the start of the pretreatment. As for barley straw, the IL first needs to penetrate through the lignin and hemicellulose, which surrounds and binds the cellulose. Penetration and dissolution processes are both energy dependent.

With 150°C clearly shown to be the better temperature for barley straw hydrolysis, further investigations on the effects of pretreatment time and lignocellulose concentration were carried out. Models of glucose and xylose recoveries at either low (A, B) or high (C, D) levels of pretreatment time and substrate concentration were shown in Figure 5. Two different ranges were used in the construction of the models in order to ensure: 1) that correlation ranges were not too wide, thereby resulting in very rough statistical correlations, and 2) that ranges were not too narrow, thereby resulting in a loss of the overall trend. All-in-all, optimal pretreatment conditions for glucose and xylose were found to be similar in both cases, with around 55-60 minutes and barley straw concentration of 8-10% as the optimum. Note that higher dosage levels of the IL are not necessarily better, as increasing quantities of IL require a longer time to heat up and consequently the energy input into the system goes towards heating up rather than dissolving lignocellulose.

Influence of [EMIM]Ac on enzyme activity

After IL pretreatment, regeneration of lignocellulose and removal of the IL are accomplished through the addition of water. Since the mechanism of cellulose dissolution by ILs is through competition for hydrogen bonding, it follows that the 3-D structure of enzymes can also be changed by ILs due to a loss of hydrogen bonding interactions between amino acids. The removal of excess IL is therefore important. In order to find the maximum tolerance level of [EMIM]Ac towards the biocatalyst, enzymatic activity was investigated. Figure 6 shows that an [EMIM]Ac concentration below 0.5% did not significantly affect hydrolytic efficiency, unlike [EMIM]Ac concentrations greater than 1% which had the effect of steadily decreasing efficiency. Thus in production process the ILs should be less than 0.5% when the substrate is subjected to enzymatic hydrolysis.

Enzymatic hydrolysis kinetics of pretreated barley straw at different temperatures

Zhao (2009) [12] showed that not only could Avicel pretreated by [EMIM]Ac be hydrolyzed at 60°C, but it also yielded higher sugar recoveries than at 50°C. This was reportedly because IL pretreated cellulose had a surface that was accessible to the enzyme, helping to protect it against thermal denaturation at 60°C. In order to investigate whether IL pretreated barley straw was influenced in a similar manner, both IL and HW pretreated barley straw were enzymatically hydrolyzed at 50°C and 60°C. As seen in Figure 7, IL pretreated barley straw exuded a protective effect as compared with the hydrolysis of HW pretreated substrate. The protection efficiencies (the ratio of released glucose at 60°C and 50°C) at 72 hours were 82.4% and 38.5%, respectively, for IL and HW pretreated barley straw. It has been reported that enzyme thermal stability may be improved through immobilization technologies, such as adsorption (reviewed by Iyer 2008 [21]). From this perspective, structural attributes such as high surface area and fine porous structure of IL pretreated lignocellulose, with higher adsorption capacity for enzyme molecules, may be regarded as the support of the enzyme. As such, this reaction may be likened to a semi-immobilized enzymatic system, in which its structure protects the enzyme from thermal denaturation. Within the first 6 hours, the hydrolysis reaction at 60°C is faster than at 50°C (Figure 7); however, as the substrate was hydrolyzed over time, its porous structure was disrupted, no longer accommodate and protect much enzyme from thermo deactivation. As such, resulting hydrolysis efficiency decreases dramatically after 6 hours. Still, this theory cannot explain the finding of Zhao (2009) [12] whom reported that the glucose yield after hydrolysis efficiency of IL pretreated Avicel at 60°C was higher than that at 50°C. Detailed mechanisms are to be investigated in the future. It should be emphasized that the protective nature of the IL pretreated substrate might permit easier development of a high temperature hydrolysis process through thermal stabilization of the enzyme.

Regarding to the glucose yield after enzymatic hydrolysis of 5% pretreated barley straw, if it is based on pretreated substrate, IL and HW pretreatments yielded glucose recoveries of 80.7 % and 62.4 %, respectively. Example of calculation:

$$\frac{50}{120*0.516}*100\% = 80.7\%$$

where

50: total weight of released glucose (mg)

120: initial substrate weight (mg)

0.516: glucose content of IL pretreated barley straw (in Table 1)

When based on native substrate, the yields become 70.4% and 71.9%, respectively. Example of calculation:

$$\frac{50}{120/0.73 * 0.432} * 100\% = 70.4\%$$

where

50: total weight of released glucose (mg)

120: initial substrate weight (mg)

0.73: mass recovery after pretreatment

0.432: glucose content of native barley straw (in Table 1)

Although HW pretreated substrate contains more potential glucose, a range of factors, such as those relating to enzyme stability and product inhibition mean that almost 37.6% (calculated from 100% - 62.4%) of the glucose present was not released. This may due to product inhibition and the high content lignin (26.6%, Table 1), in the substrate. Lignin non-specifically adsorbs enzyme and reduce hydrolysis efficiency. Another difference between IL and HW pretreatment is that at 50°C, the hydrolysis rate of the former is faster than the later up until 24 hours. This may be because IL pretreated barley straw has a more porous structure which allows for greater accessibility of the enzyme into the interior structure of the substrate, not only accelerate reaction rate but also stabilize the enzyme.

Enzymatic hydrolysis at different enzyme dosage

The finding that IL pretreated barley straw can protect the enzyme at elevated temperatures leads to the hypothesis that a lower enzyme dosage may be sufficient to hydrolyze the IL pretreated lignocellulose. Figure 8 shows that when the enzyme dosage was reduced, glucose recovery from HW pretreated barley straw decreased faster than following hydrolysis of the IL pretreated barley straw. This observation combined with previous kinetic results (Figure 7) illustrate that the reaction environment of the IL pretreated barley straw is more favourable for enzymatic hydrolysis.

Effect of high lignocellulose concentration on enzymatic hydrolysis efficiency

In an industrial process, water and ethanol are separated by distillation following the conversion of glucose to ethanol. Distillation is an energy intensive process [22]. As such, it is preferable that the glucose concentration in the fermentation reactor is high, thereby producing a higher concentration of ethanol. This can reduce energy input for heating up excess water. In the past years, enzymatic hydrolysis of more concentrated mixtures was widely investigated for the production of high glucose substrates [23, 24]. However, IL pretreated lignocellulose hydrolyzed at higher substrate concentration was not previously reported. In this research, IL and HW pretreated barley straw were compared following hydrolysis of increasing levels of substrate, based on glucose recovery as well as resulting glucose concentration. It shows that glucose recoveries of both pretreatment samples decreased with substrate

concentration (Figure 9). The slopes were similar, illustrating that although IL pretreated barley straw was previously shown to help maintain enzymatic activity; product inhibition was inevitable [25]. Intersection of recovery and concentration curves occurred around a 15% substrate concentration. When glucose recovery and glucose concentration of hydrolysis of 5% and 15% substrate were compared, the values are 67.4 %, 21.2 mg/mL, and 57.3 %, 60.4 mg/mL, respectively. This means that if 10.1 % glucose recovery is sacrificed, 2.86 times of glucose concentration can be obtained.

Conclusions

In the point of view of large-scale processes, yield of product is not the only consideration. The required input of energy for pretreatment and distillation, the size of reactor, consumption of water and subsequent treatment of byproducts from the system (e.g. recycling of ILs and upgrading of lignin) are also important. Every aspect needs to be properly evaluated.

Upon reduction of the amount of IL employed during the pretreatment step, the following benefits may be obtained: (1) the need for costly ILs can be reduced, resulting in significant savings, (2) reduced impact on the environment based on a reduced need for energy and ILs, (3) reduced size of the reactor, and (4) less water is required for regeneration of lignocellulose and removal of the IL. This research shows that while optimal IL pretreatment conditions include 150°C, 55~60 minutes and 8~10% substrate concentration, glucose yields may be balanced against economic considerations, whereby barley straw concentrations may be increased to 20% and reaction time may be decreased to 50 minutes. Compared with HW pretreatment, IL pretreated barley straw did not yield a significantly better glucose recovery after enzymatic hydrolysis. Although the initial hydrolysis rate for IL pretreated barley straw was faster than that of HW pretreated, after 24 hours the rate of the former decreases faster than the later, and finally at 72 hours the glucose concentration are similar. This is the result of product inhibition, due to the nature of this catalytic system. Still, IL pretreated barley straw can protect the enzyme at higher temperatures and is less sensitive to the reductions of enzyme dosage. As such, IL pretreatment can improve the thermal stability of the enzyme while allowing for a reduction in costs. Overall, several key parameters relating to [EMIM]Ac pretreatment for a lignocellulosic bioethanol production process were investigated, and compared with HW pretreatment. In most research including this research, due to the high viscosity of the IL-substrate mixture under high substrate concentration, the pretreatment were conducted under stationary conditions without further mixing, meaning that the penetration of ILs into plant tissue only depend on diffusion, thus longer time or higher temperature are needed to elevate the pretreatment efficiency. We expect that with mild mixing and squeezing, the pretreatment efficiency may significantly be improved. With the aid of a reactor designed according to the structure of extruder, which is used in polymer process,

the mixing of viscous ILs-lignocellulose mixture can be easily achieved. As proved in this research, pretreatment under 150°C start degradation reaction, which reduce sugar recovery. Mixing may be a feasible way to decrease pretreatment temperature and time, thus reduce degradation reaction. The hypothesis needs further investigation in the future.

Methods

Chemicals and enzymes

The following chemicals were purchased from Sigma-Aldrich (St. Louis, MO, USA): Avicel PH-101 cellulose, sodium acetate, sodium azide, 3,5-dinitrosalicylic acid, Rochelle salt (K-Na tartrate tetrahydrate), phenol, sodium metabisulfite, 1-ethyl-3-methylimidazolium acetate, adenosine 5′-triphosphate disodium salt, β-nicotinamide adenine dinucleotide phosphate sodium salt hydrate, and EPPS. The following two enzymes were provided from Novozymes A/S (Bagsværd, Denmark): Celluclast 1.5L derived from *Trichoderma reesei* and Novozyme 188 derived from *Aspergillus niger*. Celluclast 1.5L had an activity of 65 FPU/g (FPU = filter paper units). The FPU activity was determined by NREL standardized filter paper assay. Novozyme 188 had an activity of 860 CBU/g (CBU = cellobiose units). The CBU activity was determined by measuring glucose production from cellobiose at 50°C, pH 4.8 [26, 27]. Hexokinase (420 U/ml) + Glucose-6-phosphate-dehydrogenase (210 U/ml) was purchased from Megazyme (Wicklow, Ireland).

Preparation of barley straw and pretreatment

Barley straw for ILs pretreatment was grown in Grumløse (Southern Zealand, Denmark) in 2003 and obtained from The Danish Cooperative Farm Supply (Bårse, Denmark). It was ground by universal mill (M20, IKA, Germany) until particles passed through a stainless steel sieve with a 0.5 mm aperture (Endecotts, London, UK). Pretreatment parameters such as temperature, time and substrate concentration ranged from 90-150°C, 30-85 minutes, and 5-40% (w/w), respectively. In order to model this system, the software MODDE (Umetrics AB, Sweden) was used to suggest combinations of these parameters for investigation. Overall, 0.3 g of barley straw particles or cellulose (Avicel) substrate was mixed together with different amounts of [EMIM]Ac, and then incubated in an oven at a set temperature for a defined period of time without stirring. The pretreated substrates were regenerated through addition of 40 mL water to the still-hot IL-substrate mixtures with vigorous stirring for 30 seconds. Next, the mixtures were incubated for 15 minutes at room temperature with mild shaking, centrifuged at 5000 × g for 10 minutes and the supernatant was discarded. Additional water (40 mL) was added to the system and the mixture was incubated for at least 12 hours at room temperature with mild shaking, followed by centrifugation at

5000 × g for 10 minutes and discarding of the supernatant. This washing step was repeated once more prior to freeze-drying of the samples.

Barley straw pretreated via hot-water-extraction was grown and harvested in 2006 on the island of Funen, Denmark. Thereafter, the barley straw was transported to DONG Energy (Danish Oil and Natural Gas Energy), Denmark for pretreatment. The pretreatment method consisted of a three-stage process, whereby the straw was subject to three successive heat-treatment steps at progressively higher temperatures (60°C, 15 min; liquids removed; 180°C, 10 min; 195°C, 3 min). Following pretreatment, the liquids were removed from the system.

Mass recoveries of regenerated substrates were calculated based on their weights. As such, mass recoveries (Y_{mass}) were calculated according to the following equation:

$$Y_{mass}(\%) = \frac{W_{pretreated}(g)}{W_{unpretreated}(g)} \times 100\%$$

Hydrolysis and compositional analysis

Standard procedures for acid hydrolysis and compositional calculation analysis were carried out according to the U.S. National Renewable Energy Laboratory [28].

Enzymatic hydrolysis of substrates was carried out in 0.1 M sodium acetate buffer containing 0.02% sodium azide. The dosage of Celluclast 1.5L used was 5.1 FPU/g-pretreated substrate while the dosage of Novozyme 188 was 45 CBU/g-pretreated substrate. The reactions were incubated in a 50°C or 60°C water bath with shaking, and were deactivated via heating at 100°C for 10 minutes. After cooling to room temperature, reaction samples were centrifuged at 5000 rpm for 10 minutes and the supernatant was subject to compositional analysis.

Concentrations of liberated monosaccharides were determined according to the DNS reducing sugar method, Hexokinase + Glucose-6-phosphate-dehydrogenase assay and through high-performance anion exchange chromatography (HPAEC) on a Dionex® BioLC system (Dionex Denmark A/S, Hvidovre, DK). Sugar recoveries (Y_{sugar}) were calculated according to the following formula:

$$Y_{sugar}(\%) = \frac{W_{monosaccharide}(g)}{W_{potential\ \ monosaccharide}(g)} \times 100\%$$

(Note that the maximum potential sugar content was based on data from the acid hydrolysis of native barley straw)

Construction of models

Multiple linear regression (MLR) statistical analysis and multi-variable models of the pretreatment and hydrolysis were calculated and simulated using MODDE software.

Abbreviations

[AMIM]Cl, 1-allyl-3-methylimidazolium-chloride; [BMIM]Cl, 1-butyl-3-methylimidazolium-chloride; DNS, 3,5-dinitrosalicylic; DM, Dry matter; IL, Ionic liquid; ILs, Ionic liquids; [EMIM]Ac, 1-ethyl-3-methylimidazolium acetate; HW, Hot-water-extraction; MLR, Multiple linear regression

Authors' contributions

CTT participated in the design of experiments, collected the data and drafted the manuscript. ASM coordinated the research and helped to finalize the manuscript. Both authors read and approved the final manuscript.

References

1. Lynd LR, Laser MS, Bransby D, Dale BE, Davison B, Hamilton R, Himmel M, Keller M, McMillan JD, Sheehan J, Wyman CE: **How biotech can transform biofuels.** *Na. Biotechnol* 2008, **26:** 169-172.
2. Regalbuto JR: **Cellulosic biofuels--got gasoline?** *Science* 2009, **325:** 822-824.
3. Zhbankov RG: **Hydrogen bonds on the structures of carbohydrates.** *J Mol Struct* 1992, **270:** 523-539.
4. Zeng M, Mosier NS, Huang CP, Sherman DM, Ladisch MR: **Microscopic examination of changes of plant cell structure in corn stover due to hot water pretreatment and enzymatic hydrolysis.** *Biotechnol Bioeng* 2007, **97:** 265-278.
5. Lu Y, Yang B, Gregg D, Saddler JN, Mansfield SD: **Cellulase adsorption and an evaluation of enzyme recycle during hydrolysis of steam-exploded softwood residues.** *Appl Biochem Biotechnol* 2002, **98-100:** 641-654.
6. Berlin A, Gilkes N, Kurabi A, Bura R, Tu M, Kilburn D, Saddler J: **Weak lignin-binding enzymes: a novel approach to improve activity of cellulases for hydrolysis of lignocellulosics.** Appl Biochem Biotechnol 2005, **121-124:**163-70.
7. Mosier N, Wyman C, Dale B, Elander R, Lee YY, Holtzapple M, Ladisch M: **Features of promising technologies for pretreatment of lignocellulosic biomass.** *Bioresour Technol* 2005, **96:** 673-686.
8. Tan SSY, MacFarlane DR, Upfal J, Edye LA, Doherty WOS, Patti AF, Pringlea JM, Scotta JL: **Extraction of lignin from lignocellulose at atmospheric pressure using alkylbenzenesulfonate ionic liquid**. *Green Chem* 2009, **11:** 339-345.
9. Sheldon RA, Lau RM, Sorgedrager MJ, van Rantwijk F; **Biocatalysis in ionic liquids.** *Green Chem* **4:** 147-151.
10. Dadi AP, Varanasi S, Schall CA: **Enhancement of Cellulose Saccharification Kinetics Using an**

Ionic Liquid Pretreatment Step. *Biotechnol Bioeng* 2006, **95:** 904-910.

11. Liu L, Chen H: **Enzymatic hydrolysis of cellulose materials treated with ionic liquid [BMIM]Cl**. *Chin Sci Bull* 2006, **51:** 2432-2346.
12. Zhao H, Jones CL, Baker GA, Xia S, Olubajo O, Person VN: **Regenerating cellulose from ionic liquids for an accelerated enzymatic hydrolysis.** *J Biotechnol* 2009, **139:** 47-54.
13. Zhu S, Wu Y, Chen Q, Yu Z, Wang C, Jin S, Ding Y, Wu G: **Dissolution of cellulose with ionic liquids and its application: a mini-review.** *Green Chem* 2006, **8:** 325-327.
14. Zavrel M, Bross D, Funke M, Büchs J, Spiess AC: **High-throughput screening for ionic liquids dissolving (ligno-)cellulose.** *Bioresour Technol* 2009, **100:** 2580-2587.
15. Olivier-Bourbigou H, Magna L, Morvan D: **Ionic liquids and catalysis: Recent progress from knowledge to applications**, *Applied Catalysis A: General* 2010, **373:** 1-56.
16. Nguyen TAD, Kim KR, Han SJ, Cho HY, Park SM, Park JC, Sim SJ, Kim JW: **Pretreatment of rice straw with ammonia and ionic liquid for lignocellulose conversion to fermentable sugars.** *Bioresource Technology* 2010, **101:** 7432-7438.
17. Singh S, Simmons BA, Vogel KP: **Visualization of Biomass Solubilization and Cellulose Regeneration During Ionic Liquid Pretreatment of Switchgrass.** *Biotechnol Bioeng* 2009, **104:** 68-75.
18. Sun N, Rahman M, Qin Y, Maxim ML, Rodríguez H, Rogers RD: **Complete dissolution and partial delignification of wood in the ionic liquid 1ethyl-3-methylimidazolium acetate.** *Green Chem* 2009, **11:** 646–655.
19. Kim JY, Shin EJ, Eom IY, Won K, Kim YH, Choi D, Choi IG, Choi WJ: **Structural features of lignin macromolecules extracted with ionic liquid from poplar wood.** *Bioresource Technology* 2011, **102:** 9020-9025.
20. Huber GW, Iborra S, Corma A: **Synthesis of Transportation Fuels from Biomass: Chemistry, Catalysts, and Engineering.** *Chem. Rev.* 2006, **106:** 4044-4098.
21. Iyer PV, Ananthanarayan L: **Enzyme stability and stabilization—Aqueous and non-aqueous environment.** *Process Biochem* 2008, **43:** 1019-1032.
22. Fan ZL, South C, Lyford K, Munsie J, van Walsum P, Lynd LR: **Conversion of paper sludge to ethanol in a semicontinuous solids-fed reactor.** *Bioprocess Biosyst Eng* 2003, **26:** 93-101.
23. Jørgensen H, Vibe-Pedersen J, Larsen J, Felby C: **Liquefaction of Lignocellulose at High-Solids Concentrations.** *Biotechnol Bioeng* 2007, **96:** 862-870.
24. Rosgaard L, Pedersen S, Meyer AS: **Comparison of Different Pretreatment Strategies for Enzymatic Hydrolysis of Wheat and Barley Straw.** *Appl Biochem Biotechnol* 2007, **143:** 284-296.
25. Gruno M, Valjamae P, Pettersson G, Johansson G: **Inhibition of the *Trichoderma reesei* Cellulases**

by Cellobiose Is Strongly Dependent on the Nature of the Substrate. *Biotechnol Bioeng* 2004, **86:** 503-511.

26. Ghose TK: **Measurement of Cellulase Activities**. *Pure and Applied Chemistry* 1987, **59:** 257-268.

27. Sternberg D, Vijayakumar P, Reese ET: **β-Glucosidase: microbial production and effect on enzymatic hydrolysis of cellulose**. *Can J Microbiol* 1977, **23:** 139-147.

28. Sluiter, A; Hames B; Ruiz R; Scarlata C; Sluiter J; Templeton D; Crocker D (2006): *Laboratory analytical procedure 002, Determination of structural carbohydrate and lignin in biomass. NREL.* http://www.nrel.gov/biomass/analytical_procedures.html.

Table 1 Composition of potential sugar and solid fraction of native and pretreated barley straw; values are given in % (w/w)

Pretreatment condition	Glucose	Xylose	Arabinose	Acid insoluble lignin	Ash	Not assayed or unknown
Native barley straw	43.2	20.2	2.7	17.0	1.2	15.7
HW	66.3	3.5	0.3	26.6	1.6	1.7
IL, DM 8%, 60 min	49.6	21.9	3.0	13.6	0.8	11.1
IL, DM 20%, 50 min	51.6	19.4	2.7	14.4	1.3	10.6

Pretreatment condition	Mass recovery (%)	Glucose recovery (%)	Xylose recovery (%)	Acid insoluble lignin recovery (%)
Native barley straw	-	100.0	100.0	100.0
HW	75.0[b]	-	-	-
IL, DM 8%, 60 min	71.0	81.5	77.0	56.8
IL, DM 20%, 50 min	73.0	87.1	70.1	61.8

[a] $\text{Recovery} = \frac{(fraction\ \ of\ \ component\ \ in\ \ pretreated\ \ substrate)\times(mass\ \ recovery)}{(fraction\ \ of\ \ component\ \ in\ \ native\ \ barley\ \ straw)}$

[b] The value was roughly estimated from compositional analysis of native and HW pretreated barley straw.

Table 2 Raw experimental data for multiple linear regression statistical analysis and multi-variable models

	Pretreatment condition			Recovery after pretreatment		
#	Temperature (°C)	Substrate concentration (%)	Time (min)	Mass recovery (%)	Glucose recovery (%)	Xylose recovery (%)
1	90	5.0	30	87.6	31.7	18.7
2		5.0	60	87.8	34.1	20.2
3		12.5	45	86.2	33.8	19.6
4		20.0	30	86.7	31.4	18.5
5		20.0	60	86.6	32.6	19.2
6	120	5.0	45	85.7	49.0	31.4
7		12.5	30	85.6	44.9	27.9
8		12.5	45	84.6	49.8	32.8
9		12.5	60	84.2	54.8	36.6
10		20.0	45	84.4	44.8	30.0
11	150	5.0	30	82.2	69.3	55.7
12		5.0	60	72.0	78.2	60.4
13		12.5	45	74.3	76.9	61.4
14		20.0	30	79.7	72.5	58.7
15		20.0	60	68.3	69.0	53.7

Table 3 Raw experimental data at 150°C for multiple linear regression statistical analysis and multi-variable models

	Pretreatment condition		Recovery after pretreatment		
#	Substrate concentration (%)	Time (min)	Mass recovery (%)	Glucose recovery (%)	Xylose recovery (%)
1	10	45	77.8	74.5	57.1
2		65	69.8	72.3	41.8
3		85	65.1	67.6	34.0
4	25	45	76.7	69.0	53.6
5		65	62.2	66.5	51.3
6		85	56.5	56.3	35.6
7	40	45	70.2	57.5	41.4
8		65	57.6	56.8	40.5
9		85	45.5	37.2	25.9

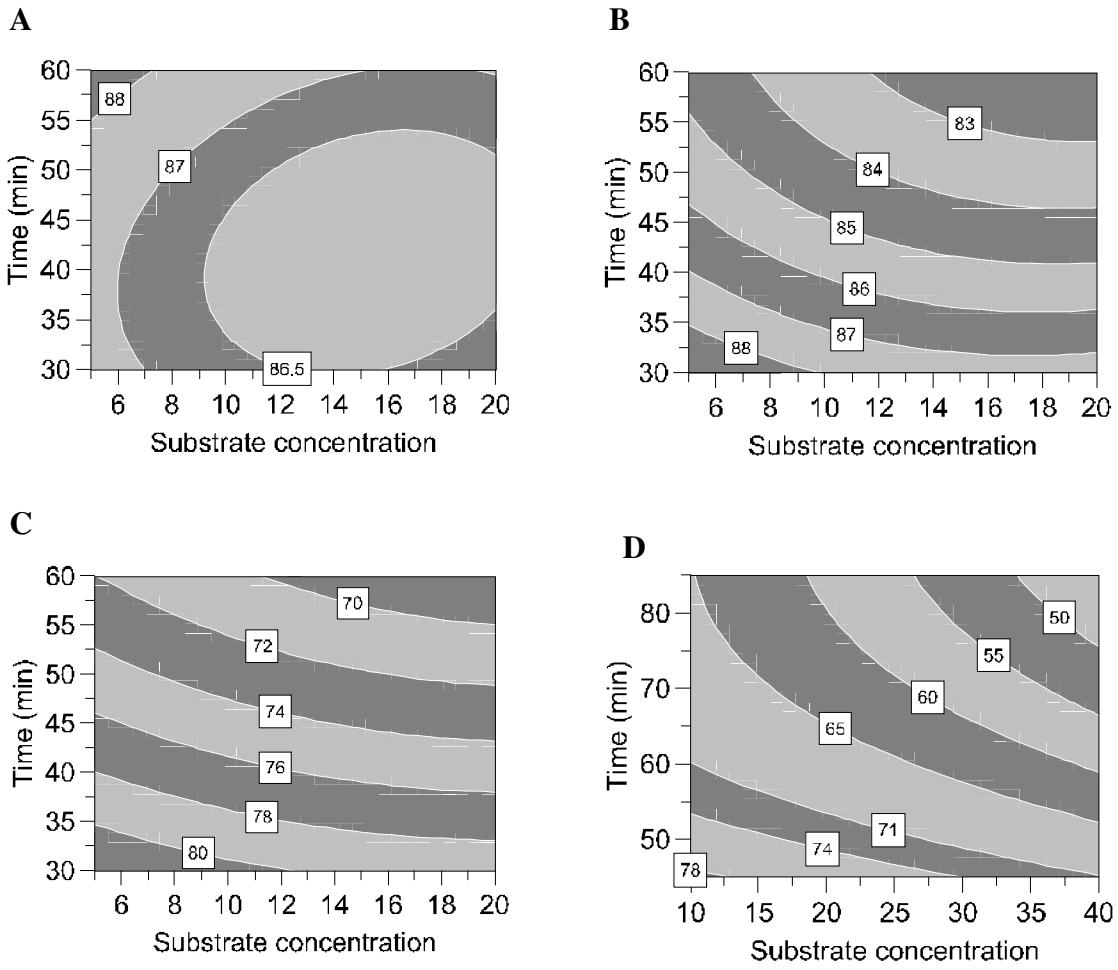

Figure 1 Effect of pretreatment time and substrate concentration on the recovery of lignocellulose (% w/w) under different temperature. (a) 90°C, (b) 120°C, (c) and (d) 150°C; simulated by multiple linear regression from data in table 2 and 3 . (a), (b) and (c) were derived from raw experimental data in Table 2, (d) was from Table 3.

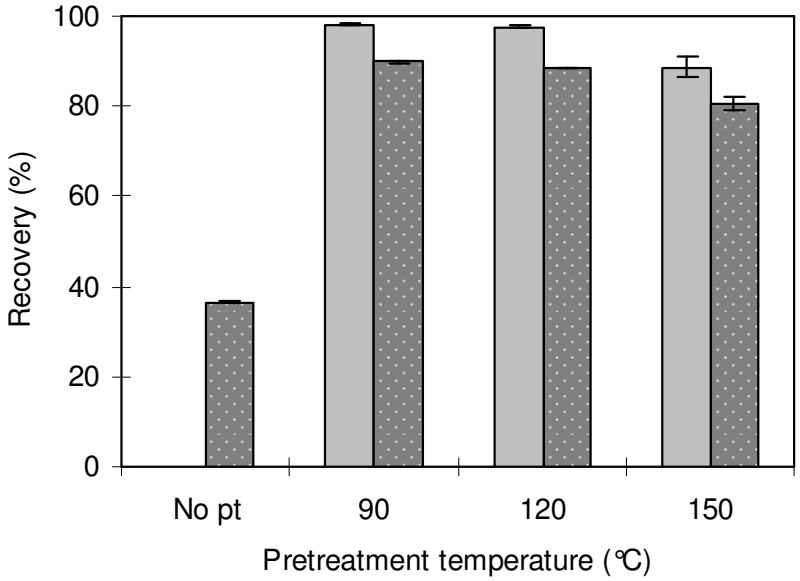

Figure 2 Effect of pretreatment temperature on Avicel mass recovery and glucose recovery after enzymatic hydrolysis. Gray bar: Weight of Avicel left after pretreatment, black with dot bar: Glucose recovery after enzymatic hydrolysis. Substrate concentrations for pretreatment and hydrolysis were 12.5 and 5% (w/w) respectively. Pretreatment time was 45 minutes. Hydrolysis time was 48 hours; two replications.

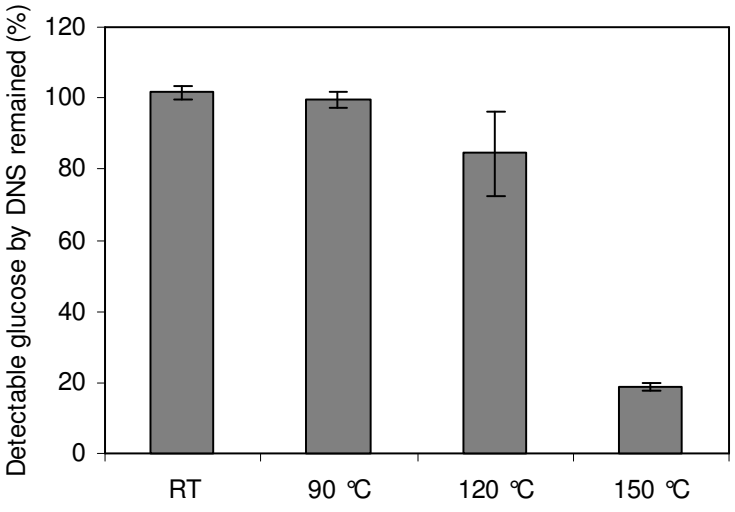

Figure 3 DNS assay detectable glucose after different IL pretreatment temperatures. Glucose powder was incubated in ILs with final concentration of 12.5% (w/w) for 45 minutes; two replications.

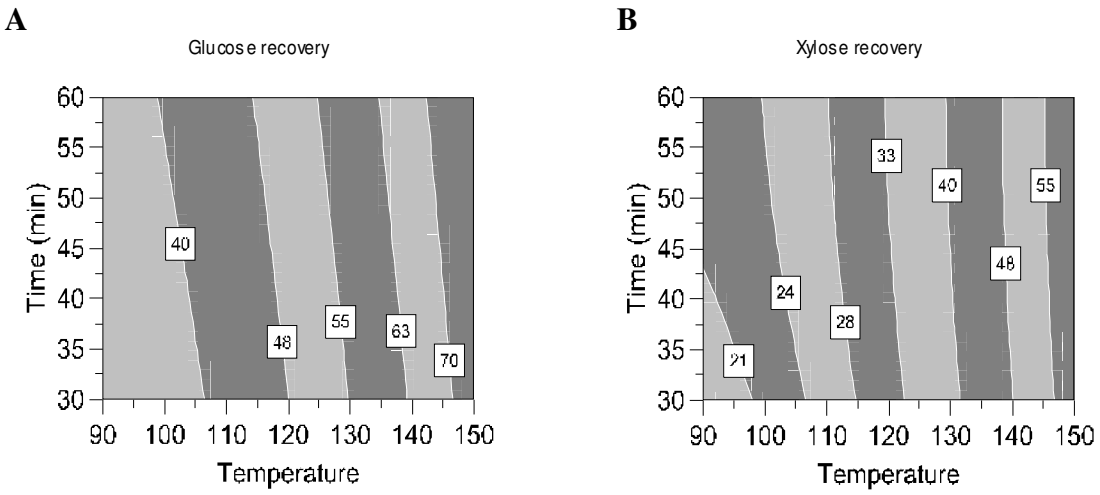

Figure 4 Effect of pretreatment temperature and time on sugar recovery after enzymatic hydrolysis of lignocellulose. (a) Glucose, (b) Xylose; simulated from data in table 2 by multiple linear regression. Substrate concentrations for pretreatment and hydrolysis were 12.5 and 5% (w/w) respectively. Both were derived from raw experimental data in Table 2.

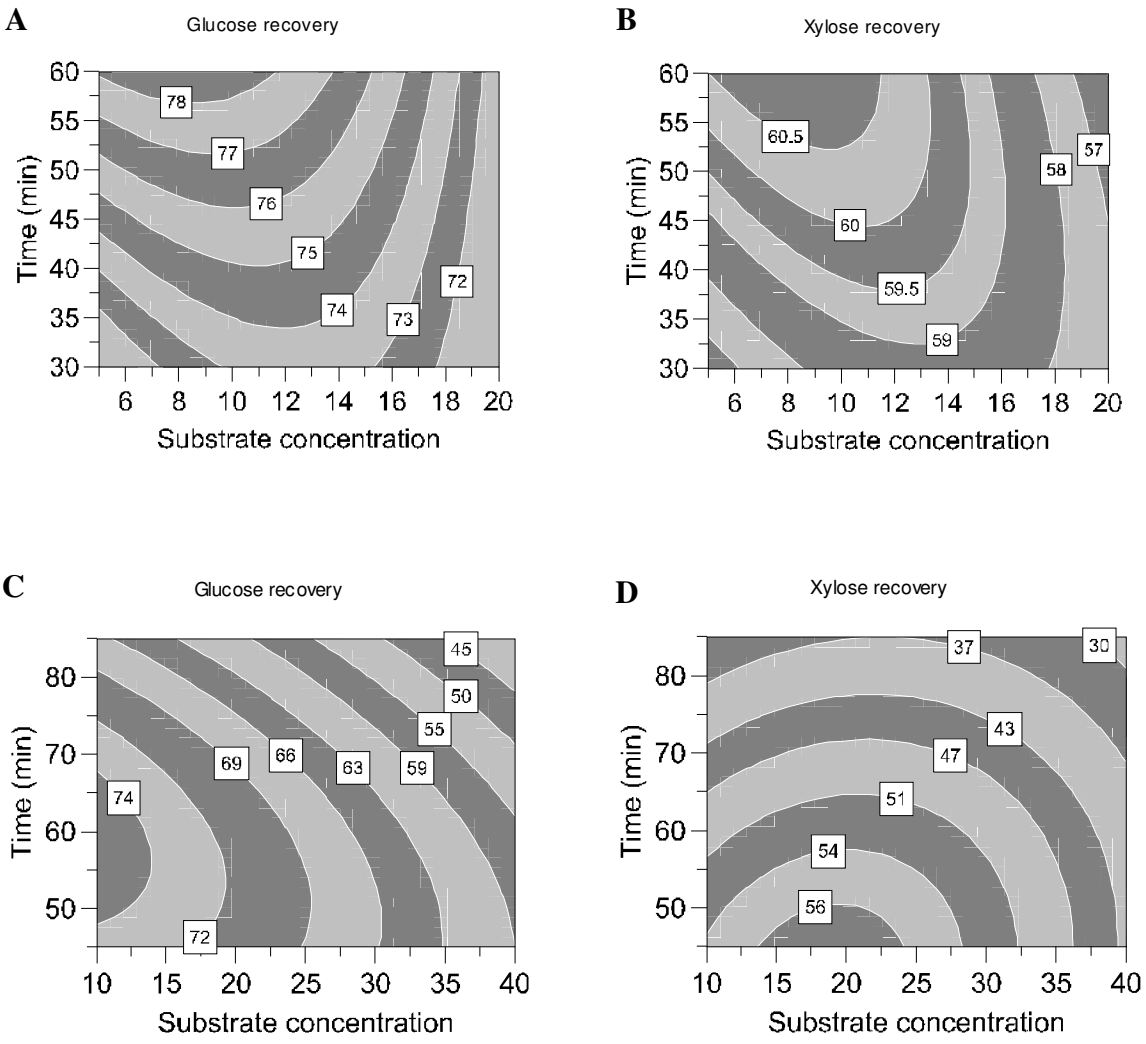

Figure 5 Effect of glucose and xylose recoveries after enzymatic hydrolysis of IL pretreated barley straw at 150°C with different time and substrate concentration. Simulated by multiple linear regression from data in table 2 and 3. (a) and (b) were derived from the raw experimental data in Table 2; (c) and (d) were from Table 3. Substrate concentration for hydrolysis was 5% (w/w).

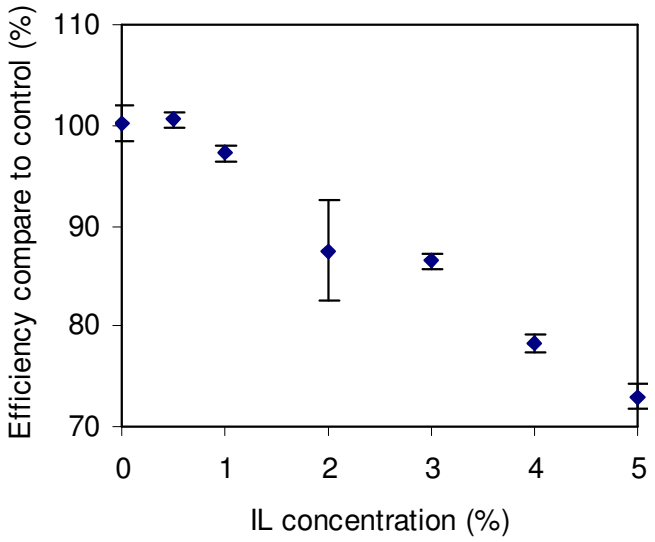

Figure 6 Influence of [EMIM]Ac on enzymatic hydrolysis efficiency. Different concentrations of ILs were added to the reactions hydrolyzing 5% (w/w) hot water-extracted pretreated barley straw; two replications.

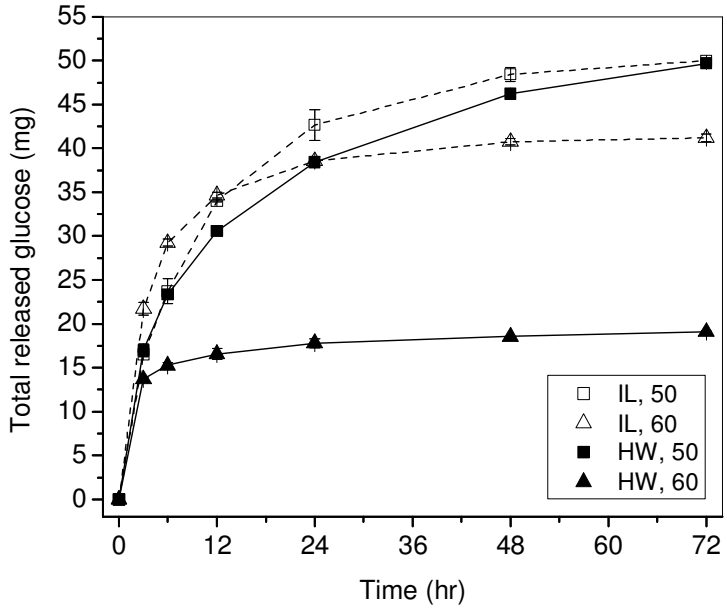

Figure 7 Time course enzymatic hydrolysis of ionic liquid (IL) and hot water-extracted (HW) pretreated barley straw under different temperature. Open square: IL at 50°C, open triangle: IL at 60°C, closed square: HW at 50°C, closed triangle: HW at 60°C; 120 mg substrate per reaction. Substrate concentration was 5% (w/w); shaking speed was 200 rpm; two replications.

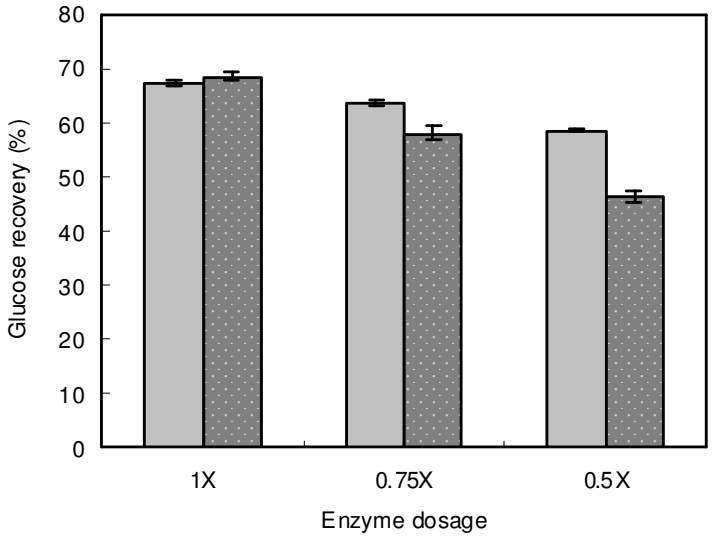

Figure 8 Enzymatic hydrolysis of IL (gray) and HW (black with dot) pretreated barley straw with different enzyme dosage. 1X: 5.1 FPU of Celluclast 1.5L and 45 CBU of Novozyme 188 per gram of pretreated substrate; three replications.

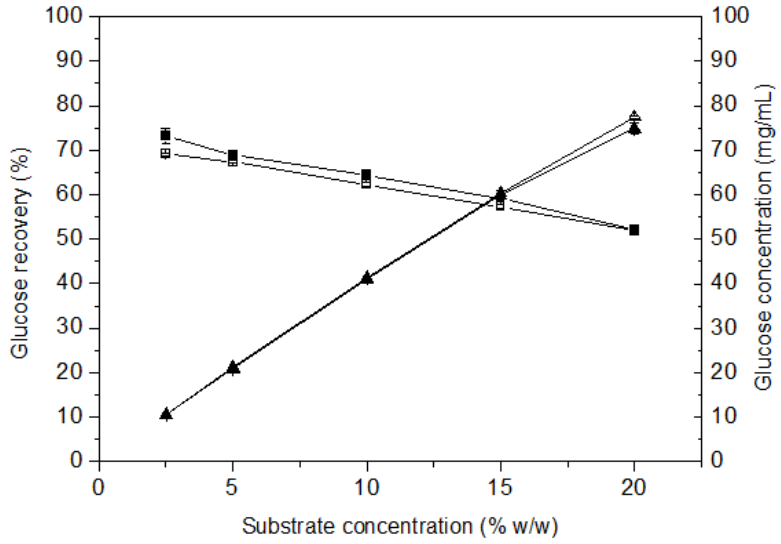

Figure 9 Effect of substrate (% w/w) concentration during enzymatic hydrolysis (50°C, 100 rpm) to glucose recovery and glucose concentration. Recovery was based on potential glucose in native substrate. Open and closed square: glucose recovery of IL and HW pretreatment; open and close triangle: glucose concentration of IL and HW pretreatment; three replications

Chapter 4

Enzymatic Cellulose Hydrolysis: Reusability and Visualization of Crosslinked β-Glucosidase Immobilized in Calcium Alginate

In bioethanol industry, the cost of enzyme is one of the bottlenecks. Recycle the enzyme through immobilization is an alternative way to reduce the cost.

4.1 Key point of this research

This study investigated the reusability of immobilized β-glucosidase (BG), which was crosslinked by glutaraldehyde followed by entrapment in calcium alginate. The reason to choose this method is economic consideration. The prices of some common used materials for immobilization are shown in table 4.1. Although some methods for immobilized BG had been reported, most research focused on basic analyses of enzymatic parameters (*eg.* K_m, K_i and V_{max}). Only few investigated the reusability of immobilized enzyme for hydrolysis of cellulose or lignocellulose. In addition, this is the first time that BG aggregation entrapped in calcium alginate was visualized by confocal laser scanning microscope (CLSM) to see the distribution of enzyme.

Table 4.1 Comparison of selected commercialized materials for enzyme immobilization.

Material	Price
1. Eupergit C	1818 DKK/25 g
2. CNBr/NHS -activated sepharose	5064 DKK/15 g (Activated CH-Sepharose® 4B) 4829 DKK/15 g (Epoxy-activated–Sepharose® 6B) 2060 DKK/10 g (Cyanogen bromide-activated-Sepharose® 4 Fast Flow)
3. Chitosan	874 DKK/250 g
4. Sodium alginate	455 DKK/250 g

* Price is from SIGMA-ALDRICH (April 2010)

4.2 Conclusion

The experimental procedures are shown in Figure 4.1. Glutaraldehyde treated BG forms aggregation and successfully entrapped in calcium alginate. Enzyme distributions were visualized by CLSM. The concentration of glutaraldehyde has significant effect on the overall performance of immobilization. Different combinations of BG and glutaraldehyde for crosslinking are listed in Table 4.2. Figure 4.2 shows that higher glutaraldehyde concentration inactivates more enzymes but also prevents the leakage of enzyme from calcium alginate. Total leakage of the enzyme was the sum of leakage form curing to the 3rd time of buffer change (Figure 4.3). In the optimized treatment (A), less than 40% of enzyme activity was lost due to crosslinking and leakage.

In order to get higher enzyme density in calcium alginate beads, the concentrations of enzyme and glutaraldehyde were increased at the same time (Table 4.3; results are shown in Figure 4.4). When we compare "A" (7.33 mg/L BG + 0.75% glutaraldehyde, in Figure 4.2) and "I" (22 mg/L BG + 3% glutaraldehyde, in figure 4.4), total loss activities due to crosslinking and leakage did not differ too much. This means the optimized crosslinking condition might depend more on the molar ratio of BG and glutaraldehyde rather than individual concentration respectively.

The immobilized BG could be recycled for cellulose hydrolysis up to 20 times without any significant loss of activity. Therefore the cost of BG in industrial processes can be reduced significantly for its high stability.

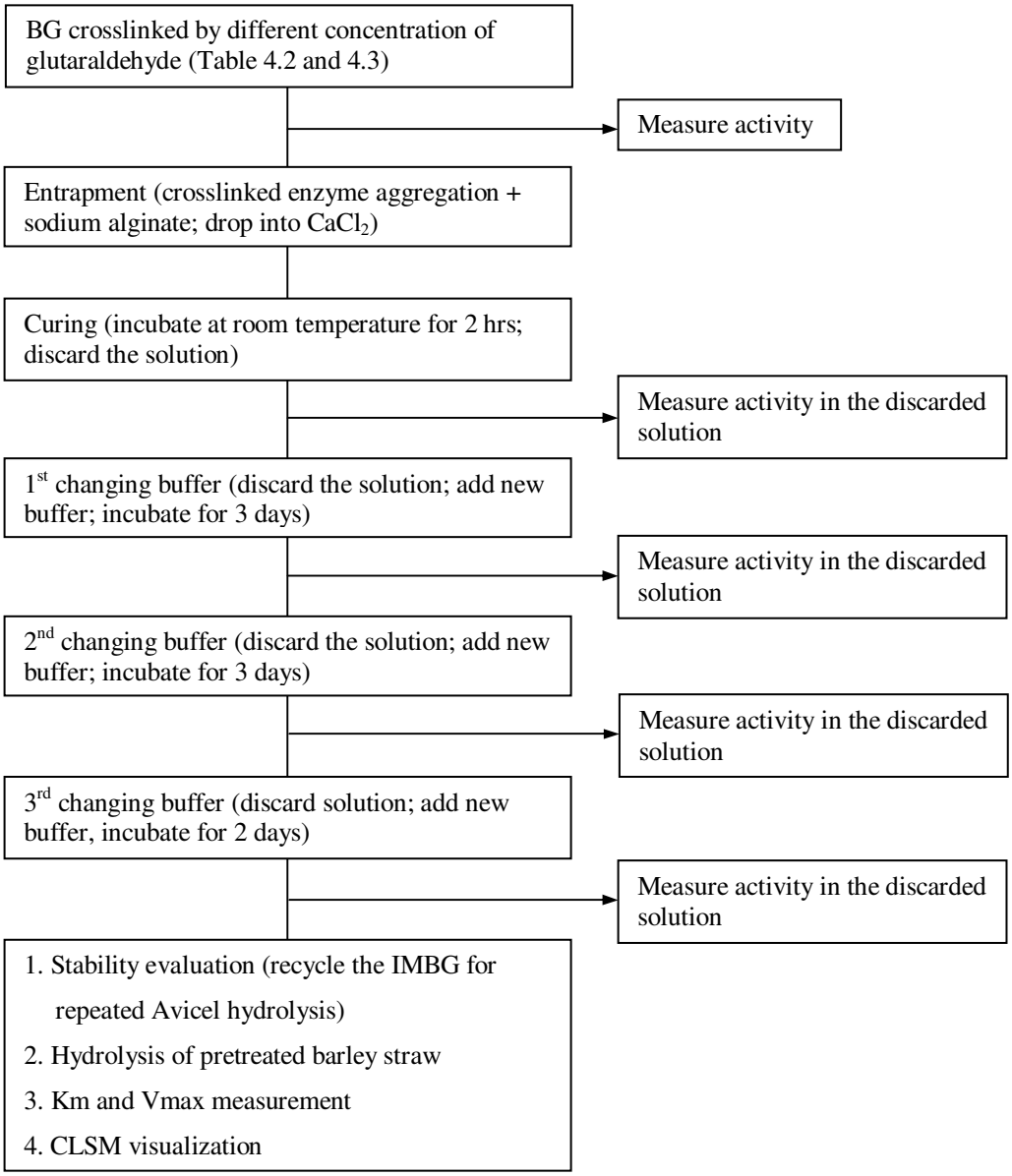

Figure 4.1 Experimental procedure of enzyme immobilization.

Table 4.2 Conditions of crosslinking at lower BG and glutaraldehyde concentration.

	BG (mg/mL)	BSA (mg/mL)	Glutaraldehyde (%)
A	7.33	0	0.75
B			0.5
C			0.25
D			0
E		3	0.75
F			0.5
G			0.25

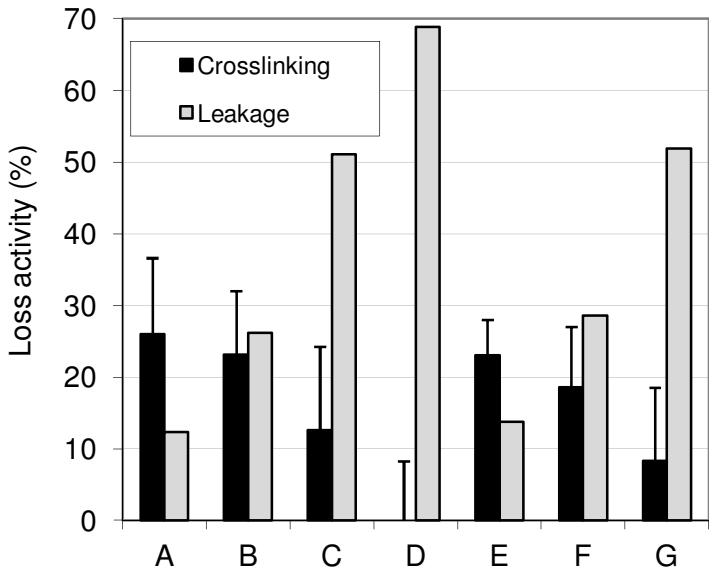

Figure 4.2 Loss BG activity due to crosslinking (3 replication) and leakage. (A~G refer to different crosslinking conditions shown in table 4.2)

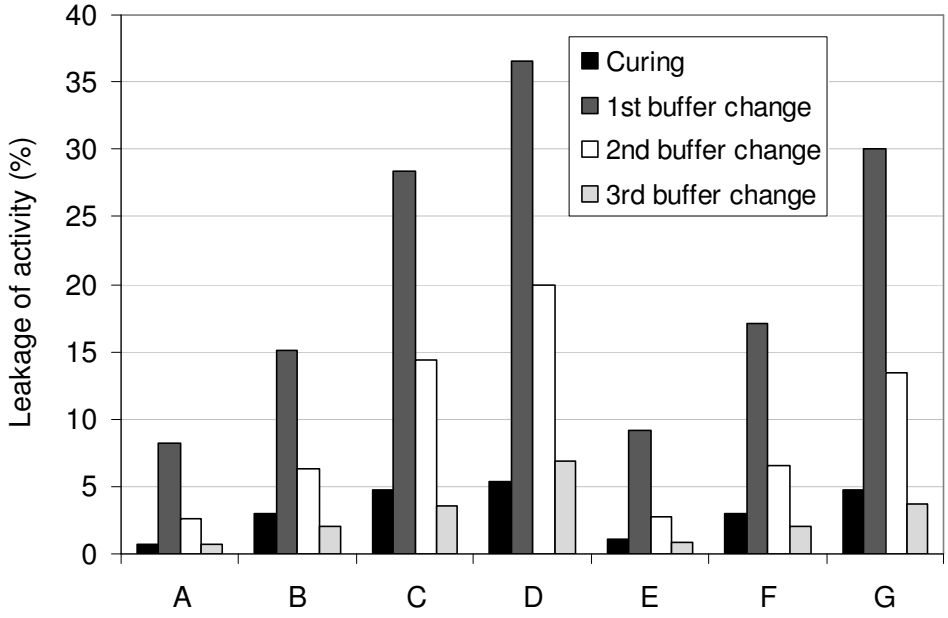

Figure 4.3 Leakage of BG from calcium alginate at different time intervals. (Curing and buffer change procedures see figure 4.1. A~G refer to different crosslinking conditions shown in table 4.2) The sum of four valuess in each sample is equal to the value (total leakage) shwon in Figure 4.2 as gray bars.

Table 4.3 Conditions of crosslinking at higher BG and glutaraldehyde concentration.

	BG (mg/mL)	Glutaraldehyde (%)
H	22	3
I		2.25

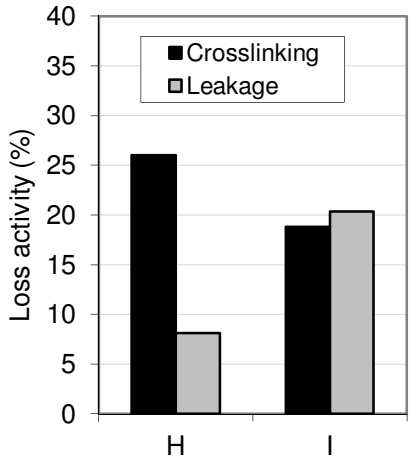

Figure 4.4 Loss BG activity due to crosslinking and leakage. (H and I refer to different glutaraldehyde treatment shown in Table 4.3)

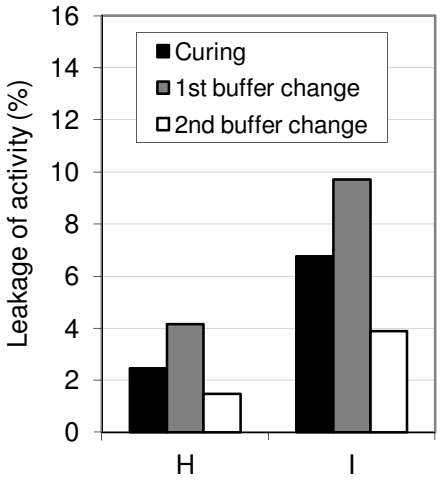

Figure 4.5 Leakage of BG from calcium alginate at different time intervals. (Curing and buffer change procedures see Figure 4.1. H and I refer to different crosslinking conditions shown in Table 4.3) The sum of four valuess in each sample is equal to the value (total leakage) shwon in Figure 4.4 as gray bars.

Enzymatic Cellulose Hydrolysis: Reusability and Visualization of Crosslinked β-Glucosidase Immobilized in Calcium Alginate

Chien Tai Tsai,[a] and Anne S. Meyer*[,a]

[a] Center for Bioprocess Engineering, Department of Chemical and Biochemical Engineering, Technical University of Denmark, DK-2800 Kgs. Lyngby, Denmark

* Corresponding author , telephone: +45-45252800; e-mail: am@kt.dtu.dk

ABSTRACT

One of the major bottlenecks in production of ethanol from lignocellulose is the required high cellulase enzyme dosages that increase the processing costs. One method to decrease the enzyme dosage is to re-use β-glucosidase (BG) and increase the biocatalytic productivity of this enzyme via immobilization. In this research, glutaraldehyde cross-linked β-glucosidase (BG) aggregates were entrapped in 3.75% calcium alginate. The effects associated with increasing glutaraldehyde concentration for the cross-linking were investigated and the data showed that > 60% of enzymatic activity could be recovered under optimized conditions, and that glutaraldehyde pretreatment decreased leakage of the enzyme activity from the calcium alginate particles. In order to evaluate the enzyme stability and re-usability, the immobilized BG in the calcium alginate particles were recycled for cellulase catalyzed hydrolysis of Avicel. No significant loss in activity was observed for up to 20 rounds of reaction recycle steps of the BG particles of 24 h each. Similar glucose yields were obtained following enzymatic hydrolysis of hot water pretreated barley straw by immobilized and free BG. Finally, the immobilized BG aggregates in the calcium alginate matrix were visualized by confocal laser scanning microscope (CLSM). The CLSM images, which we believe are the first to be published, proved that more BG aggregates were entrapped in the matrix when the enzymes were cross-linked by glutaraldehyde as opposed to not being cross-linked.

KEYWORDS: immobilization; β-glucosidase; alginate; bioethanol; confocal

Introduction

In order to produce bioethanol from lignocellulosic biomass, the 1,4-β-D-glycosidic linkages in cellulose must be hydrolyzed to release glucose for subsequent fermentation. The currently most studied classical cellulase production organism, *Hypocrea jecorina* (*Trichoderma reesei* (Rut C-30)), secretes three main groups of cellulose degrading enzyme activities for catalyzing this enzymatic hydrolysis process: 1. endo-1,4-β-D-glucanase (EG, EC 3.2.1.4), which catalyzes the random cleavage the internal β-1,4 bonds in the cellulosic polymers, 2. exo-1,4-β-D-glucanase or cellobiohydrolase (CBH, EC 3.2.1.91), which catalyzes the hydrolysis of the β-1,4 bonds by attacking the cellulose from the ends only, releasing mainly cellobiose; CBH1 (or Cel7A) attacks the reducing ends, whereas CBHII (or Cel6A) attacks the non-reducing ends of the cellulose polymers, and 3. β-glucosidase (BG, EC 3.2.1.21) which catalyzes the hydrolysis of cellobiose and other short cellulo-oligomers to liberate glucose [Vinzant et al., 2001]. Notably cellobiose, but to a certain extent also glucose, exert significant product inhibition on the enzymatic cellulose hydrolysis accomplished by these enzymes [Andrić, et al. 2010]. Improvements in the hydrolytic efficiencies of EG and CBH can thus be seen following removal of the strongly inhibitory cellobiose from the reaction [Andrić, et al. 2010; Lee, et al. 1983a]. While the *Trichoderma reesei* cellulase system does exhibit BG activity, the activity is not sufficiently high to hydrolyze the accumulated cellobiose, because a major part of the BG activity is bound to the fungal mycelium and hence not recovered during the industrial cellulase production process [Rosgaard et al., 2007]. Additional BG is therefore required to achieve sufficiently high glucose yields as well as for securing satisfactory efficiencies of EG and CBH. Overall, higher glucose yields may be attained through increased dosing of EG, CBH or BG, but addition of higher enzyme dosages of course results in higher enzyme costs. In addition to constantly improving the composition of the cellulase enzyme cocktail to improve cellulase productivity [Harris et al., 2010; Rosgaard et al. 2006], two general approaches can be used to overcome the problem of the high enzyme dosage requirements that increase the lignocellulose conversion costs: 1. Lowering of the enzyme production costs, and 2. Recycling of the enzymes for reuse; the latter e.g. by immobilization.

Hydrolysis reactions involving EG and CBH are heterogeneous in nature due to the water insoluble properties of the cellulose and the putative presence of cellulo-oligo-saccharides and the cellobiose product. Immobilization of these enzymes will therefore cause the enzyme catalysis to be mass transfer limited due to the slow diffusion of the substrate and products of these reactions, leaving this option futile. In contrast, the water soluble properties of cellobiose and the much faster mass transfer of this substrate and its hydrolysis products make BG a much better candidate for immobilization. In the last 30 years, different BG immobilization technologies have been intensively investigated and various support

materials have been tested, including concanavalin A-Sepharose, CNBr activated Sepharose [Woodward, et al. 1982], chitosan [Bissett, et al. 1978, Martino, et al. 1996], calcium alginate [Magalhães, et al. 1991, Busto, et al. 1995, Shen, et al. 2004], alginate-bone gelatin [Woodward, et al. 1991], polyacrylamide [Ortega, et al. 1998], soil humates [Busto, et al. 1997a], silica [Calsavara, et al. 2001] and Eupergit C [Tu, et al. 2006]). Among those, calcium alginate entrapment is a cheap and convenient method for enzyme immobilization. This methodology furthermore allows easy enzyme recycling by simple recovery of the calcium alginate beads (containing the immobilized enzyme) from the reaction slurry, e.g. by arranging that the beads are physically confined to allow repeated or contiuous use. However, leakage of enzyme from the matrix has been reported [Magalhães, et al. 1991, Woodward, et al. 1982, Tanaka, et al. 1984]. To overcome this problem, BG may be cross-linked with glutaraldehyde to form larger aggregates [Magalhães, et al. 1991, Woodward, et al. 1992] or immobilized onto other small particles like concanavalin A-Sepharose [Lee, et al. 1983b]. BG rich spores from *Aspergillus niger* ZU-07 have also been employed to prevent the leakage of BG from calcium alginate [Shen, et al. 2004].

Although enzyme immobilization technologies are already well developed, the application of immobilized BG (IMBG) in the bioethanol industry has not been widely evaluated. To date, most research has been restricted to fundamental analyses of enzymatic parameters and there is limited knowledge of extensive recycling of IMBG through prolonged hydrolysis cycles of cellulase catalyzed degradation of cellulose or authentic pretreated lignocellulose. Moreover, the distribution of the entrapped BG in the calcium alginate polymer network of the immobilization material has to our knowledge not been visualized. The objective of the present work was to evaluate the recyclability of BG immobilized in calcium alginate particles with the purpose of assessing the options for improving enzyme productivity during enzymatic cellulose hydrolysis. A sub-purpose was to examine the significance of the cross-linking with glutaraldehyde (GA) for the immobilization efficiency, notably with respect to avoiding leakage of enzyme activity from calcium alginate beads. Hence, in this research, BG was cross-linked with glutaraldehyde (GA) to yield aggregates which were then entrapped in 3.75% calcium alginate. The residual activity and recyclability of the immobilized BG were investigated. Enzyme aggregation and distribution within the alginate matrix were also observed by confocal laser scanning microscope (CLSM).

Materials and Methods

Chemicals and enzymes

Sodium alginate, glutaraldehyde, Avicel PH-101 cellulose, sodium acetate, sodium azide, adenosine 5′-triphosphate disodium salt, β-Nicotinamide adenine dinucleotide phosphate sodium salt hydrate, EPPS and Dimethylsulfoxide (DMSO) were purchased from Sigma – Aldrich (St. Louis, MO, USA). The two

enzyme preparations, Celluclast 1.5L and Novozyme 188, were from Novozymes A/S (Bagsværd, Denmark). Celluclast 1.5L derived from *Trichoderma reesei*, mainly composed of EG and CBH (Rosgaard et al., 2006), had an activity of 65 FPU/mL (FPU = filter paper unit) and 10 CBU/mL (CBU = cellobiose units). The FPU activity was determined by the NREL standardized filter paper assay. The CBU activity was determined by measuring glucose production on cellobiose at 50°C, pH 4.8 [Ghose 1987, Sternberg, et al. 1977]. Novozyme 188, harbouring BG derived from *Aspergillus niger*, had an activity of 856 CBU/mL. The hexokinase (420 U/ml) + glucose-6-phosphate dehydrogenase (G6P-DH) (210 U/ml) used for glucose analysis was purchased from Megazyme (Wicklow, Ireland). Fluorescein-5-EX succinimidyl ester was from Invitrogen (Carlsbad, California, USA). The bicinchoninic acid (BCA) Protein Assay Kit was from Thermo Scientific Life Science (Rockford, IL, USA).

Immobilization of β-glucosidase

Novozyme 188 was the source of the BG employed in this study. Prior to immobilization, the crude enzyme was centrifuged at 5,000 g for 10 min and the precipitate was discarded. Protein concentration in the supernatant was determined by the Quick Start Bradford Protein Assay (Bio-Rad, Hercules, CA, USA) to be 88 mg/mL (γ-globulin as reference). The enzyme was cross-linked using different concentrations of glutaraldehyde with/without bovine serum albumin (BSA) according to Table 1, and then incubated with shaking at 100 rpm at 25°C for 4 hr. For the crosslinking procedure, enzyme and glutaraldehyde were diluted by 200 mM EPPS, pH 10.5 (this buffer was used in order to make the final solution around neutral because Novozym 188 is acid). Next, a solution of 5% (w/w) sodium alginate in 5 mM sodium acetate, pH 4.8 with 0.02% sodium azide was prepared. The sodium alginate was then mixed with the cross-linked enzyme to yield a final alginate and enzyme concentrations of 3.75% and 1.46 mg protein/mL, respectively. Following incubation at 4°C overnight, the alginate-enzyme gel was dropped into a 200 mM $CaCl_2$ solution in 5 mM, pH 4.8 sodium acetate buffer with stirring (the diameter of the aperture of the syringe tip was 3 mm). The beads were stirred for another 2 hrs at room temperature to improve toughness (curing) and then stored at 4°C in 50 mM sodium acetate, pH 4.8 with 20 mM $CaCl_2$ solution.

Analysis of residual activity

The residual activities after glutaraldehyde treatment and following additional losses due to enzyme leakage during curing and incubation steps were assayed according to a standard cellobiase assat procedure [Ghose 1987, Sternberg, et al. 1977]. In order to measure enzyme leakage, discarded solutions were collected and assayed after curing for 2 hrs and following subsequent buffer exchanges (repeated 3 times, using 50 mM sodium acetate buffer, pH 4.8 with 20 mM $CaCl_2$ and incubated at 4°C). The enzyme

activities in the discarded buffer solutions were assayed immediately after collection. Residual enzyme activities in the calcium alginate were calculated as shown in equation 1:

(Residual activity) = (Original activity) – (Lost activity due to cross-linking) – (Leakage) (1)

Measurement of Km and Vmax of BG

For free BG (FRBG), 7000X diluted enzyme was reacted with 0.9, 2.25, 4.5, 9, 13.5, 18 and 22.5 mM of cellobiose and incubated at 50°C with shaking at 650 rpm in a thermomixer for 8 minutes. For IMBG, the beads were mixed with different concentrations of cellobiose in a ratio of 1:9 (v/v, IMBG bead vs. substrate solution) and incubated at 50°C with shaking at 100 rpm in water bath for 15 minutes. All reactions were stopped by heating at 100°C for 5 minutes. The K_m and V_{max} values were derived from the Hanes-Woolf plot.

Repeated hydrolysis for evaluating the stability of the recycled enzyme

Using Avicel as the cellulose substrate (10%, w/v), hydrolysis reactions were carried out in 50 mM sodium acetate buffer solutions, pH 4.8 containing 0.02% sodium azide and 20 mM calcium chloride. The total volume was 25 mL. Dosage of Celluclast 1.5L was 16 FPU/g-substrate while the dosage of BG was 13 CBU/g-substrate for FRBG or the same bead weight of IMBGs prepared under different conditions (i.e. corresponding to the original 13 CBU/g-substrate). The negative control contained Celluclast 1.5L only (i.e. with no added BG). Reaction flasks were incubated in a 50°C water bath with shaking. To facilitate recycling and washing of the beads, the beads were maintained in a small cylinder cell, both sides were covered by nets with mesh size of 2 mm for substrate diffusion (Fig. 1).

Samples withdrawn from reactions were deactivated via heating at 100°C for 5 minutes. After cooling to room temperature, samples were centrifuged at 16,000 g for 2 minutes and the supernatant was subject to glucose analysis. Concentrations of liberated glucose were determined by the hexokinase + G6P-DH assay. Glucose yields ($Y_{glucose}$) were calculated as detailed in equation 2; W indicates weight. (hydrated glucose)

$$Y_{glucose}(\%) = \frac{W_{glucose}(g)}{W_{potential\ \ glucose}(g)} \times 100\% \qquad (2)$$

Hot water pre-treatment of barley straw

Barley straw was grown and harvested in 2006 on the island of Funen, Denmark. Thereafter, a sample was transported to DONG Energy (Danish Oil and Natural Gas Energy, Denmark) for pre-treatment. The pre-treatment method consisted of a three-stage process, which involved heat treating the straw three times at progressively higher temperatures (60°C, 15 minutes; liquids removed; 180°C, 10 minutes; 195°C, 3

minutes). After pre-treatment, the liquids were removed. Standard procedures for acid hydrolysis and compositional calculation analysis were carried out according to the U.S. National Renewable Energy Laboratory [Sluiter, et al. 2006].

Enzymatic hydrolysis of hot water pre-treated barley straw

Pre-treated barley straw was cut to allow its passage through a sieve with an aperture of 2 mm (Endecotts, London, England). Hydrolysis reactions of the barley straw were carried out in the same buffer as described previously for cellulose (Avicel) hydrolysis. The substrate concentration was 5% (w/v) and the enzyme dose was made up of 8 FPU/g-substrate Celluclast 1.5L as well as 13 or 26 CBU/g-substrate BG. Flasks were incubated in a 50°C water bath with shaking. Samples were removed from reactions at different time intervals for subsequent glucose analysis. Glucose yields were also calculated according to equation 2.

Visualization of enzyme distribution in calcium alginate by confocal laser scanning microscope

Fluorescein-5-EX, succinimidyl ester was dissolved in DMSO to 10 mg/mL according to manufacturer's instruction. Small, thin pieces of IMBG were placed in 100 mM EPPS with 20 mM $CaCl_2$, pH 8. Fluorescein was then added to the mixture, and the samples were incubated for 1.5 hrs at 25°C. At the end of this interval, un-conjugated fluorescein was removed from the IMBG samples through repeated washings (5 times) using sodium acetate buffer. Microscopic observations and image acquisitions were performed on an LSM 510 confocal laser scanning microscope (CLSM) (Carl Zeiss, Jena, Germany) equipped with detectors and filter sets for monitoring fluorescence (500~550 nm). Images were obtained using a 63X/0.95W objective. Images were processed using Imaris software (Bitplane AG, Zürich, Switzerland).

Results and Discussion

The effects of immobilization conditions on residual activity

Prior to calcium alginate entrapment, the enzyme BG was cross-linked using different concentrations of glutaraldehyde with/without BSA. The purpose of cross-linking was to aggregate the BG into larger particles, thereby hindering their diffusion from the calcium alginate matrix. However, in practice it seems that glutaraldehyde also blocked the active sites of the enzyme, resulting in reduced enzymatic activities. Fig. 2 shows the loss activities of BG after different cross-linking conditions. Overall, increased incorporation of glutaraldehyde during the cross-linking step resulted in greater inactivation of BG. In contrast, the addition of BSA during cross-linking with glutaraldehyde improved residual activities. One

explanation might be that BSA provided some amine groups for cross-linking, thus reducing the probability that BG active sites would be blocked by glutaraldehyde. Nonetheless, when the BSA concentration was doubled (6 mg/mL) and glutaraldehyde concentration was 1%, the residual activity was lower than that obtained without BSA (data not shown). One reason for this could be that the aggregates were simply too large, with some BGs embedded in BSA clusters resulting in decreased accessibility of the substrates and the enzyme.

After cross-linking, BG enzymes were entrapped within calcium alginate. In most previous literature, the concentration of calcium alginate employed was reportedly between 2~3%. However, in order to reduce leakage of the enzyme and mechanical strength of the beads, a concentration of 3.75% was used in this study. At this concentration, the viscosity of the system was high and the resulting beads appeared circular (4~5 mm in diameter) with short tails. When the concentration was increased to 4% calcium alginate, the viscosity was so high that the tails were too long; as such, concentrations higher than 3.75% were not used in this research. Overall, it was apparent that increasing the concentration of glutaraldehyde served to inactivate BG to a greater extent. Still, lower quantities of the enzyme diffused out of the beads due to improved entrapment of the enzyme aggregates by the matrix (Fig. 2). Optimal conditions, whereby the enzyme was cross-linked with 0.75% glutaraldehyde and then entrapped in 3.75% calcium alginate (sample A, Table 1) yielded more than 60% residual activity.

Km and Vmax of BG

From the Hanes-Woolf plot (Fig. 3), the Km of FRBG and IMBG were 1.69 and 17.62 mM, respectively (Table 2). The latter was much larger than the former. In contrast, the Vmax of FRBG was larger than that of IMBG. This was due to diffusion limitations resulting from the matrix and is consistent with previous literature [Magalhães, et al. 1991]. Due to an upturn in the FRBG data depicted on the Hanes-Woolf plot (Fig. 3), estimations of Km and Vmax were based on extrapolations using substrate concentrations between 0 and 10 mM. The upturn was attributed to substrate inhibition. However, this tendency was not observed in IMBG because the diffusion effect increased not only the Km, but also the threshold for substrate inhibition. This was consistent with that reported by Lee and Woodward (1983) [Lee, et al. 1983b]. Conversely, Magalhães reported that no decrease in the reaction rate was observed for either FRBG or IMBG at a 50 mM cellobiose concentration. The discrepancies among different researchers need further investigation.

Repeated hydrolysis and stability of the recycled enzyme

The standard method for monitoring enzyme stability is to incubate the enzyme in buffer at a defined temperature, followed by measuring of the activity at different time intervals. In doing so, one can

calculate the half-life of the enzyme from the decay curves. However, these environments are usually different from real industrial processes. For example, the presence of substrate may serve to protect the enzyme. In addition, the mechanical forces imposed on the enzyme may differ due to agitation or shaking. Moreover, lignocellulose hydrolysis is a heterogeneous reaction, which means that collision and friction between substrate and enzyme must also be considered. In order to evaluate enzyme stability under hydrolytic reaction conditions, the IMBG was recycled repeatedly following hydrolysis of 10% Avicel at 50°C with vigorous shaking.

Fig. 4 compares time course curves depicting the hydrolysis kinetics of IMBG, obtained from BG cross-linked with different concentrations of glutaraldehyde, as well as FRBG (positive control, 13 CBU/g-substrate) and a sample containing no BG (negative control). Glucose was released from the negative control, which is consistent with previous work [Tu, et al. 2006]. This occurrence may be explained by two reasons: Firstly, Celluclast 1.5L still contains small amounts of BG, which is why 10 CBU could still be measured in each millilitre of enzyme. The second reason is that CBH can also cleave oligosaccharides into smaller molecules, including glucose [Nidetzky, et al. 1994, Schmid, et al. 1990, Schülein 1997]. Each hydrolysis reaction contained 2.46 CBU/g-substrate due to Celluclast 1.5L, which was calculated as follows:

The enzyme activity of Celluclast 1.5L is 65 FPU/mL and 10 CBU/mL respectively, and the dosage in the reaction was 16 FPU/g-substrate. The volume of Celluclast 1.5L added was:

$$16\ (\text{FPU/g-substrate}) / 65\ (\text{FPU/mL}) = 0.246\ (\text{mL/g-substrate})$$

The dosage of CBU in the reaction contributed from Celluclast 1.5L was:

$$0.246\ (\text{mL/g-substrate}) \times 10\ (\text{CBU/mL}) = 2.46\ \text{CBU/g-substrate}$$

When we consider the two factors detailed above, the appearance of glucose in the negative control can therefore be explained.

The quantity of IMBG employed in each reaction corresponded to 2.25 g of immobilized beads. In the event that no BG was inactivated during cross-linking or lost due to leakage after entrapment, the dosage should have corresponded to 13 CBU/g-substrate. However, some activity was lost during the immobilization process. As such, the active IMBG remaining in each system was less than 13 CBU/g-substrate (e.g. the dosage of active IMBG in sample A was around $13 \times 0.62 = 8$ CBU/g-substrate). Prior to use in hydrolysis reactions, the beads were incubated in buffer for 8 days and changed buffer three times to remove non-entrapped, which might interfere in subsequent experiments. This means that the glucose released during the reaction (Fig. 4 and 5) was a hydrolysis product of the entrapped BG. Using increasing glutaraldehyde concentrations during cross-linking resulted in increased reaction efficiencies

within the range investigated. This also supports results (Fig. 2) showing that more BG was retained in the matrix when cross-linking efficiency was higher. It should be noted that some BG could still be entrapped within the beads even without glutaraldehyde treatment, since more glucose was released from the non-glutaraldehyde treated BG samples (Fig. 4, sample D) compared with the negative control. This is because there were already small amounts of BG aggregates existing in Novozyme 188 before glutaraldehyde treatment (further evidence confirming this will be discussed later in the CLSM section). All IMBG samples prepared using different levels of glutaraldehyde were very stable when recycled up to 8 times, suggesting that BG was stabilized for as long as BG aggregates could be entrapped in the matrix. It was reported that entrapped uncross-linked BG had a higher thermo stability than FRBG [Busto, et al. 1997b]. Glutaraldehyde treated BG also had higher thermo stability than FRBG [Woodward, et al. 1992, Baker, et al. 1988]. Moreover, BG was also more resistant to higher temperatures when immobilized onto chitosan [Bissett, et al. 1978]. These examples reveal that BG was stabilized by molecular interactions, widely accepted as the mechanism of stabilization for these immobilized enzymes.

IMBG prepared through cross-linking with 0.75% glutaraldehyde (i.e. sample A only) was evaluated after >8 rounds of recycling. Specifically, hydrolysis efficiencies following each reuse, given after 9, 24 and 48 hr reaction periods, were shown in Fig. 5. Comparison of these three time points allows for a more accurate assessment of enzyme performance. In most enzymatic hydrolysis reactions, reaction rates slow down significantly after 12 hrs due to the depletion of substrate and accumulation of product. As 48 hrs corresponds to most industrial processing times (48~72 hrs), the hydrolytic efficiency at this late stage can reflect the overall performance. Glucose yields from beginning and middle stages of the reaction can reveal the initial reaction rate and how the rate slows down as the reaction proceeds. It shows that there was no significant decrease in efficiency until the 20 th round. From the 9th round, a hydrolysis reaction containing only 6.5 CBU/g-substrate of FRBG was used as a“1/2 positive control”, which is a base line representing/mimicking if half of “positive control” FRBG were inactivated. It is easier to evaluate the performance of IMBG when we have more base line for reference. After 9 hrs, the reaction rate of the 1/2 positive control appeared faster than the IMBG due to internal diffusion limitations. In contrast, glucose yields of the IMBG were higher after 24 to 48 hrs. This means that the apparent dosage of IMBG was still higher than 6.5 CBU/g-substrate, and it confirmed the high stability of IMBG.

Enzymatic hydrolysis of hot water pre-treated barley straw

To evaluate the performance of hydrolysis of lignocellulose, the IMBG was used for hydrolyzing pretreated barley straw (Fig. 6). According to compositional analysis, the potential glucose content in the pre-treated barley straw is 66% (w/w). The dosage of Celluclast 1.5L employed in this hydrolysis reaction was 8 FPU/g-substrate. The initial reaction rate using FRBG was faster than IMBG, and can be explained

by a significant difference in Km values resulting from the diffusional limitations of the IMBG matrix. However, the final yields of glucose obtained from FRBG and IMBG reaction systems were similar. This proves that it is possible for IMBG to be used in real industrial processes. Yet in this study, it was difficult to perform the reaction when substrate concentration was higher than 10% (w/v) since the state of the reaction was almost solid and viscous. For a diffusion limited IMBG reaction system, it is a problem. Further investigations are needed to overcome this dilemma.

Confocal laser scanning microscope observation

Entrapment of BG without cross-linking in calcium alginate was investigated by Ortega [Ortega, et al. 1998], Magalhaes [Magalhães, et al. 1991] and in this research. While large amounts of enzyme diffused out of the matrix, 10 to 60% of active BG (depending on preparation conditions during the study) was still retained in the beads. An exact description of inside the matrix has not been presented before. In this research, IMBG was stained by fluorescein and observed under CLSM. Fig. 7(b) and 7(e) show that even without glutaraldehyde treatment, there were still some BG aggregates in the IMBG matrix. This explains why stable BG activity was found in the IMBG beads without any glutaraldehyde treatment, as shown in Fig. 4 and in previous reports. As the mechanism for protein aggregation is complicated and the exact composition of Novozyme 188 is not known, an explanation is beyond the scope of this research. IMBG treated with 0.75% glutaraldehyde showed a very strong signal due to the presence of aggregates (Fig. 7(c) and 7(f)), with most aggregates measuring >1 μm. This is consistent with the finding that BG leakage decreased due to the entrapment of cross-linked aggregates within the matrix.

Conclusions

In this paper, glutaraldehyde treated BG aggregates were entrapped in 3.75% calcium alginate. Overall, 60% of BG residual activity could be recovered. The immobilized BG enzyme could be recycled in a hydrolysis reaction up to 20 times without any significant loss of activity. The performance of IMBG on lignocellulose hydrolysis was comparable to FRBG. More than 50% of the glucose was released from hot water pre-treated barley straw. BG aggregates in the matrix were visualized by CLSM. The images showed that more BG aggregates were entrapped in the matrix following cross-linking by glutaraldehyde. In conclusion, the cost of BG in industrial processes can be reduced significantly because of its high stability. However, application of BGs in the bioethanol industry, particularly for hydrolysis reactions at higher substrate concentrations, still needs to be investigated and improved in the future.

Abbreviation: BG (β-glucosidase), IMBG (immobilized β-glucosidase), FRBG (free β-glucosidase), CLSM (Confocal laser scanning microscope), GA (glutaraldehyde), BSA (bovine serum albumin)

Table 1

Cross-linking conditions

	BG (mg/mL)	BSA (mg/mL)	Glutaraldehyde (%)
A	7.33	0	0.75
B			0.5
C			0.25
D			0
E		3	0.75
F			0.5
G			0.25

Table 2

Km and Vmax of BG

	Km (mM)	Vmax (umol/(min*mg BG))
FRBG	1.70 ± 0.12	12.71 ± 0.26
IMBG	17.62 ± 0.11	5.39 ± 0.06

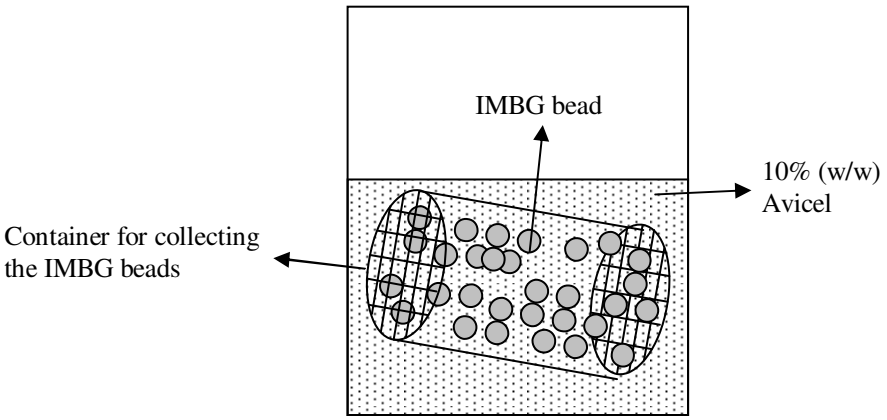

Fig. 1. Hydrolysis of Avicel by IMBG. For the ease of recycling and washing the beads, the beads were contained in a small cylinder cell and immersed in substrate. Avicel suspension was able to mix with IMBG through the meshed at both sides.

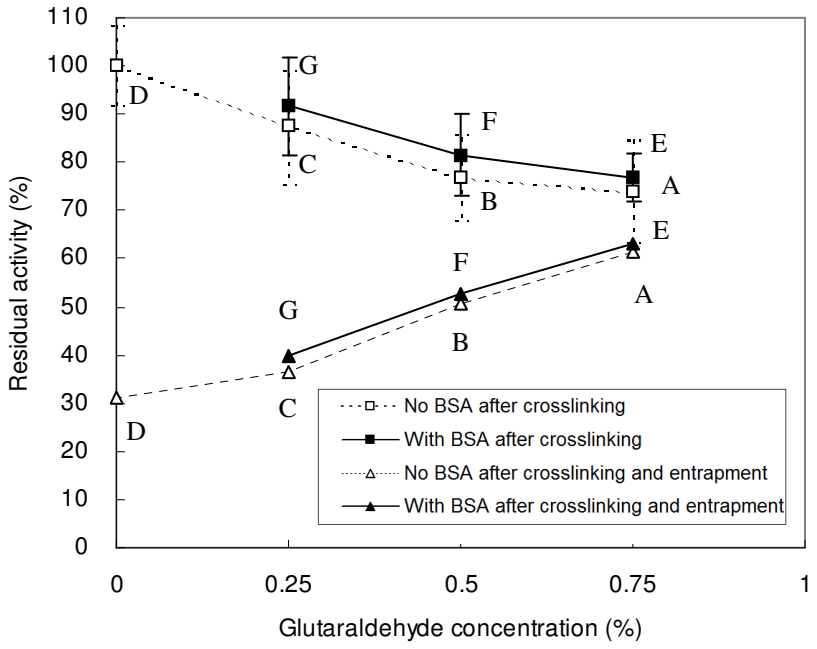

Fig. 2. Residual activity of BG after crosslinking (3 replications) and full immobilization process (crosslinking + entrapment).

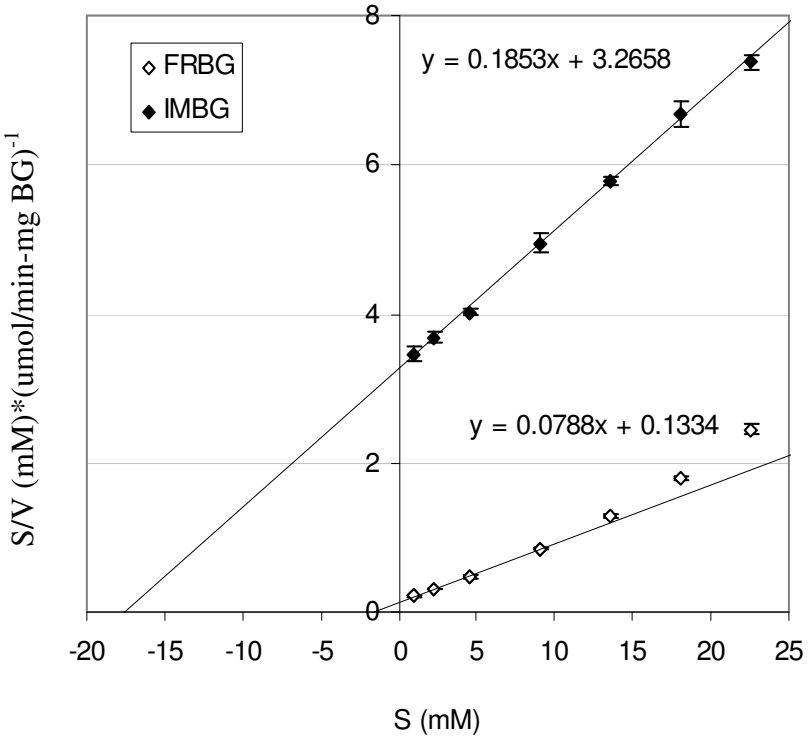

Fig. 3. Hanes-Woolf plot of free and immobilized BG. The straight line for free BG was fitted to the substrate concentrations between 0 and 9 mM.

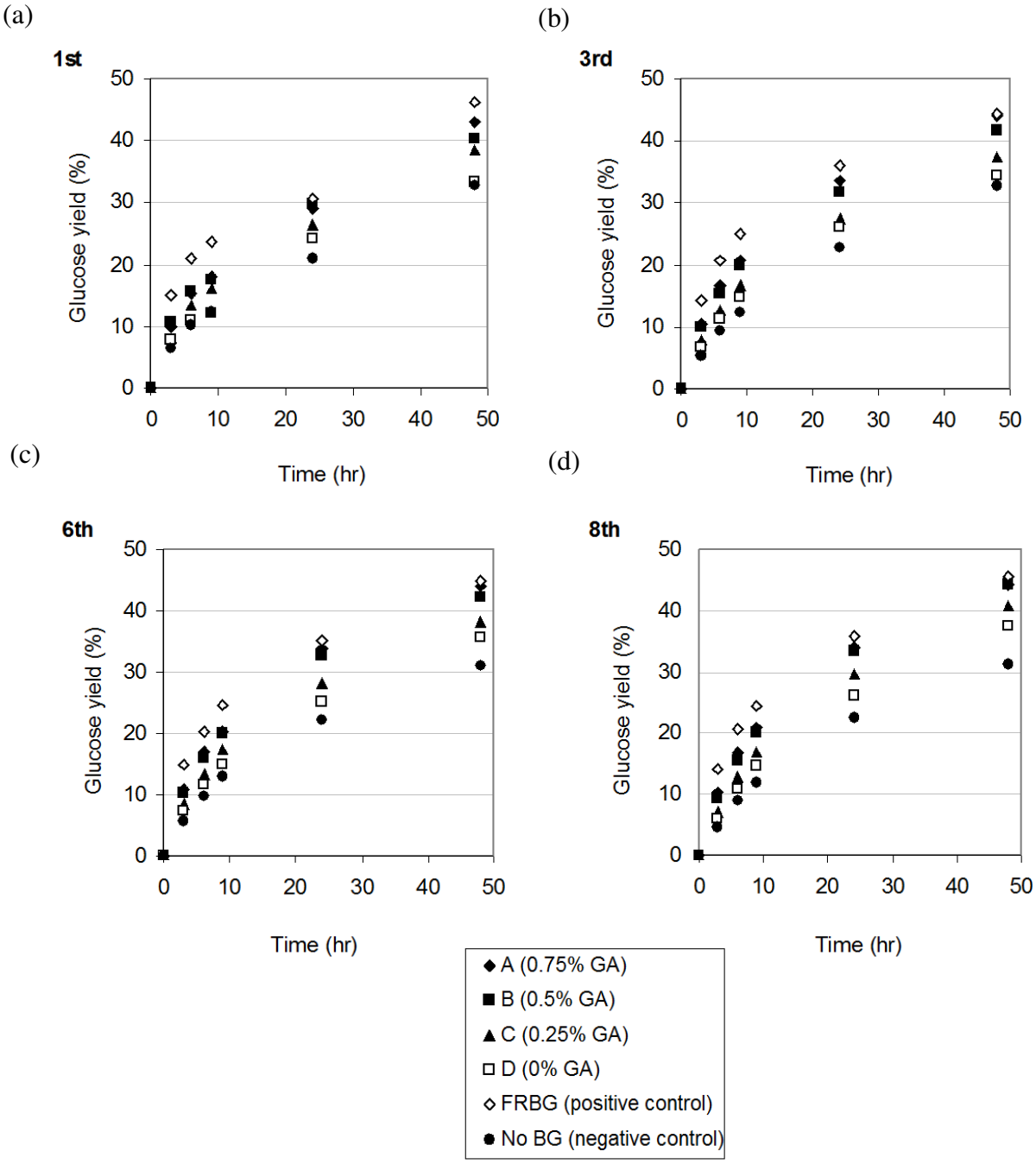

Fig. 4. Time course kinetics of free and immobilized BG under repeated hydrolysis reaction. (a), (b), (c) and (d) are 1st, 3rd, 6th and 8th rounds respectively. A, B, C and D are IMBG prepared by different cross-linking conditions referring to Table 1 (Data of samples that were cross-linked with additional BSA were not shown). FRBG and No BG are positive and negative controls respectively.

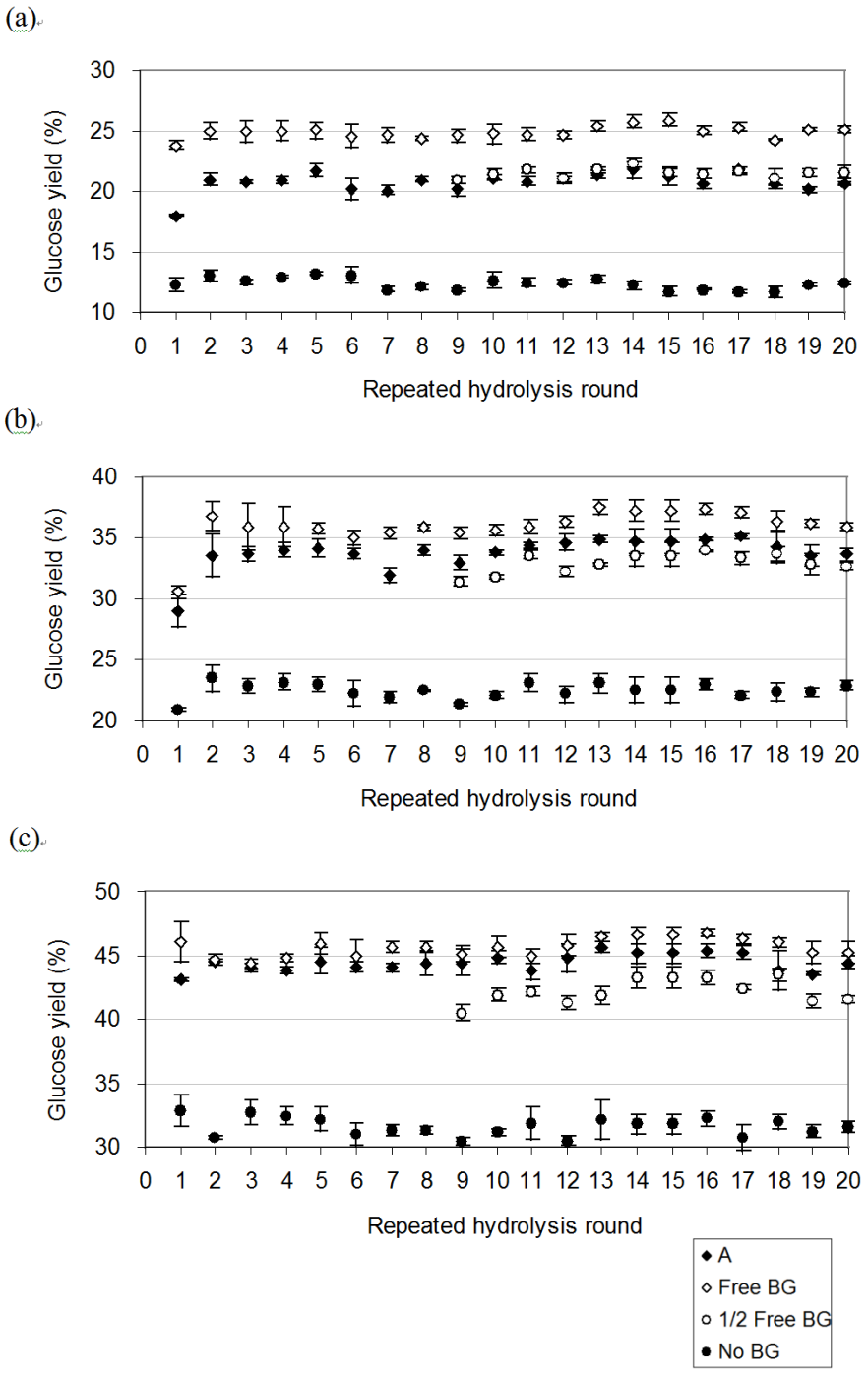

Fig. 5. Stability of immobilized BG under repeated hydrolysis reaction. (a), (b) and (c) are glucose yields at 9, 24 and 48 hr. 'A' is IMBG prepared under condition referring to Table 1.

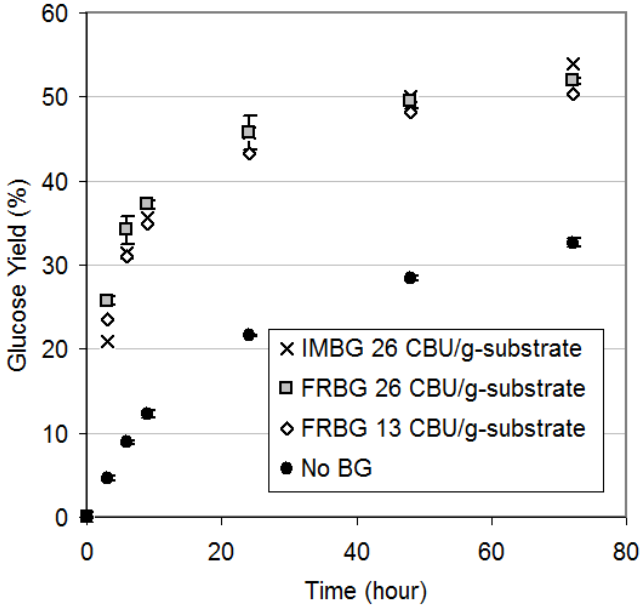

Fig. 6. Time course enzymatic hydrolysis of hot water pretreated barley straw in the presence of free or immobilized BG with different dosage.

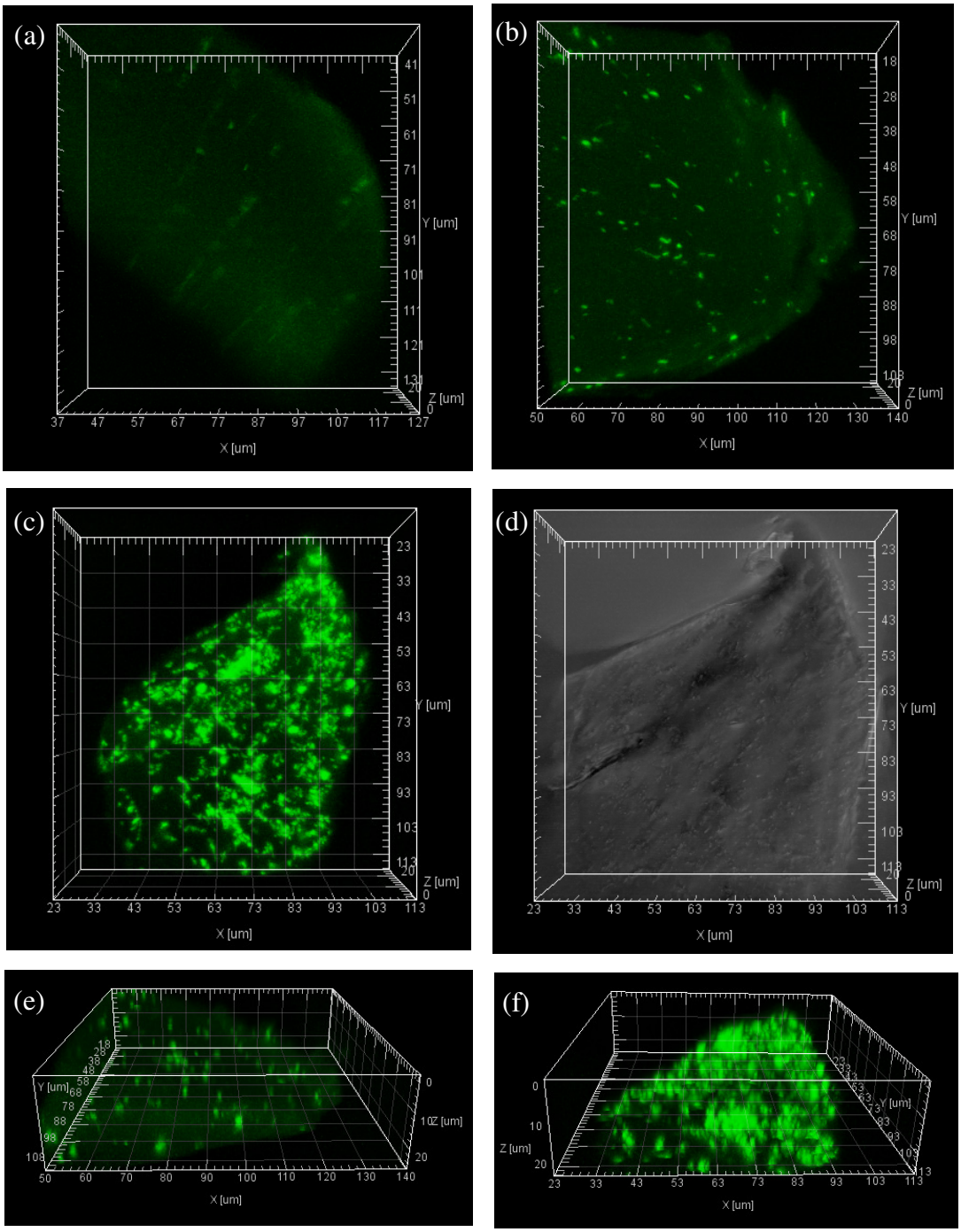

Fig. 7. CLSM Image of BG distribution in calcium alginate. (a) Calcium alginate only, which shows very weak background from the nonspecific binding of fluorescein. (b) and (e) IMBG without glutaraldehyde treatment. (c) and (f) IMBG with 0.75% glutaraldehyde treatment. (d) Image of (c) but without fluorescence.

References

[1] Andric P, Meyer AS, Jensen PA, Dam-Johansen K. Reactor design for minimizing product inhibition during enzymatic lignocellulose hydrolysis: I. Significance and mechanism of cellobiose and glucose inhibition on cellulolytic enzymes. Biotechnology Advances 2010;28:308-324.

[2] Jørgensen H, Kristensen JB, Felby C. Enzymatic conversion of lignocellulose into fermentable sugars: challenges and opportunities Biofuels. Biofuels, Bioproducts and Biorefining 2007;1:119-134.

[3] Lee YH, Fan LT. Kinetic studies of enzymatic hydrolysis of insoluble cellulose II. Analysis of extended hydrolysis times. Biotechnology and Bioengineering 1983a;25:939-966.

[4] Woodward J, Wohlpart DL. The properties of native and immobilized β-glucosidase preparations from *Aspergillus niger*. Journal of Chemical Technology and Biotechnology 1982;32:547-552.

[5] Bissett F, Sternberg D. Immobilization of *Aspergillus* β-glucosidase on chitosan. Applied and Environmental Microbiology 1978;35:750-755.

[6] Martino A, Pifferi PG, Spagna G. Immobilization of β-glucosidase from a commercial preparation. Part 2. Optimization of the immobilization process on chitosan. Process Biochemistry 1996;31:287-293.

[7] Magalhães DB, Miguez da Rocha-Leão MH. Immobilization of β-glucosidase aggregates in calcium alginate. Biomass and Bioenergy 1991;1:213-216.

[8] Busto MD, Ortega N, Perez-Mateos M. Studies of microbial β-D-glucosidase immobilized in alginate gel beads. Process Biochemistry 1995;30:421-426.

[9] Shen X, Xia L. Production and immobilization of cellobiase from *Aspergillus niger* ZU-07. Process Biochemistry 2004;39:1363-1367.

[10] Woodward J, Clarke M. Hydrolysis of cellobiose by immobilized β-glucosidase entrapped in maintenance-free gel spheres. Applied Biochemistry and Biotechnology 1991;28/29:277-283.

[11] Ortega N, Busto MD, Perez-Mateos M. Optimisation of β-glucosidase entrapment in alginate and polyacrylamide gels. Bioresource Technology 1998;64:105-111.

[12] Busto MD, Ortega N, Perez-Mateos M. Stabilisation of cellulases by cross-linking with glutaraldehyde and soil humates. Bioresource Technology 1997a;60:27-33.

[13] Calsavara LPV, Moraes FFD, Zanin GM. Comparison of Catalytic Properties of Free and Immobilized Cellobiase Novozym 188. Applied Biochemistry and Biotechnology 2001;91–93:615-626.

[14] Tu M, Zhang X, Kurabi A, Gilkes N, Mabee W, Saddler J. Immobilization of β-glucosidase on Eupergit C for lignocellulose hydrolysis. Biotechnology Letters 2006;28:151-156.

[15] Woodward. J, Krasniak SR, Smith RD, Spielberg F. Kinetic properties of β-glucosidase preparations immobilized in calcium alginate gel spheres. Biotechnology Bioengineering Symposium 1982;12:485-489.

[16] Tanaka H, Matsumura M, Veliky A. Diffusion characteristics of substrates in Ca-alginate gel beads. Biotechnology and Bioengineering 1984;26:53-58.

[17] Woodward J, Capps KM. Cellobiose hydrolysis by glutaraldehyde-treated β-glucosidase entrapped in propylene glycol alginate/bone gelatin spheres Applied Biochemistry and Biotechnology 1992;34/35:341-347.

[18] Lee JM, Woodward J. Properties and application of immobilized β-D-glucosidase coentrapped with *Zymomonas mobilis* in calcium alginate. Biotechnology and Bioengineering 1983b;25:2441-2451.

[19] Ghose TK. Measurement of Cellulase Activities. Pure and Applied Chemistry 1987;59:257-268.

[20] Sternberg D, Vijayakumar P, Reese ET. β-Glucosidase: microbial production and effect on enzymatic hydrolysis of cellulose. Canadian Journal of Microbiology 1977;23:139-147.

[21] Sluiter A, Hames B, Ruiz R, Scarlata C, Sluiter J, Templeton D, Crocker D. Laboratory analytical procedure 002, Determination of structural carbohydrate and lignin in biomass. 2006:Retrieved from http://www.nrel.gov/biomass/analytical_procedures.html.

[22] Nidetzky B, Zachariae W, Gercken G, Hayn M, Steiner W. Hydrolysis of cellooligosaccharides by *Trichoderma reesei* cellobiohydrolases: Experimental data and kinetic modeling. Enzyme and Microbial Technology 1994;16:43-52.

[23] Schmid G, Wandrey C. Evidence for the lack of exo-cellobiohydrolase activity in the cellulase system of *Trichoderma reesei* QM 9414. Journal of Biotechnology 1990;14:393-409.

[24] Schülein M. Enzymatic properties of cellulases from *Humicola insolens*. Journal of Biotechnology 1997;57:71-81.

[25] Busto MD, Ortega N, Perez-Mateos M. Effect of immobilization on the stability of bacterial and fungal β-D-glucosidase. Process Biochemistry 1997b;32:441-449.

[26] Baker JO, Oh KK, Grohmann K, Himmel ME. Thermal stabilization of fungal β-glucosidase through glutaraldehyde crosslinking. Biotechnology Letters 1988;10:325-330.

Chapter 5

A Dynamic Model for Cellulosic Biomass Hydrolysis: Validation of Hydrolysis and Product Inhibition Mechanisms

The hydrolysis of cellulose/lignocellulose involve mutiple enzymes and different phase (homogeneous and heterogeneous). A number of mathematical models for enzymatic hydrolysis have been proposed in the literatures to describe the reaction kinetics. However, only few of those models have been independently subjected to intensive experimental validation. A model proposed by Kadam (2004) based on Michaelis-Menten (M-M), enzyme adsorption and product inhibition (eq. 2.2~2.9, in chapter 2) provides an easier way to predict the reaction kinetics because all the variables are easily obtained by regular laboratory instruments.

5.1 Key point of this research

A semimechanistic multi-reaction kinetic model consists of homogeneous and heterogeneous reaction proposed by Kadam was systematically validated and modified under a step by step analysis. The objective is to perform a comprehensive analysis, validating and further consolidating the model. A number of experiments were carried out under a wide range of initial conditions (Avicel versus pretreated barley straw as substrate, different enzyme loadings, and different product inhibitors such as glucose, cellobiose and xylose) to test the hydrolysis and product inhibition mechanism of the model. Nonlinear least squares method was used to identify the model and estimate kinetic parameters based on the experimental data. The weighted sum of square error (*WSSE*) was used to evaluate the performance of the models.

Transglycosylation reaction converts glucose back to oligosaccharides significantly under high glucose concentration. In most previous reseaches of kinetic modeling, substrate concentration were not high enough (cellulose concentrations in Kadam (2004) and Zheng (2009) were less than 65 g/L), therefore, the role of transglycosylation were ignored. In this reseach, cellulose concentration is 100 g/L, with the addition of initial glucose background, the effact of transglycosylation becomes significant. This result in that model proposed by Kadam failed to predict the hydrolysis behavior under high glucose concentration. Therefore, transglycosylation reaction should be considered.

5.2 Conclusion

The analysis showed that transglycosylation reaction at high glucose level play a key role in the model. Two transglycosylation reactions ($3G \leftrightarrow G_3 + 2H_2O$ and $G + G_3 \leftrightarrow G_4 + H_2O$) were introduced

to calibrate the deviations at higher glucose backgrounds. Although transglycosylation reactions proposed here are simplified, with the consideration of transglycosylation, precise prediction of hydrolysis behavior under high glucose background can be achieved. Therefore, the range of applicability of the model is improved.

The model over-predicts product concentrations for reaction where a extreme high substrate concentration (150 g/L Avicel) was present. This may be attributed to that the level of transglycosylation is also depends on enzyme concentration, which was not included in the mathematical equations. The relation between enzyme concentration and transglycosylation needs further investigation to solved the limitation. Two exceptions where the model fit is less good: (1) Different types of substrate. Hydrolysis of Avicel is used for parameter estimation, the estimated values can not describe the hydrolysis of pretreated barley straw very well. (2) Different enzyme source. It is observed that different types of β-glucosidase shows different reaction rate.

The parameters are not universal and the variations are highly dependent on the selected experimental data sets used for parameter estimation. However, this model provides a simple way for predicting hydrolysis kinetics over a broad range of substrate and enzyme loading. As long as the models is applied with caution of its limitations, it is easy and usful for supporting process design and technology improvement efforts at pilot and full-scale studies especially under high cellulose loading.

5.3 Reference

Kadam, K.L., Rydholm, E.C., and McMillan, J.D. (2004) Development and Validation of a Kinetic Model for Enzymatic Saccharification of Lignocellulosic Biomass. Biotechnology Progress 20, 698-705

Zheng, Y., Pan, A., Zhang, R., and Jenkins, B.M. (2009) Kinetic Modeling for Enzymatic Hydrolysis of Pretreated Creeping Wild Ryegrass. Biotechnology and Bioengineering 102 (6) 1558-1569.

A Dynamic Model for Cellulosic Biomass Hydrolysis: A Comprehensive Analysis and Validation of Hydrolysis and Product Inhibition Mechanisms

Chien-Tai Tsai [a], Ricardo Morales-Rodriguez [c], Gürkan Sin [b], Anne S Meyer [a,*]

[a] Center for BioProcess Engineering, Technical University of Denmark, DK-2800 Lyngby, Denmark. **e-mail: am@kt.dtu.dk ; Tel: +45 45252909

[b] Computer Aided Process-Product Engineering Center, Technical University of Denmark, DK-2800 Lyngby, Denmark. **e-mail: gsi@kt.dtu.dk

[c] Departamento de Ingeniería de Procesos e Hidráulica, Universidad Autónoma Metropolitana-Iztapalapa, Av. San Rafael Atlixco 186, C.P. 09340, México, D.F., México. **e-mail: rmro@xanum.uam.mx

Abstract

Background: The objective of this study is to perform a comprehensive analysis in view of validating and further consolidating a semimechanistic kinetic model consisting of homogenous and heterogeneous reactions for enzymatic hydrolysis of lignocellulosic biomass proposed by Kadam et al. and its variations proposed in this work.

Methods: A number of dedicated experiments were carried out under a wide range of initial conditions (Avicel® versus pretreated barley straw as substrate, different enzyme loadings, and different product inhibitors as glucose, cellobiose and xylose) to test the hydrolysis and product inhibition mechanism of the model. Nonlinear least squares method was used to identify the model and estimate kinetic parameters based on the experimental data. The suitable mathematical model for industrial application was selected among the proposed models based on statistical information (weighted sum of square errors).

Results: The analysis showed that transglycosylation plays a key role at high glucose level. It also showed the values of parameters depend on the selected experimental data used for parameter estimation. Therefore, the parameter values are not universal and should be used with caution. Semimechanistic model proposed by Kadam et al. failed to predict the hydrolysis phenomena at high glucose level, but when combined with transglycosylation reaction, the prediction of cellulose hydrolysis behavior over a broad range of substrate concentration (50-150 g/L) and enzyme loading (15.8-31.6 and 1-5.9 mg-protein/g-cellulose for Celluclast and Novozyme 188 respectively) is possible.

Conclusions: This is the first study introducing transglycosylation into the semimechanistic model. As long as these type of models are used within the boundary of their validity (substrate type, enzyme source and substrate concentration), they can support process design and technology improvement efforts at pilot and full-scale studies.

Keywords: lignocellulose; kinetic model; enzymatic hydrolysis; Langmuir adsorption isotherm; validation; process design; bio-ethanol; transglycosylation

Nomenclature

BG	β-glucosidase
CBH	exo-1,4-β-D-glucanases
Cel	Celluclast 1.5L
DP	degree of polymerization
EG	endo-1,4-β-D-glucanase
E_{iT}	total enzyme concentration (g protein/L) (i = 1 for Cel; i = 2 for N188)
E_{iB}	bound enzyme concentration (i = 1 for Cel 1.5L; i = 2 for N188)
E_{iF}	concentration of free enzyme in solution (i = 1 for Cel 1.5L; i = 2 for N188)
G_i	glucose (i = 1), cellobiose (i = 2), cellotriose (i = 3) and cellotetraose (i = 4) concentration
$G_{cr,\ tri}$	(g/L)
$G_{cr,\ tetra}$	critical glucose concentration of transglycosylation for cellotriose production (g/L)
K_{iad}	critical glucose concentration of transglycosylation for cellotetraose production (g/L)
	dissociation constant for enzyme adsorption/desorption reaction (L/g protein) (i = 1 for Cel; i
K_{3M}	= 2 for N188)
K_{iIG2}	substrate (cellobiose) saturation constants (g/L)
K_{iIG}	inhibition constant cellobiose (g/L) (i = 1 for r_1; i = 2 for r_2)
K_{iIX}	inhibition constant glucose (g/L) (i = 1 for r_1; i = 2 for r_2; i = 3 for r_3)
k_{ir}	inhibition constant xylose (g/L) (i = 1 for r_1; i = 2 for r_2; i = 3 for r_3)
k_{G3}	reaction rate constant (i = 1 and 2, L/ g•h ; i = 3, h^{-1})
k_{G4}	reaction rate constant of transglycosylation for cellotriose production
N188	reaction rate constant of transglycosylation for cellotetraose production
r_i	Novozyme 188
	reaction rate (g/L•h) (i = 1 for cellulose to cellobiose; i = 2 for cellulose to glucose; i = 3 for
	cellobiose to glucose)

Nomenclature- continued

r_{tri}	overall reaction rate (g/L•h) of $3G \leftrightarrow G_3 + 2H_2O$
r_{tri+}	reaction rate (g/L•h) of $3G \rightarrow G_3 + 2H_2O$
r_{tri-}	reaction rate (g/L•h) of $3G \leftarrow G_3 + 2H_2O$
r_{tetra}	overall reaction rate (g/L•h) of $G + G_3 \leftrightarrow G_4 + H_2O$
r_{tetra+}	reaction rate (g/L•h) of $G + G_3 \rightarrow G_4 + H_2O$
r_{tetra-}	reaction rate (g/L•h) of $G + G_3 \leftarrow G_4 + H_2O$
R_S	substrate reactivity
S	substrate concentration (g/L) (suffix with "0" meas initial substrate concentration)
X	xylose concentration (g/L)
Xbg	a BG other than N188
α	dimensionless constant for substrate reactivity

Background

Ethanol produced from lignocellulose has become an alternative source of fuel (Gnansounou, 2010; Larsen et al., 2008). In order to release glucose from biomass to be fermented into ethanol, cellulose contained in the lignocellulosic matrix firstly needs to be hydrolyzed. Enzymatic hydrolysis besides chemical hydrolysis is a promising method for decomposing the cellulose into small molecules The enzymatic hydrolysis reactions involved three groups of enzyme: endo-1,4-β-D-glucanase (EG) (EC 3.2.1.4), exo-1,4-β-D-glucanases (or cellobiohydrolase, CBH) (EC 3.2.1.91) and β-glucosidase (BG) (EC 3.2.1.21). The EG cuts the cellulose from inside randomly. CBH hydrolyzes the cellulose from the ends and releases mainly cellobiose. Finally, BG hydrolyze cellobiose into glucose (Zhang & Lynd, 2004).

The mechanism of converting insoluble polymeric substrate into soluble sugars by the action of cellulase enzymes has not yet been completely understood due to the complexity of the involved phenomena (such as, adsorption, desorption, enzyme deactivation, accessible area, crystallinity, degree of polymerization, lignin content, enzyme synergism, etc.), which affect the reaction kinetics. Nevertheless, a number of mathematical models for enzymatic hydrolysis have been proposed in the literature (Gan et al., 2003; Gharpuray et al., 1983; Kadam et al., 2004; Movagarnejad et al., 2000; Philippidis et al., 1993) as reviewed in Bansal et al. (Bansal et al., 2009).

Among the models proposed in the past, none of them were validated rigorously. This may call into question the credibility of such models for engineering applications. Among the factors that can explain the variability are different enzyme sources, substrate type, conceptual framework of the model (model structure), experimental data quality and quantity as argued by Sin et al. (Sin et al., 2010). Hence the

purpose of this study is to validate the conceptual framework of Kadam model (model structure) with focused and dedicated rigorous experimental testing (improved data quality and quantity) in systematic and iterative manner and to expand the model structure as necessary in view of improving range of applicability of the model. In addition, transglycosylation reactions which convert glucose back to oligosaccarides under high glucose and cellulose concentrations were first introduced in the modelling and investigated. Further guidelines will be elucidated to help use the model for supporting process design and optimization studies for lignocellulosic ethanol production.

Review of hydrolysis model proposed by Kadam

The mathematical model proposed by Kadam et al. (2004) describes the conversion of cellulose to cellobiose (r_1), the conversion of cellulose to glucose (r_2) and the conversion of cellobiose to glucose (r_3) as illustrate in the bold dashed-dot square in Fig. 1. The mathematical model was based on a number of assumptions such as:

- Enzyme adsorption follows a Langmuir-type isotherm with first order reactions occurring on the cellulose surface.
- Amorphous and crystalline cellulose are lumped and uniform in terms of its susceptibility to enzymatic attack,
- Enzyme activity remains constant throughout the reaction,
- Conversion of cellobiose to glucose occurs in solution and follows classical Michaelis-Menten kinetics.
- Considers separate cellulase (mainly a mixture of EG and CBH) and β-glucosidases activities on cellulose breakdown and competitive inhibition by simple sugars.

The hydrolysis pathways and the inhibition effects by intermediate and final products (cellobiose, glucose and xylose) can be classified into r_1, r_2 and r_3. These can be expressed as equations (1) to (8):

Enzyme Adsorption

Langmuir isotherm $$E_{iB} = \frac{E_{i\max} K_{iad} E_{iF} S}{1 + K_{iad} E_{iF}} \qquad (1)$$

Cellulose-to-Cellobiose Reaction with Competitive Glucose, Cellobiose and Xylose Inhibition.

$$r_1 = \frac{k_{1r} E_{1B} R_S S}{1 + \frac{G_2}{K_{1IG2}} + \frac{G}{K_{1IG}} + \frac{X}{K_{1IX}}} \qquad (2)$$

Cellulose-to-Glucose Reaction with Competitive Glucose, Cellobiose and Xylose Inhibition.

$$r_2 = \frac{k_{2r}(E_{1B} + E_{2B})R_S S}{1 + \frac{G_2}{K_{2IG2}} + \frac{G}{K_{2IG}} + \frac{X}{K_{2IX}}} \quad (3)$$

Cellobiose-to-Glucose Reaction with Competitive Glucose and Xylose Inhibition Reaction.

$$r_3 = \frac{k_{3r}E_{2F}G_2}{K_{3M}(1 + \frac{G}{K_{3IG}} + \frac{X}{K_{3IX}}) + G_2} \quad (4)$$

Mass Balances

Cellulose: $\frac{dS}{dt} = -r_1 - r_2$ (5)

Cellobiose: $\frac{dG_2}{dt} = 1.056r_1 - r_3$ (6)

Glucose: $\frac{dG}{dt} = 1.111r_2 + 1.053r_3$ (7)

Enzyme: $E_{Ti} = E_{Fi} + E_{Bi}$ (8)

Since this model based on the assumption that enzyme activity remains constant. Factors decreasing the reaction rate are: 1. product inhibition, 2. inactivation of enzyme (BG) after the adsorption to the substrate and 3. the change of substrate reactivity (R_S). Substrate reactivity is derived from the secondary hydrolysis rate of the residual substrate at given time (Kadam et al., 2004; Yang et al., 2006; Zheng et al., 2009). It is expressed as:

$$R_S = \alpha \frac{S}{S_0} \quad (9)$$

S_0 is the initial substrate concentration and S is the substrate concentration at a given time (g/L). α is a dimensionless constant derived from experimental data, *e.g.* the relation between secondary initial hydrolysis rate and S/S_0. The introduction of R_S in the model based on the observation/assumption that the substrate may become less susceptible to be hydrolyzed by enzyme over time. Since the reasons decreasing substrate reactivity are complicated (change of the substrate structure like crystal structure, degree of polymerization, pore size distribution, etc.), in practical, these properties are difficult to be

evaluated by many labaratories. Therefore, R_S represents an empirical factor for the correction and consideration of the phenomena mentioned above in the reaction rate equations.

Transglycosylation

The model proposed by Kadam et al. (2004) did not include transglycosylation reaction. To the best of our knowledge, transglycosylation was not considered in previous studies. However, this reaction transferring glucose back to cello-oligosaccharides by β-glucosidase at high glucose or cellobiose concentrations were reported in different studies (Andrić et al., 2010; Bhiri et al., 2008; Gusakov et al., 1984; Kono et al., 1999; Pal et al., 2010; Watanabe et al., 1992). It might be a relevant mechanism to be considered for kinetic models, because in bioethanol industry, the hydrolysis process is typically operated above 15% (w/w) dry matter of biomass to obtain higher glucose concentration, so after fermentation the higher distillation efficiency can be achieved (Jørgensen et al., 2007; Morales-Rodriguez et al., 2011). Therefore, it becomes important to include transglycosylation reaction for the sake of completeness. Gusakuv et al. (Gusakov et al., 1984) proposed very detailed mechanism of transglycosylation with certain degree of complexity. Therefore two simplified reactions were proposed and tested in this research. The first reaction is for cellotriose production $3G \leftrightarrow G_3 + 2H_2O$ (r_{tri}). The reaction rate can be expressed as:

$$r_{tri} = r_{tri+} - r_{tri-} \tag{10}$$

Where

$$r_{tri+} = k_{G3+}\left[\frac{1}{1+e^{(G_{cr,tri}-G)}}\right]G \tag{11}$$

$$r_{tri-} = k_{G3-}\left[\frac{1}{1+e^{(G_{cr,tri}-G)}}\right]G_3 \tag{12}$$

$G_{cr,tri}$ is critical glucose concentration, which means when glucose level is above this concentration the transglycosylation for cellotriose production is significant. The second reaction is for cellotetraose production $G + G_3 \leftrightarrow G_4 + H_2O$ (r_{tetra}) and the reaction rate can be expressed as:

$$r_{tetra} = r_{tetra+} - r_{tetra-} \tag{13}$$

Where

$$r_{tetra+} = k_{G4+}\left[\frac{1}{1+e^{(G_{cr,tetra}-G)}}\right]G \tag{14}$$

$$r_{tetra-} = k_{G4-}\left[\frac{1}{1+e^{(G_{cr,tetra}-G)}}\right]G_4 \qquad (15)$$

$G_{cr,tetra}$ is critical glucose concentration, which means when glucose level is above this concentration the transglycosylation for cellotetraose production is significant. Fig. 1 illustrates all reaction pathways for glucose production from cellulose.

Methods

Substrate and enzyme

The substrate in this research were Avicel® PH-101 (Sigma, USA) and pretreated barley straw. Barley straw was grown and harvested in Denmark and then was transported to DONG Energy (Danish Oil and Natural Gas Energy, Denmark) for pretreatment. The pretreatment method consisted of a three-stage heating process, which involved triple heating treatment of the straw at increasing temperatures (15 min at 60°C; liquids removal; 10 min at 180°C; 3 min at 195°C) (Rosgaard et al., 2007). After pretreatment, the liquids were removed. Standard procedure for acid hydrolysis and compositional calculation analysis of the dry solid was according to the U.S. National Renewable Energy Laboratory (Sluiter et al., 2006). The cellulose, xylose and acid insoluble lignin contents in barley straw are 66.3, 3.5 and 26.6 %, respectively.

The following three enzymes were obtained from Novozymes A/S (Bagsværd, Denmark): Celluclast 1.5L, Novozyme 188 and another type of BG (not commerciallized, named Xbg in this research). Celluclast 1.5L (Cel, mainly EG+CBH) derived from *Trichoderma reesei*, having an activity of 65 FPU/mL (FPU = filter paper unit), 10 CBU/mL (CBU = Cellobiose units) and protein concentration of 79 mg/mL. Novozyme 188 (N188, mainly BG) derived from *Aspergillus niger*, having an activity of 870 CBU/mL and protein concentration of 88 mg/mL. Xbg has protein concentration of 60 mg/mL. The CBU activity was determined by measuring glucose production from hydrolysis of cellobiose at 50°C, pH 4.8 (Ghose, 1987; Sternberg et al., 1977).

Analysis of protein and sugars

Protein concentrations of the enzymes were measured by Quick Start Bradford protein assay (Bio-Rad, Hercules, CA) and γ-globulin was used as standard. Hexokinase (420 U/ml) + Glucose-6-phosphate-dehydrogenase (210 U/ml) purchased from Megazyme (Wicklow, Ireland) were used for glucose analysis. The concentration of cellobiose followed previous research (Drissen et al., 2007) by calculated from the increase of glucose after treatment of excess of N188 for 24 h at 50°*C*. Xylose contents in the pretreated

barley straw is only 3.5%, even completely released after hydrolysis, the concentration is only 3.15 g/L, which was ignored and no further measurements in this research were performed.

Experimental design and hydrolysis reaction

Hydrolysis reactions under different enzyme concentration/combination, substrate and inhibitors concentrations are shown in Table 1. These data were used for parameters estimation or validation, depending on the modeling strategies. All reactions were conducted in 2 mL eppendorf tubes and incubated in thermomixer at 50°C and mixed at 1000 rpm. Reaction buffer was 50 mM sodium acetate pH 4.8 with 0.04% sodium azide.

Determination of Langmuir adsorption constants

10 g/L of Avicel or 5 g/L pretreated barley straw was mixed with different concentrations of enzyme and incubated for 1 h at 50°C with mixing at 1000 rpm. Free enzymes were measured as the protein concentrations in the supernatant. Adsorbed enzymes were calculated by subtracting free enzyme concentrations from the initial enzyme concentrations. K_{ad} and E_{max} were determined by Eq. (16), which was rearranged from Eq. (1).

$$\frac{E_F}{(E_B / S)} = \frac{1}{E_{\max} K_{ad}} + \frac{E_F}{E_{\max}} \qquad (16)$$

The obtained Langmuir adsorption constants were shown in Table 3.

Transglycosylation reaction

N188 and Xbg (0.585 and 0.293 mg/mL), Celluclast 1.5L (1.58 and 0.585 mg/mL) were mixed with different glucose concentration. Reactitons were incubated at 50°C for 48 hr. Final glucose concentrations were analyzed and compared with initial concentration. The decreased glucose was regarded as being converted to oligosaccharides by transglycosylation reaction.

Estimation of kinetic parameters and model validation methodology

To achieve the goal of the study, a systematic framework was introduced and used, the framework consists of the following steps: model construction, experimental data collection, estimation of the parameters and validation (see Fig. 2). Three kinetic parameters (k_{3r}, K_{3M}, K_{3IG} and K_{3IX}) of the cellobiose-to-glucose conversion (r_3) were calculated using data set E1-E5 (see Table 1), glucose and xylose were

used as initial inhibitor. Then the parameters were validated by data sets with different enzyme concentrations (data set D1-D5, see Table 1). If the fitting and validation seems not being completely correct, it was possible to return and make a further analysis of the mathematical model by introducing the cellotriose production transglycosylation reaction (r_{tri}) into the original Kadam model. Two parameters (k_{+G3}, k_{-G3}) involved in transglycosylation were estimated. The next step of the procedure was estimating eight unknown parameters (k_{1r}, k_{2r}, K_{1IG2}, K_{2IG2}, K_{1IG}, K_{2IG}, K_{1IX} and K_{2IX}) in the kinetic reactions for cellulose conversion to cellobiose (r_1) and glucose (r_2) using experimental data set A1-A4 (Celluclast + N188) or B1-B7 (Celluclast only) which involved the analysis of the hydrolysis and product inhibition mechanism (see Table 2). Different initial concentration of inhibitory agents, glucose, cellobiose and xylose, were used to quantify their inhibition effects on the cellulosic hydrolysis. R_S of Avicel in cellulose-to-cellobiose reaction (r_1) and cellullose-to-glucose reaction (r_2) (Eqs. (2) and (3)) were regarded as constant by setting as 1, according to the report by Yang et al. (Yang et al., 2006) and Ooshima et al. (Ooshima et al., 1991) that the reactivity of Avicel did not change over time. The validation of the models was performed using data sets with a different enzyme combination and concentration, substrate concentration, and pretreated barley straw (data set C-Q, see Table 1). The R_S of pretreated barley straw was not constant and α was set as 1, according to the values derived from other types of lignocellulose in previous researches (Kadam et al., 2004; Zheng et al., 2009). If mathematical model predictions did not fit or predict very well with the experimental data, then return to the modeling step and introduce another transglycosylation reaction (production for cellotetraose, r_{tetra}). The expresssion of r_1 and r_2 also could be revised by introducing K_{1M} and K_{2M} (see Table 2, Model 3). Then start the implementation of the framework for parameter estimation and validation for further investigation.

To this end, three different variations of the original mathematical model proposed by Kadam et al. (2004) were proposed in this research (Table 2) and evaluated. Model 1 only considered the transglycosylation for cellotriose production. Model 2 and Model 3 involved both cellotriose and cellotetraose production. Therefore, Eq. (7) for mass balance of glucose was modified for Model 1 as following:

$$\frac{dG}{dt} = 1.111r_2 + 1.053r_3 - 1.071r_{tri+} + 1.071r_{tri-} \qquad (17)$$

and Eqs. (7) and (10) were modified for Model 2 and 3 as is shown below, respectively:

$$\frac{dG}{dt} = 1.111r_2 + 1.053r_3 - 1.071r_{tri+} + 1.071r_{tri-} - 0.2702r_{tetra+} + 0.2702r_{tetra-} \qquad (18)$$

$$\frac{dG_3}{dt} = r_{tri+} + r_{tri-} - 0.7567 r_{tetra+} + 0.7567 r_{tetra-} \quad (19)$$

in order to fulfill the mass balances of the compounds following the reaction pathway proposed in Fig. 1.

The modelling and estimation of the parameters was done using MatLab (The Mathworks, Natick, MA). Nonlinear least squared method was used for the parameter estimation. The Initial values for the parameter estimation were taken from Kadam et al. (2004). The fminseach function from Matlab and the Levenberg-Marquardt search were used to solve the objective function, $J(\boldsymbol{\theta})$:

$$\arg\min \quad J(\boldsymbol{\theta}) = \sum_{j=1}^{M} \sum_{i=1}^{N} \left(ym_{i,j} - f_{i,j}(\boldsymbol{\theta}) \right) \quad (20)$$

where $J(\boldsymbol{\theta})$ is the sum of squared errors, $ym_{i,j}$ is the *ith* measurement in the *jth* experiment and $f_{i,j}(\boldsymbol{\theta})$ is the corresponding model prediction for the measurement and $\boldsymbol{\theta}$ is the parameter subset used for parameter estimation. This is to mean that for parameter estimation a set of experiments are typically used in view of better identifying the parameter subset in questions. This is explained below.

Experimental data sets under different hydrolysis conditions used for parameter estimation and validation were shown in Table 1. Each data set was given a specific code from A to Q where different initial substrate concentration, substrate type, enzyme loading and combinations, and inhibitors loading were related with the different data sets. To make the article concise, these codes will be used repeatedly in this paper.

The comparison and selection for the proper mathematical structure among the proposed mathematical models was performed relying on the weighted sum of square error (*WSSE*) as following:

$$WSSE = \sum_{j} \sum_{i} \left(\frac{y_{i,j} - f(x_{i,j.k})}{\sigma_{i,j}} \right)^2 \quad (21)$$

where, $y_{i,j}$ is the experimental value i of the dataset j, $f(x_{i,j})$ is the value of the function evaluated at the same experimental conditions i of the data set j in the model k and σ is the standard deviation of the measurement error (in this study a similar value was assumed for all measurement points which was calculated from triplicate measurements).

Kinetic parameters derived from standard enzymatic procedure

In enzymology, standard procedure for deriving kintic properties of enzyme is through the measurement of initial reaction rate. Then plot the data according to functions rearranged form Michaelis-Menten equation, such as Hanes-Woolf plot (Hanes, 1932).The values of kinetic parameters can be calculated from the intercept and slop. In order to compare the paremeters estimated from standard procedure and numerical method in this research, kinetic parameters were also obtained through standard procedure. Proper concentration of BG was mixed with different concentrations of cellobiose and inhibitors (glucose or xylose) and incubated at 50°C with gental shaking for 8 minutes. All reactions were stopped by heating at 100°C for 5 minutes. Parameters, k_3, K_{3M}, K_{3IG} and K_{3IX}, were derived from the Hanes-Woolf plot. The vlaues were shown in Table 4.

Results and discussion

Parameter estimation and validation of cellobiose-to-glucose conversion (r_3)

The parameters of describing the rate of cellobiose hydrolysis, r_3, were obtained using the experimental data from hydrolysis of cellobiose by N188 using data set E1-E5 (see Table 1). However, the preliminary evaluation shows the deviations between the fitting/prediction and experimental data were large when glucose concentration is higher than 70 g/L (Fig. 3a). Since the product inhibition was already taken into account, this deviation may be resulted from transglycosylation. This hypothesis was tested and proved by incubating the enzymes in different concentrations of glucose solutions to see the effect of transglycosylation. It shows the higher the initial glucose concentration the more glucose disappears after incubation for 2 days (Fig. 3b). The lost glucose was assumed to be converted to cellotriose. The level of transglycosylation is approximately proportional to glucose concentration when glucose concentration is over 40 g/L. Therefore, the original model of Kadam was revised to account for this reaction step, namely by introducing transglycosylation reactions for cellotriose production (r_{tri}, Eq. (10)-(12)). The value of critical glucose concentration ($G_{cr,tri}$) was set to be 40 g/L, meaning that when glucose concentration is higher than 40 g/L, the effect of transglycosylation is taken into account. To describe the rate expression mathematically, two terms were used: the first term is a sigmoid function which switches on or off the transglycosylation reaction based on the critical glucose concentration and the other term is a first order conversion rate of glucose to cellotriose (see Eqs. (11)-(12)). With this modification, better description of the experimental data can be obtained as shown in Fig. 4. It should be noticed that under same enzyme loading (protein/substrate ratio), Xbg is less inhibited by glucose, in addition its hydrolysis efficiency is much higher than N188 as shown in Fig. 3a. This is consistent with the observation that values derived

from standard assay are totally different (Table 4). Therefore, we can expect that the parameters of N188 and Xbg derived from mathematical modelling estimation will be different.

Parameter estimation and validation of cellulose to glucose (r_1) and cellulose to cellobiose (r_2)

In this study, several model structures were proposed based on iterative analysis of data and model predictions. The models are referred to as Model 1, 2 and 3 representing modification of kinetic expressions of the original Kadam model (see Table 2). Model 1 includes tranglycosylation for cellotriose production (r_{tri}). Model 2 includes the same model structure as Model 1 with the addition of tranglycosylation for cellotetraose production (r_{tetra}). Model 3 was based on Mode 2. But K_{1M} and K_{2M} were introduced into r_1 and r_2 (Eqs. (22), (23)), that is, adding this type of kinetic for r_1 and r_2 which originally were not included in model published by Kadam. For parameter estimation strategy, in addition to data set A1-A4, data set I (150 g/L of Avicel) was also included. Each model candidate was evaluated step by step from Model 1 to Model 3 to optimize the performance of r_1 and r_2. Therefore, several factors, such as experimental data selected for parameters estimation, transglycosylation for cellotetraose (r_{tetra}, Eqs. (13)-(15)), values of critical glucose concentration ($G_{cr,tetra}$) and the mathematical expression of r_1 and r_2, were analyzed. Due to the space of this article, only selected results of fitting and validation were shown and discussed. The rest results and figures are shown in Appendix. The comparison and evaluation of the models were performed by *WSSE* analysis (Table 5). It should be noticed in this research, "fitting" means the values or curves were derived from nonlinear least squared method according to the experimental data sets used for parameter estimation, while "prediction" means the values or curves were calculated using the parameters estimated from fitting and the initial conditions used in validation experiments.

In Model 1, transglycosylation for cellotetraose production (r_{tetra}) were not involved. Two strategies for parameter estimation were conducted: the first strategy was using data set B1-B7 for parameters estimation. The fitting of data set B is good (*WSSE* value is small). The predicted values of data set A2 and A3 were higher than experimental value when glucose concentration is higher than around 70~80 g/L (Fig. 5b). The second stragety used data set A1-A4 used for parameter estimation instead of data set B1-B7. The fitted values of data set A2 and A3 were still higher than experimental value under high glucose concentration, besides, the prediction of data set C1-C7 (Fig. 6b) became worse than stategy 1 (Fig. 5a). *WSSE* values of prediction of data set C of strategy 1 and strategy 2 are 1835 and 5254 respectively (Table 5).

According to the curves in data set A2 and A3 of Model 1, the "over-prediction" problem (for strategy 1) and "over-fitting" problem (for strategy 2) were observed when glucose concentration is higher than around 70~80 g/L (see Figs. 5b and 6a). That means the equations r_1, r_2, r_3 and r_{tri}, are not enough to

describe the hydrolysis kinetic behaviors under high glucose concentration. In order to address this issue, an additional transglycosylation reaction for cellotetraose production, r_{tetra}, was proposed in Model 2 (see Fig. 1). Of which the critical value of transglycosylation ($G_{cr,tetra}$) was set as 75 and 80 g/L, and both were evaluated. Data set A1-A4 were used for parameter estimation. In each case the "over-fitting" problem under high glucose concentration in data set A2 and A3 (Fig. 7a) as well as "over-prediction" problem in data set O and P were solved (Fig. 7b).

However, when Avicel concentration was up to 150 g/L (data set I), the "over-prediction" problem were not solved by Model 2. Therefore, Model 2 was then further modified by changing the expression of cellulose-to-cellobiose (r_1) (Eq. (22)) and cellulose-to-glucose (r_2) (Eq. (23)). The modified model was called Model 3:

$$r_1 = \frac{k_{1r} E_{1B} R_S S}{K_{1M}(1 + \frac{G_2}{K_{1IG2}} + \frac{G}{K_{1IG}} + \frac{X}{K_{1IX}}) + S} \qquad (22)$$

$$r_2 = \frac{k_{2r}(E_{1B} + E_{2B}) R_S S}{K_{2M}(1 + \frac{G_2}{K_{2IG2}} + \frac{G}{K_{2IG}} + \frac{X}{K_{2IX}}) + S} \qquad (23)$$

Of which the denominators of both equations were espressed according to Michaelis-Menten equation. In addition to data set A1-A4, data set I (150 g/L Avicel concentration) was also used for parameter estimation. Critical value of transglycosylation for cellotetraose production ($G_{cr,tetra}$) was set as 75 and 80 g/L and both were evaluated. The fitting curve of data set I was much close to the experimental data (Fig. 8). Among the *WSSE* values of data set I, model 3 is smaller than the others (Table 5).

For hydrolysis of barley straw (data set N, O, P and Q) the predicted values in all models were smaller than experimental value during initial phase (before 24 h) and then "over-shoot"(Fig. 7b). This can be ascribed to the difference of physical and chemical properties between Avicel and pretreated barley straw.

When we compare two strategies of Model 1 (strategy 1: data set B1-B7 for parameter estimation; strategy 2: data set A1-A4 for parameter estimation), we can find in strategy 2 the values were over predicted under xylose background (data set B6 and B7) (Fig. 6b). However, in strategy 1 the fitting curves of data set B1-B7 are good and at the meantime the prediction curves of data set A1-A4 are similar to the fitting curves of data set A1-A4 in strategy 2. The reason is not fully understood because synergistic effect can not explain this observation. This is discussed as following: In strategy 1, the parameters of r_1 and r_2 are derived from the effect of Celluclast alone (data set B1-B7), therefore the synergism effects contributed from the cooperation of BG are not included in the paramers. That means, when we use the parameters derived from strategy 1 to describe the kinetic behaviors under the conditions of data set A1-

A7 (Celluclast + BG), the predicted value should be lower than the experimental data. Owing to that experimental values include the effect of synergistism, but the prediction values do not count in the effect of synergism. However, this hypothesis is not consistent with the observed results. The predicted curves of data set A1 and A4 fit the experimental data very well by strategy 1 (not lower, as we expected). This discrepancy needs further investigation in the future.

The reason that Model 2 failed to predict the kinetics under Avicel concentration 150 g/L is not well known. However, Fig. 3b reveals that the degree of transglycosyation not only depends on glucose concentration but also enzyme concentation. The higher enzyme concentration the more transglycosylation is. In this research, enzyme concentration was not considered in the equation of transglycosylation (either r_{tri} or r_{tetra}). Therefore, although the ratio of enzyme to cellulose in data set A1-A4 and data set I are the same (see Table 1), since cellulose concentration are 100 g/L (data set A1-A4) and 150 g/L (data set I), respectively, that means enzyme concentration of the later is 1.5 time of the former. It is possible that the level of transglycosylation reaction under the condition of data set I is higher than Model 2 predicted. The same concept can be supported from the fact that parameters of transglycosylation for cellotriose production (r_3) were estimated from data set E1-E5, but the enzyme concentation of BG in those experiments were only 3.9 mg-protein/g-cellobiose, therefore, BG concentration in the reaction is 3.9×37.5 =146 mg/L (enzyme to substrate ratio×substrate concentration=enzyme concentration). Compare with BG concentration in data set I, which is 5.9×150=885, is six times of data set E. We can say the parameters of r_3 estimated form data set E1-E5 "hypo-estimated" the transglycosylation reaction of data set I. Detailed relation between enzyme concentration and transglycosylation need further investigation. The other explanation is the parameters are derived from data fitting by numerical analysis based on kinetic principles (enzyme adsorption, product inhibition and transglycosylation). Thus, when data set I was included in parameter estimation, certain unkown factors not considered in the semimechanistic model were lumped into the other parameters. That explains why data set I fitted by Model 3 is better than the predictions by Model 1 and Model 2.

In all models the validation of hydrolysis of Avicel under different ratio of Celluclast and N188 with 40 g/L xylose background (data F, G and H, Fig. 9) are good, meaning that the variation of enzyme combination within normally used range (Celluclast, 15.8-31.6 and N188, 1-5.9 mg-protein/g-cellulose) the models can describe the reaction kinetics precisely. The predictions of hydrolysis kinetics at lower cellulose concentration (50 g/L Avicel, data set J) are also good (Fig. 10). From the sum of *WSSE* values in Table 5, we can see the performance of the models not only influenced by the reaction equations selected in the models, but also influenced by the critical glucose concentration ($G_{cr,\ tetra}$) of transglycosylation. If the reaction is conducted under cellulose concentration up to 150 g/L, Model 3 with $G_{cr,\ tetra}$ = 80 is the

best choice (sum of *WSSE* = 7827). However, if the cellulose concentration is below 100 g/L, Model 1 is enough to predict the kinetics because the reaction for cellotetraose production (r_{tetra}) is not significant.

Limitations of Models proposed in this research

The models proposed in this study can predict the cellulose hydrolysis kinetics well within certain ranges of different conditions, such as enzyme-substrate ratio and substrate dry matter. However there are still two limitations, under these conditions the model can not predict very well: (1) Substrate with very different properties. The composition and physical structures of Avicel and pretreated barley straw are different. Most pretreated biomass contains more than 15% of lignin, which non-specific absorbs the enzymes and then the absorbed enzymes lose their activity. But in this research all bound enzymes were regarded as active, thus, non-productive adsorption was not considered. This can explain the model over-estimated released glucose concentration after around 48 h (Fig. 7b). The other explanation is the crystallinity of Avicel is higher than pretreated barley straw. Therefore the hydrolysis curve of pretreated barley straw bends earlier than Avicel. In addition, the less crystallinty of pretreated barley straw can adsorb (hold) more water. That means under same dry matter, more free water exists in the Avicel system. This results in different physical environment in both systems. (2) Enzyme from different source. It reveals that the intrinsic properties of N188 and Xbg derived from Hanes-Woolf plot (Table 4) are different, especially for k_{3r}, the later is more than 8 times of the former. Fig. 3B also shows Xbg triggers less transglycosylation reaction than N188. The influence of above differences on the hydrolysis kinetics is shown in Fig. 3a. The hydrolysis efficiency of Xbg is higher than N188, meaning that this model is not valid to predict the reaction kinetics when different enzyme is used.

The significance of the parameters derived from this research and real reactions

Although semimechanistic kinetic model proposed by Kadam and modified models in this research provide an easier way to predict the kinetics of enzymatic hydrolysis reaction because all the variables are easily obtained by regular laboratory instruments. However, the reaction pathways of r_1 and r_2 described here are oversimplified. As far as Celluclast 1.5L is concerned, this is a mixture of different enzyme, mainly EG I, EG II, CBH I and CBH II; the hydrolysis mechanisms of each individual enzyme are different. The main products of CBH I are cellobiose accompanied with some glucose and cellotriose, (Medve et al., 1998; Nidetzky et al., 1994) but for CBH II most products are cellobiose and cellotriose; only very trace amount of glucose was observed (Nidetzky et al., 1994). The products of EG II are cellobiose, glucose and cellotriose, nor oligosaccharides with DP>3 were observed. Furthermore, it was reported that CBH I and EG II have negative effects to each other on substrate adsorption but positive

effect for synergism for hydrolysis (Medve et al., 1998). Thus, the parameters of r_1 and r_2 derived here are "lumped properties" of EG I, EG II, CBH I and CBH II.

The enzyme-cellulose interaction here is described by Langmuir isotherm. Based on this theory, only enzymes absorbing to insoluble cellulose are defined as bound enzyme and regarded to be active. However, EG II, CBH I and CBH II were reported being able to hydrolyze soluble oligosaccharides with DP<8 (Medve et al., 1998; Nidetzky et al., 1994). For enzymes acting on soluble substrates, they are classified as free enzyme rather than bounded enzyme. In the equations presented in this work, free Celluclast (EG + CBH) were regarded not having contributions to the reactions. The role of BG in r_2 is also ambiguous. BG works on small soluble oligosaccharide (Watanabe et al., 1992) rather than cellulose. Thus, maybe bound BG dose not really contribute in r_2. This was proved by Zheng, et al. (2009) in which assumed that BG only adsorbs onto lignin but not cellulose. Therefore, in their model BG did not exist in cellulose-to glucose-reaction (r_2). It showed precise predictions still could be obtained. In addition, the values of the parameters were very close to those reported by Kadam et al. (2004).

The parameters here were derived from numerical estimation from the time course reaction curves rather than initial reaction rates reported by other researcher (Drissen et al., 2007). It is shown in Table 4 that kinetic parameters of N188 derived from these models and standard enzymatic assay are quite different. Thus, the parameters estimated from these models could not represent real properties of the enzymes. Furthermore, parameters of r_3 proposed by Kadam et al (2004) and this research are different. As far as our understanding, in Kadam's study, all values were derived from the hydrolysis of lignocellulose with a mixture of cellulase and BG. In this research, parameters of r_3 were obtained from hydrolysis of cellobiose by BG without the participation of Celluclast. Similar observation was also found that two strategies in Model 1 used different experimental data for parameter estimation, and resulted in different parameter values of r_1 and r_2. Thus, it can be concluded that the parameters derived from these models should not be regarded as "universal values". However, for engineering application, these semimechanistic models are good for describing the observed/measured enzyme-substrate conversion kinetics and product inhibition mechanism fairly well. Therefore, as long as these type of models are used under the range of their validity (substrate type, enzyme source and substrate concentration), they can support process design and technology improvement efforts at pilot and full-scale studies (Morales-Rodriguez et al., 2011) and optimization studies (Morales-Rodriguez et al., 2012).

Conclusions

Semimechanistic model proposed by Kadam was modified and validated by individual experimental data with different enzyme loading/combination and substrate loading/type. Factors such as experimental

data used for parameters estimation and transglycosylation were evaluated step by step during the modification of the models. Among the models, Model 3 can describe the hydrolysis behavior under high cellulose concentration up to 150 g/L, except when (1) substrate properties differs in parameter estimation and validation, and (2) different enzyme source are found. Lastly, the parameters are not universal, the variation depend on the experimental conditions used for parameters estimation. However, this model provides a simple and useful way of describing the dynamics of cellulose hydrolysis. As long as these types of models are used bearing in mind their limitations and staying within the range of their validity (e.g. do not extrapolate to glucose concentrations, use a proper data set to estimate parameter values), they can provide useful tools for simulations and support process design, optimisation and scale-up efforts at industrial activities.

Acknowledgements

Morales-Rodriguez, R. acknowledges the Mexican National Council for Science and Technology (CONACyT, project #145066) for the financial support for the development of part of this project. Tsai, Chien-Tai acknowledges Balduck, Guillaume for the support of experimental works.

Reference

Andrić, P., Meyer, A., Jensen, P., Dam-Johansen, K. 2010. Effect and Modeling of Glucose Inhibition and In Situ Glucose Removal During Enzymatic Hydrolysis of Pretreated Wheat Straw. *Applied Biochemistry and Biotechnology*, **160**(1), 280-297.

Bansal, P., Hall, M., Realff, M.J., Lee, J.H., Bommarius, A.S. 2009. Modeling cellulase kinetics on lignocellulosic substrates. *Biotechnology Advances*, **27**(6), 833-848.

Bhiri, F., Chaabouni, S., Limam, F., Ghrir, R., Marzouki, N. 2008. Purification and Biochemical Characterization of Extracellular β-Glucosidases from the Hypercellulolytic Pol6 Mutant of Penicillium occitanis. *Applied Biochemistry and Biotechnology*, **149**(2), 169-182.

Drissen, R.E.T., Maas, R.H.W., Van Dermaarel, M.J.E.C., Kabel, M.K., Schols, H.A., Tramper, J., Beeftink, H.H. 2007. A generic model for glucose production from various cellulose sources by a commercial cellulase complex. *Biocatalysis and Biotransformation*, **25**(6), 419-429.

Gan, Q., Allen, S.J., Taylor, G. 2003. Kinetic dynamics in heterogeneous enzymatic hydrolysis of cellulose: an overview, an experimental study and mathematical modelling. *Process Biochemistry*, **38**(7), 1003-1018.

Gharpuray, M.M., Lee, Y.-H., Fan, L.T. 1983. Structural modification of lignocellulosics by pretreatments to enhance enzymatic hydrolysis. *Biotechnology and Bioengineering*, **25**(1), 157-172.

Ghose, T.K. 1987. Measurement of Cellulase Activities. *Pure and Applied Chemistry*, **59**(2), 257-268.

Gnansounou, E. 2010. Production and use of lignocellulosic bioethanol in Europe: Current situation and perspectives. *Bioresource Technology*, **101**(13), 4842-4850.

Gusakov, A.V., Sinitsyn, A.P., Goldsteins, G.H., Klyosov, A.A. 1984. Kinetics and mathematical model of hydrolysis and transglycosylation catalysed by cellobiase. *Enzyme and Microbial Technology*, **6**(6), 275-282.

Hanes, C.S. 1932. Studies on plant amylases: The effect of starch concentration upon the velocity of hydrolysis by the amylase of germinated barley. *Biochemical Journal* **26**(5), 1406-0.

Jørgensen, H., Vibe-Pedersen, J., Larsen, J., Felby, C. 2007. Liquefaction of lignocellulose at high-solids concentrations. *Biotechnology and Bioengineering*, **96**(5), 862-870.

Kadam, K.L., Rydholm, E.C., McMillan, J.D. 2004. Development and Validation of a Kinetic Model for Enzymatic Saccharification of Lignocellulosic Biomass. *Biotechnology Progress*, **20**(3), 698-705.

Kono, H., Waelchli, M.R., Fujiwara, M., Erata, T., Takai, M. 1999. Transglycosylation of cellobiose by partially purified Trichoderma viride cellulase. *Carbohydrate Research*, **319**(1-4), 29-37.

Larsen, J., Østergaard Petersen, M., Thirup, L., Wen Li, H., Krogh Iversen, F. 2008. The IBUS Process – Lignocellulosic Bioethanol Close to a Commercial Reality. *Chemical Engineering & Technology*, **31**(5), 765-772.

Medve, J., Karlsson, J., Lee, D., Tjerneld, F. 1998. Hydrolysis of microcrystalline cellulose by cellobiohydrolase I and endoglucanase II from Trichoderma reesei: Adsorption, sugar production pattern, and synergism of the enzymes. *Biotechnology and Bioengineering*, **59**(5), 621-634.

Morales-Rodriguez, R., Meyer, A.S., Gernaey, K.V., Sin, G. 2011. Dynamic model-based evaluation of process configurations for integrated operation of hydrolysis and co-fermentation for bioethanol production from lignocellulose. *Bioresource Technology*, **102**(2), 1174-1184.

Morales-Rodriguez, R., Meyer, A.S., Gernaey, K.V., Sin, G. 2012. A framework for model-based optimization of bioprocesses under uncertainty: Lignocellulosic ethanol production case. *Computers & Chemical Engineering*, **42**, 115-129.

Movagarnejad, K., Sohrabi, M., Kaghazchi, T., Vahabzadeh, F. 2000. A model for the rate of enzymatic hydrolysis of cellulose in heterogeneous solid-liquid systems. *Biochemical Engineering Journal*, **4**(3), 197-206.

Nidetzky, B., Zachariae, W., Gercken, G., Hayn, M., Steiner, W. 1994. Hydrolysis of cellooligosaccharides by Trichoderma reesei cellobiohydrolases: Experimental data and kinetic modeling. *Enzyme and Microbial Technology*, **16**(1), 43-52.

Ooshima, H., Kurakake, M., Kato, J., Harano, Y. 1991. Enzymatic activity of cellulase adsorbed on cellulose and its change during hydrolysis. *Applied Biochemistry and Biotechnology*, **31**(3), 253-266.

Pal, S., Banik, S.P., Ghorai, S., Chowdhury, S., Khowala, S. 2010. Purification and characterization of a thermostable intra-cellular [beta]-glucosidase with transglycosylation properties from filamentous fungus Termitomyces clypeatus. *Bioresource Technology*, **101**(7), 2412-2420.

Philippidis, G.P., Smith, T.K., Wyman, C.E. 1993. Study of the enzymatic hydrolysis of cellulose for production of fuel ethanol by the simultaneous saccharification and fermentation process. *Biotechnology and Bioengineering*, **41**(9), 846-853.

Rosgaard, L., Pedersen, S., Meyer, A. 2007. Comparison of Different Pretreatment Strategies for Enzymatic Hydrolysis of Wheat and Barley Straw. *Applied Biochemistry and Biotechnology*, **143**(3), 284-296.

Sin, G., Meyer, A.S., Gernaey, K.V. 2010. Assessing reliability of cellulose hydrolysis models to support biofuel process design—Identifiability and uncertainty analysis. *Computers & Chemical Engineering*, **34**(9), 1385-1392.

Sluiter, A., Hames, B., Ruiz, R., Scarlata, C., Sluiter, J., Templeton, D., Crocker, D. 2006. Laboratory analytical procedure 002, Determination of structural carbohydrate and lignin in biomass. Retrieved from http://www.nrel.gov/biomass/analytical_procedures.html.

Sternberg, D., Vijayakumar, P., Reese, E.T. 1977. beta-Glucosidase: microbial production and effect on enzymatic hydrolysis of cellulose. *Canadian Journal of Microbiology*, **23**(2), 139-147.

Watanabe, T., Sato, T., Yoshioka, S., Koshijima, T., Kuwahara, M. 1992. Purificication and properties of Aspergillus niger β-glucosidase. *European Journal of Biochemistry*, **209**(2), 651-659.

Yang, B., Willies, D.M., Wyman, C.E. 2006. Changes in the enzymatic hydrolysis rate of Avicel cellulose with conversion. *Biotechnology and Bioengineering*, **94**(6), 1122-1128.

Zhang, Y.-H.P., Lynd, L.R. 2004. Toward an aggregated understanding of enzymatic hydrolysis of cellulose: Noncomplexed cellulase systems. *Biotechnology and Bioengineering*, **88**(7), 797-824.

Zheng, Y., Pan, Z., Zhang, R., Jenkins, B.M. 2009. Kinetic modeling for enzymatic hydrolysis of pretreated creeping wild ryegrass. *Biotechnology and Bioengineering*, **102**(6), 1558-1569.

Fig. 1.

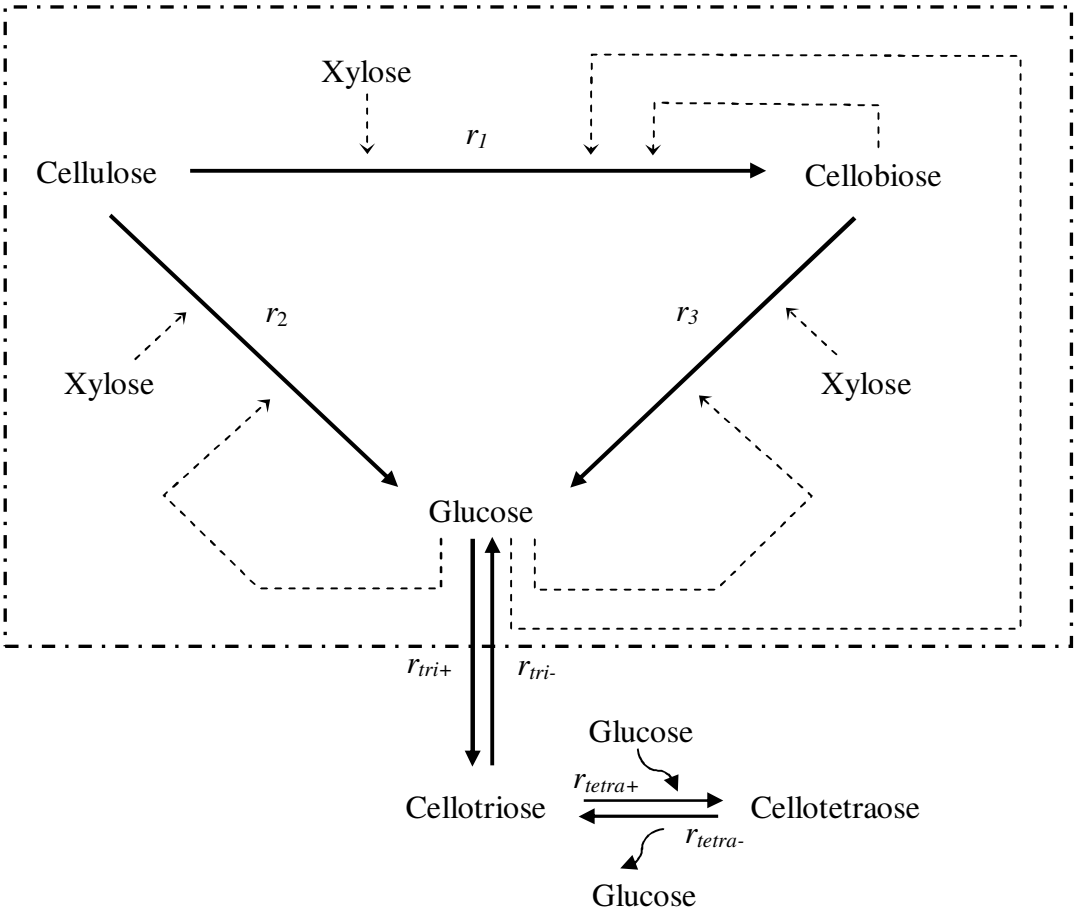

Fig. 1. Reaction scheme for modelling cellulose hydrolysis. Bold dashed-dot square illustrates the original Kadam model. Solid arrows represent the reaction routes and the dashed arrows shows the inhibition of sugars on the reactions. Modified from Kadam et al. (2004).

Fig. 2.

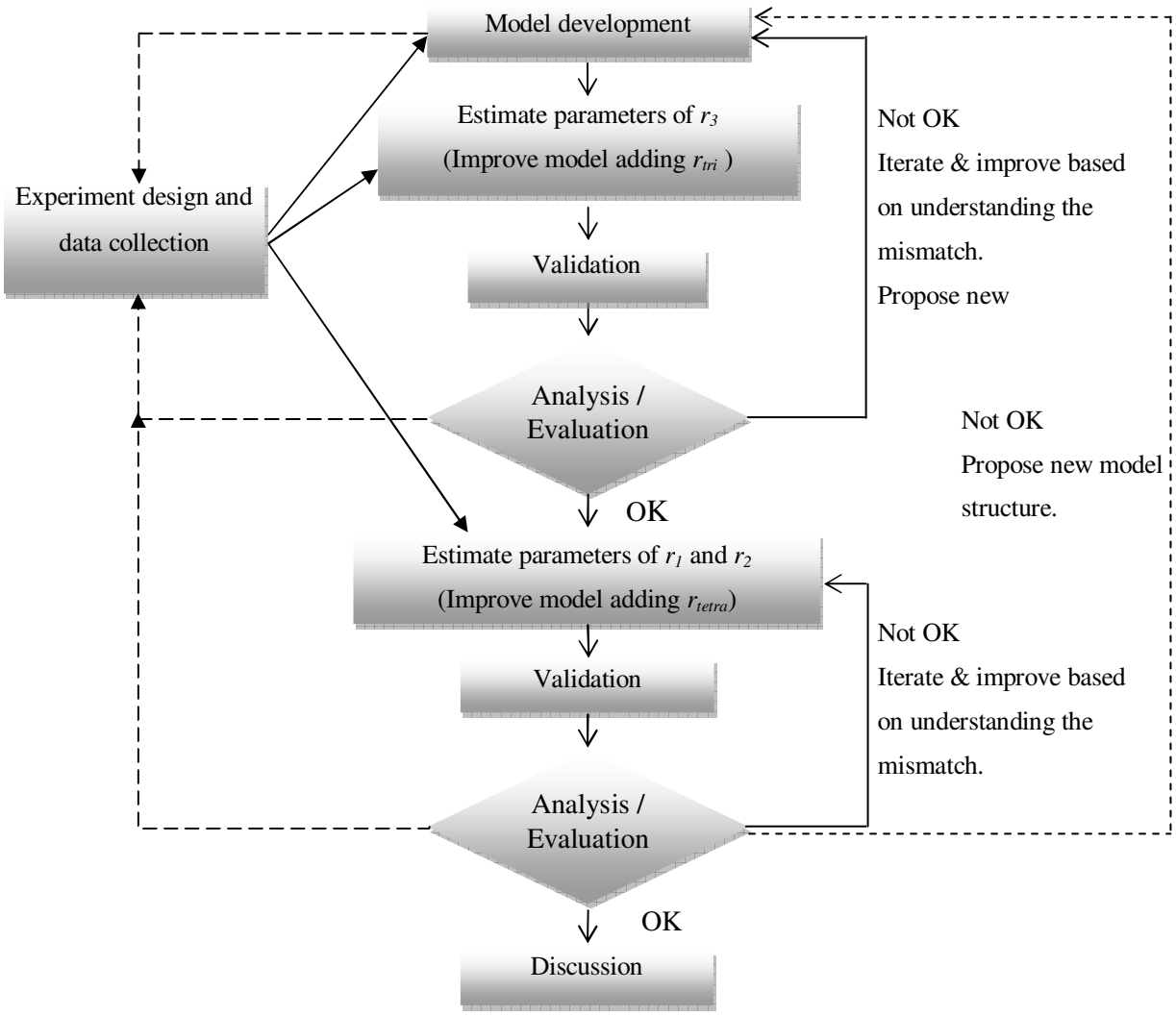

Fig. 2. Framework for construction of cellulosic hydrolysis mathematical model and parameter estimation.

Fig. 3.

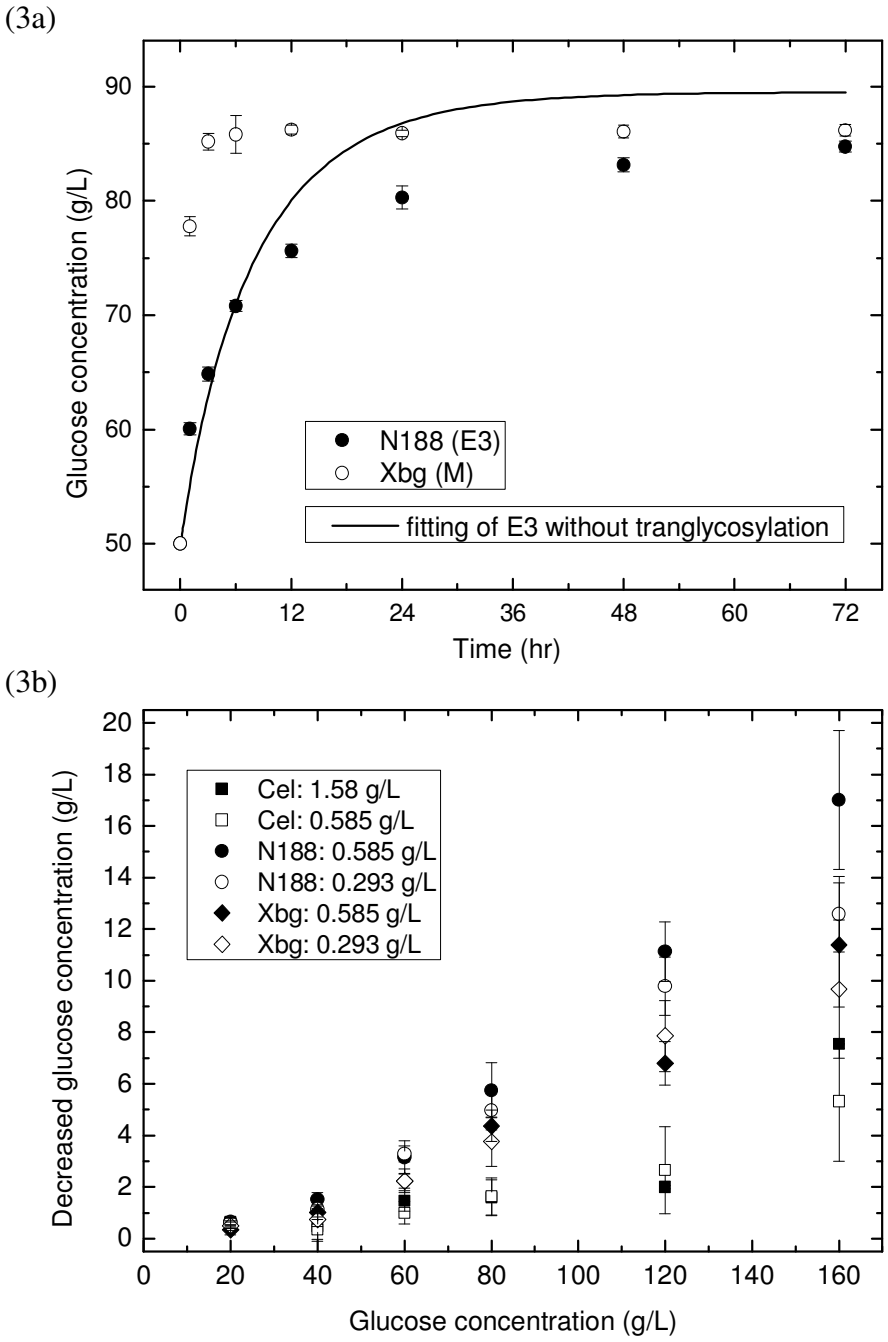

Fig. 3. The effect of transglycosylation. (a) Hydrolysis of 37.5 g/L cellobiose by N188 and Xbg (3.9 mg protein/g cellobiose) with initial background of glucose 50 g/L . Solid line indicates the fitting by model without introducing transglycosylation into the model. (b) Transglycosylation effect observed by incubating Celluclast 1.5L, N188 and Xbg at different glucose concentrations.

Fig. 4.

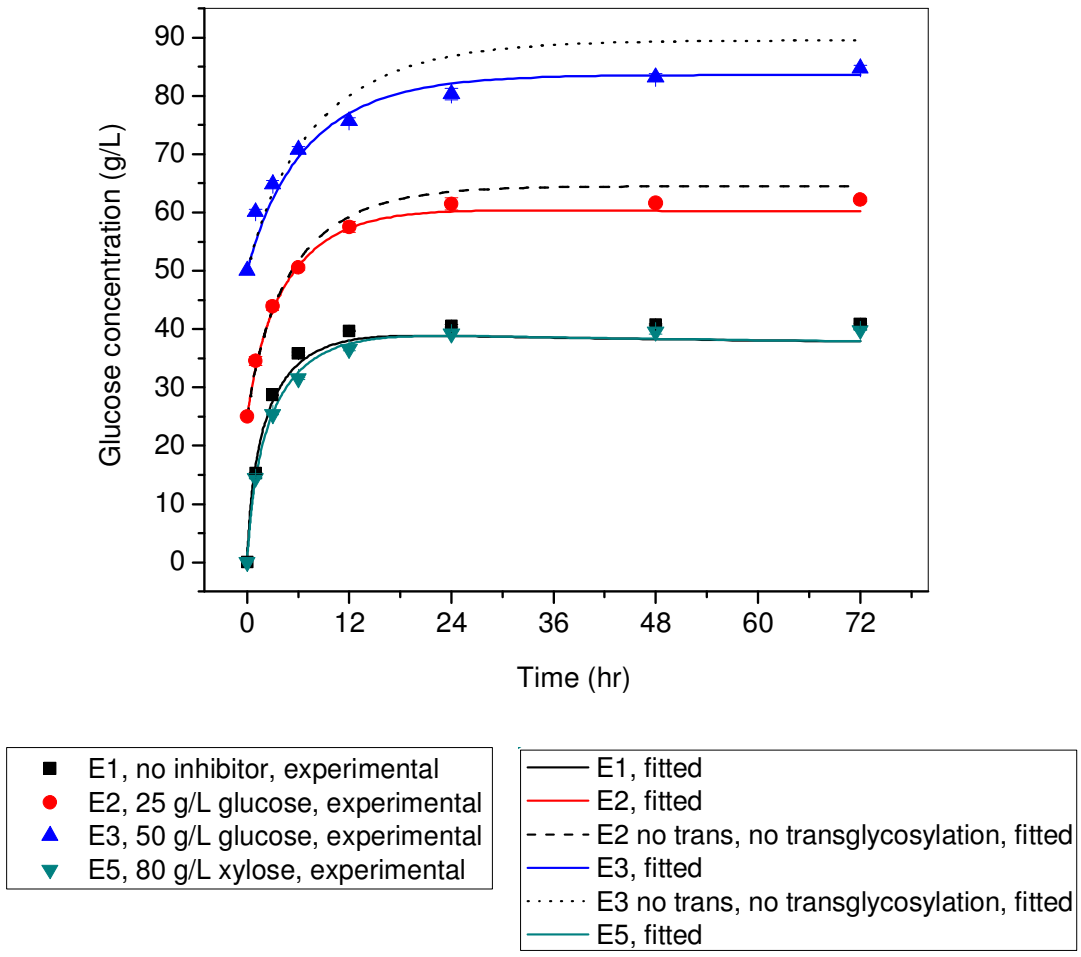

Fig. 4. Parameters estimation of cellobiose hydrolysis reaction. 37.5 g/L Avicel hydrolyzed by N188 (3.9 mg-protein/g-substrate). Different inhibitor background with 40 g/L xylose (E4) is not shown. Fitting curves without the incorporation of transglycosylation reaction are also shown.

Fig. 5a.

(5a)

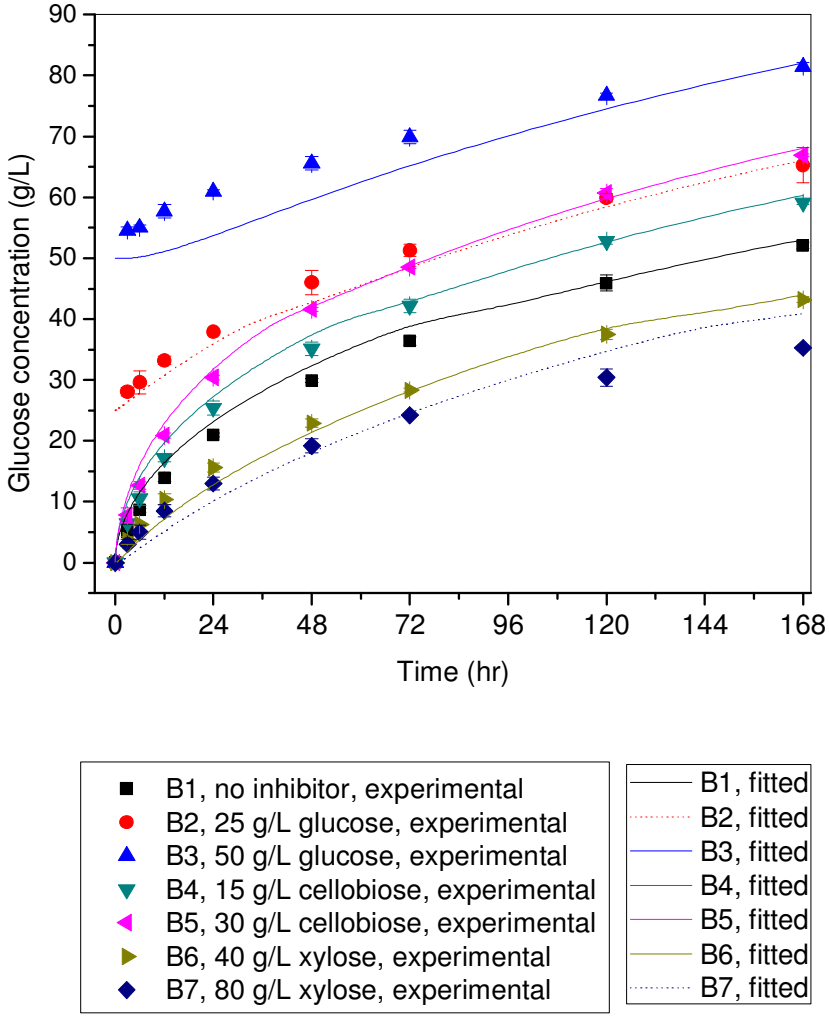
Glucose concentration (g/L)
Time (hr)
0
10
20
30
40
50
60
70
80
90
0
24
48
72
96
120
144
168
B1, no inhibitor, experimental
B2, 25 g/L glucose, experimental
B3, 50 g/L glucose, experimental
B4, 15 g/L cellobiose, experimental
B5, 30 g/L cellobiose, experimental
B6, 40 g/L xylose, experimental
B7, 80 g/L xylose, experimental
B1, fitted
B2, fitted
B3, fitted
B4, fitted
B5, fitted
B6, fitted
B7, fitted

Fig. 5b.

(5b)

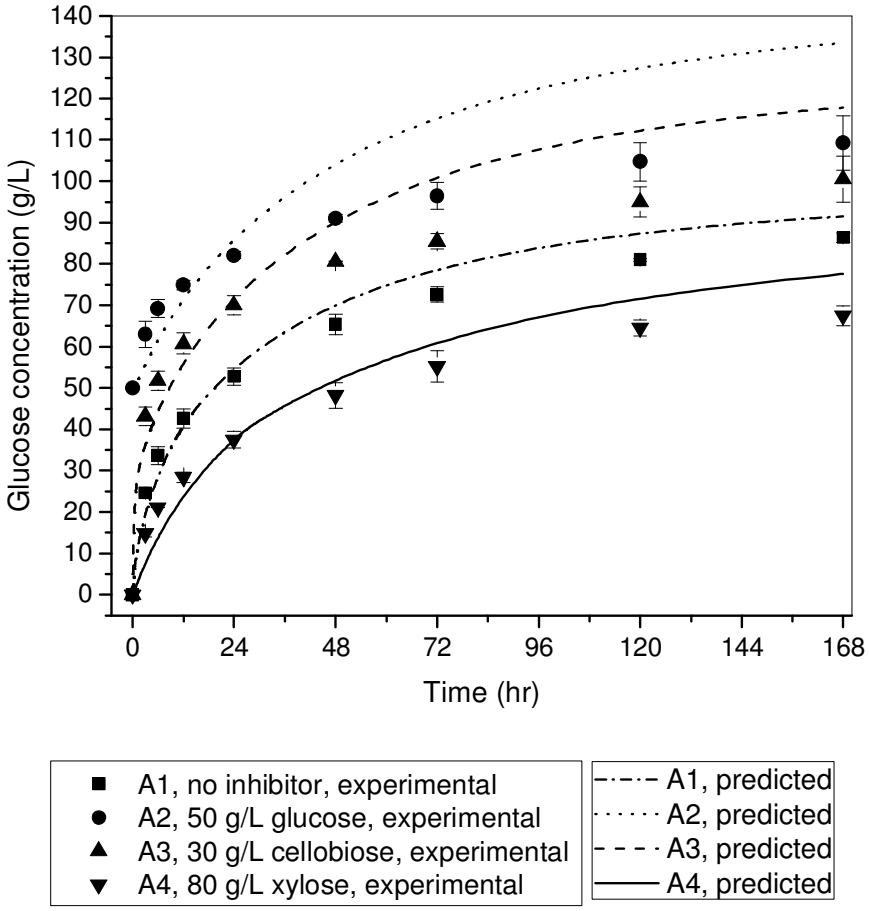

Fig. 5. Evaluation of strategy 1 of Model 1 by enzymatic hydrolysis of 100 g/L Avicel. (a) parameter estimation by data sets that hydrolyzed by Cel (10.5 mg-protein/g-substrate) with different initial background inhibitors: B1, no inhibitor; B2, 25 g/L glucose; B3, 50 g/L glucose; B4, 15 g/L cellobiose; B5, 30 g/L cellobiose; B6, 40 g/L xylose; B7, 80 g/L xylose. (b) Validation of the model by data sets that hydrolyzed by Cel (15.8 mg-protein/g-substrate) and N188 (5.9 mg-protein/g-substrate) with different background inhibitors: A1, no background; A2, 50 g/L glucose; A3, 30 g/L cellobiose; A4, 80 g/L xylose.

Fig. 6a.

(6a)

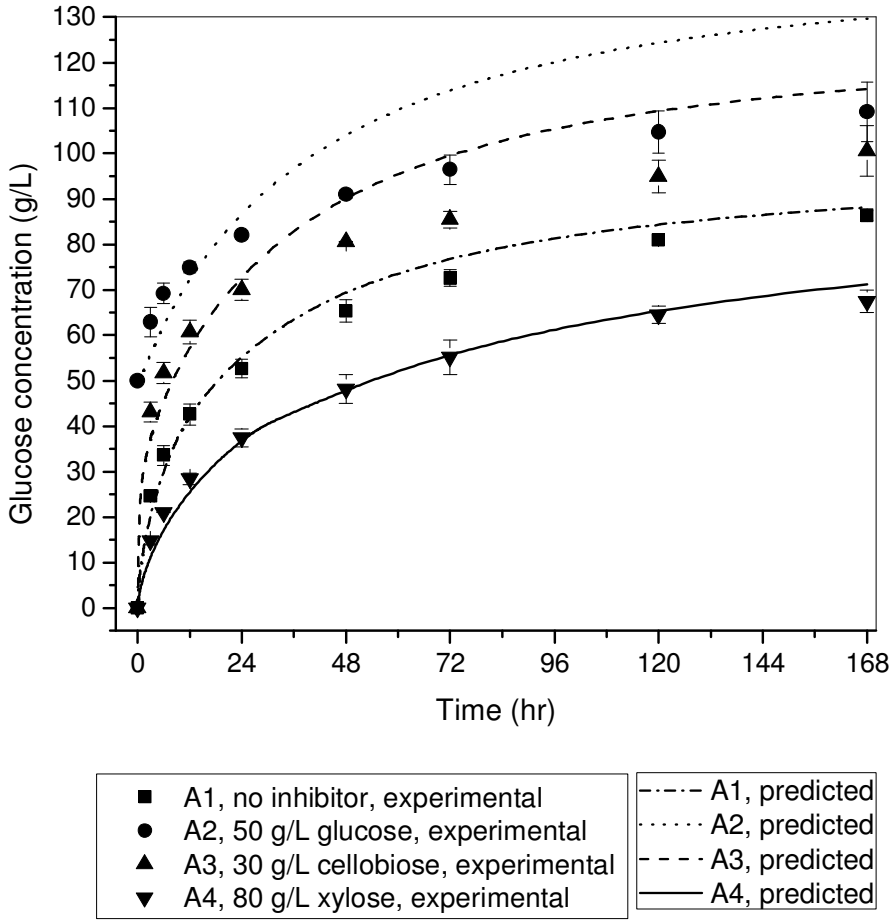
Glucose concentration (g/L)
Time (hr)
0
10
20
30
40
50
60
70
80
90
100
110
120
130
0
24
48
72
96
120
144
168
A1, no inhibitor, experimental
A2, 50 g/L glucose, experimental
A3, 30 g/L cellobiose, experimental
A4, 80 g/L xylose, experimental
A1, predicted
A2, predicted
A3, predicted
A4, predicted

Fig. 6b.

(6b)

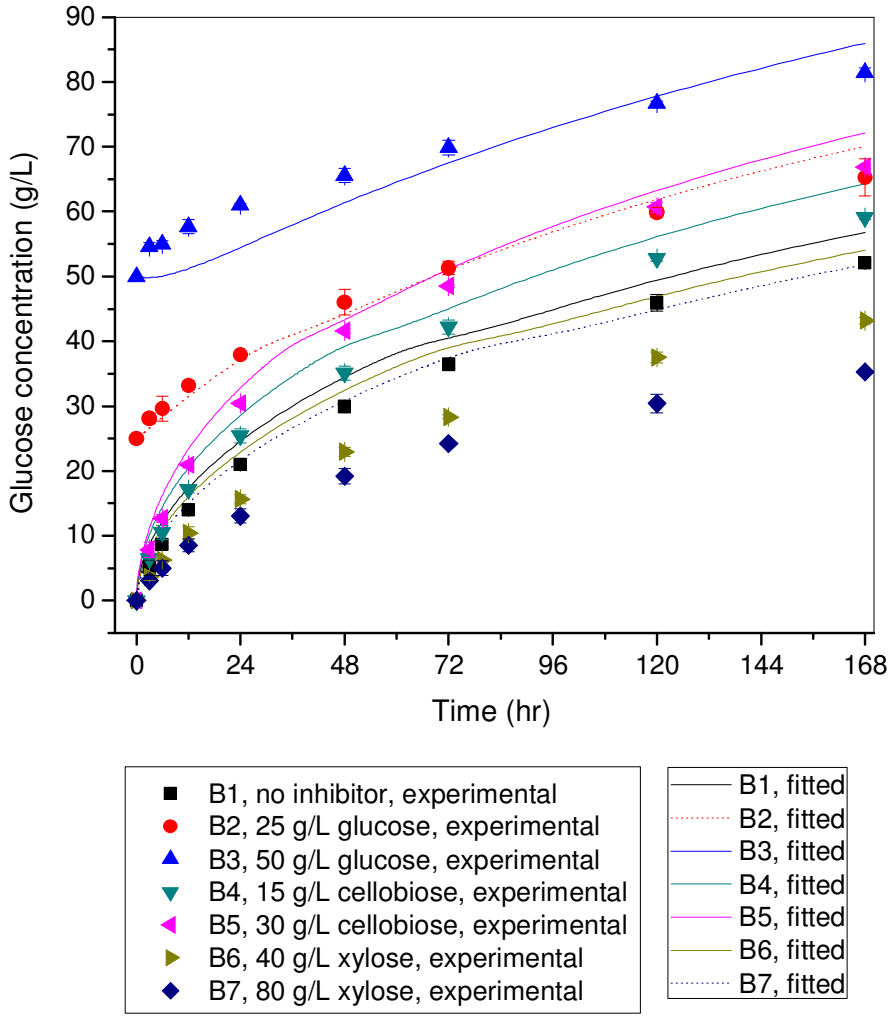

Fig. 6. Evaluation of strategy 2 of Model 1 by enzymatic hydrolysis of 100 g/L Avicel. (a) Parameter estimation by data sets that hydrolyzed by Cel (15.8 mg-protein/g-substrate) and N188 (5.9 mg-protein/g-substrate) with different background inhibitors: A1, no background; A2, 50 g/L glucose; A3, 30 g/L cellobiose; A4, 80 g/L xylose. (b) Validation by data sets that hydrolyzed by Cel (10.5 mg-protein/g-substrate) with different initial background inhibitors: B1, no inhibitor; B2, 25 g/L glucose; B3, 50 g/L glucose; B4, 15 g/L cellobiose; B5, 30 g/L cellobiose; B6, 40 g/L xylose; B7, 80 g/L xylose.

Fig. 7a.

(7a)

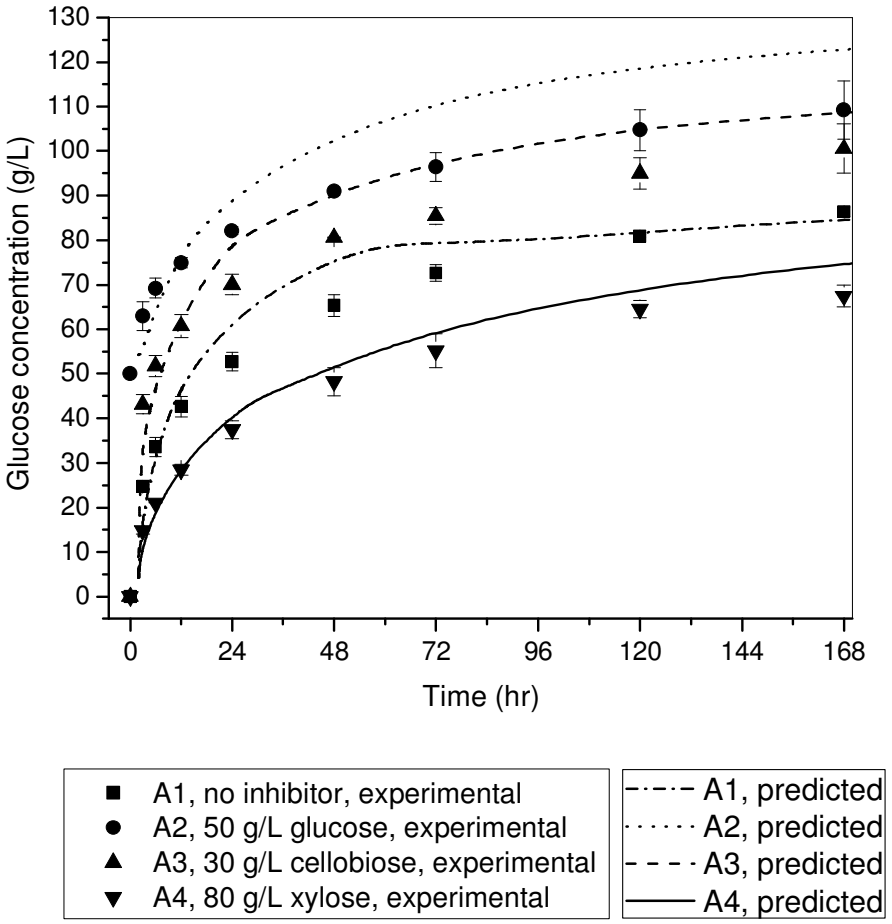
Glucose concentration (g/L)
Time (hr)
0
10
20
30
40
50
60
70
80
90
100
110
120
130
0
24
48
72
96
120
144
168
A1, no inhibitor, experimental
A2, 50 g/L glucose, experimental
A3, 30 g/L cellobiose, experimental
A4, 80 g/L xylose, experimental
A1, predicted
A2, predicted
A3, predicted
A4, predicted

Fig. 7b.

(7b)

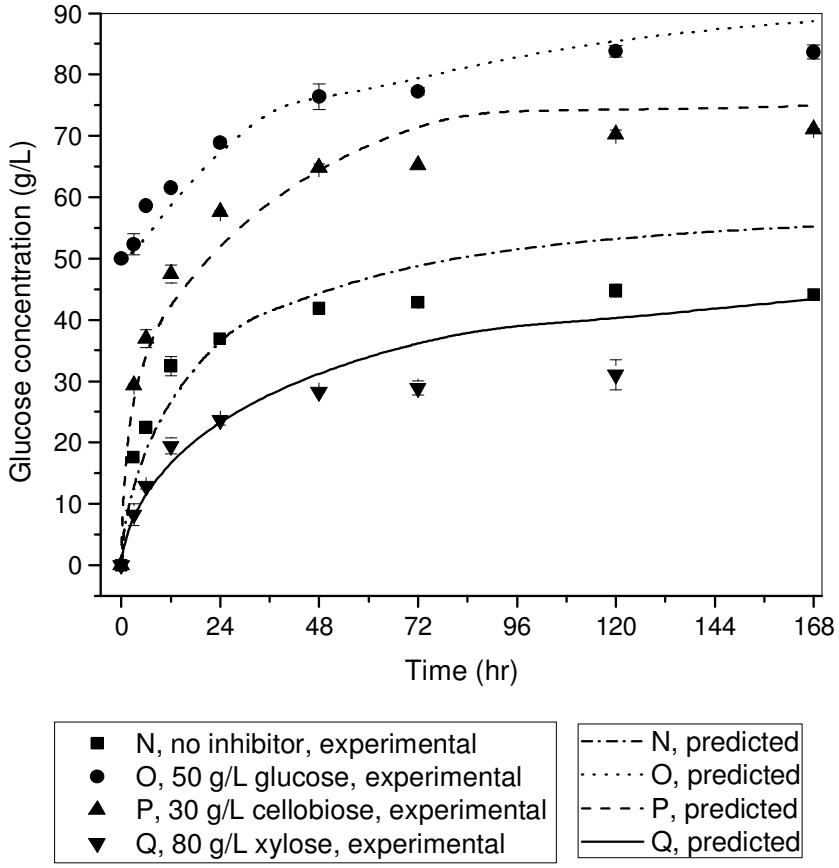

Fig. 7. Evaluation of Model 2 ($G_{cr,tetr}$=75). (a) Enzymatic hydrolysis of 100 g/L Avicel. Parameter estimation by data sets that hydrolyzed by Cel (15.8 mg-protein/g-substrate) and N188 (5.9 mg-protein/g-substrate) with different background inhibitors: A1, no background; A2, 50 g/L glucose; A3, 30 g/L cellobiose; A4, 80 g/L xylose. (b) Validation of the model by 90 g/L pretreated barley straw hydrolyzed by Cel (15.8 mg-protein/g-substrate) and N188 (5.9 mg-protein/g-substrate) with different background inhibitors: N, no background; O, 50 g/L glucose; P, 30 g/L cellobiose; Q, 80 g/L xylose.

Fig. 8.

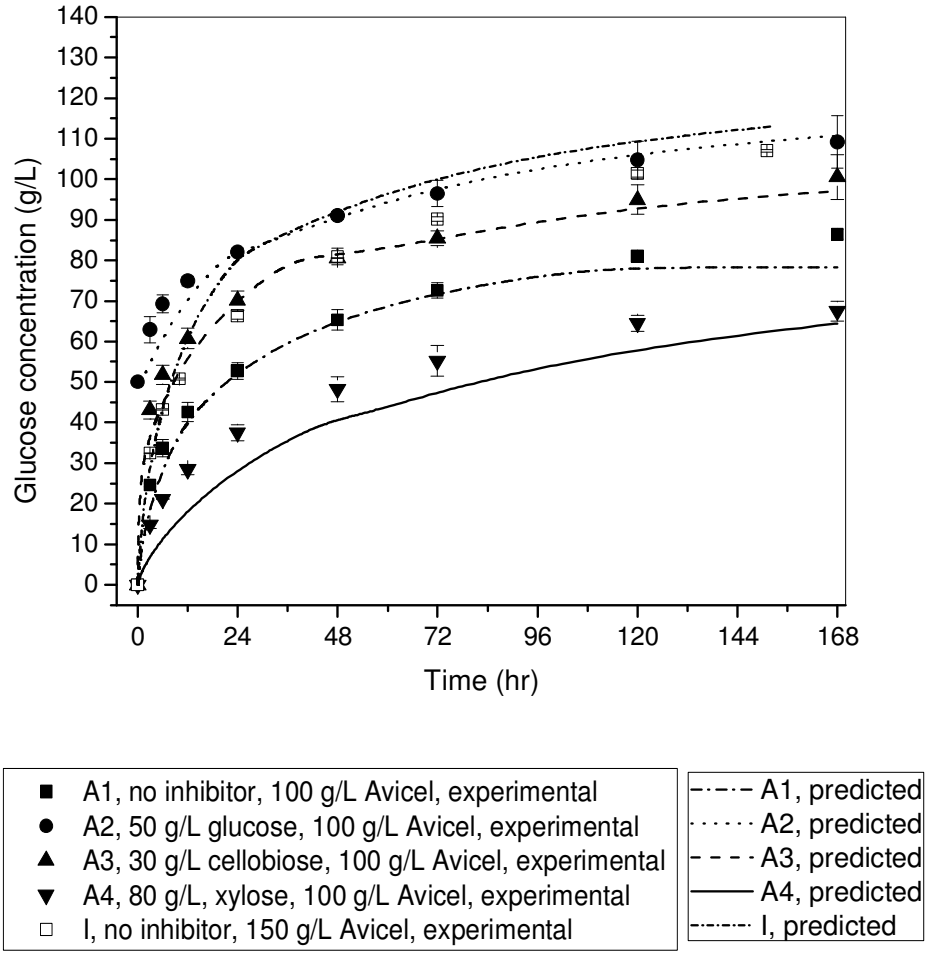

Fig. 8. Evaluation of Model 3 by enzymatic hydrolysis of 100 and 150 g/L Avicel. Parameter estimation by data sets that hydrolyzed by Cel (15.8 mg-protein/g-substrate) and N188 (5.9 mg-protein/g-substrate) with different background inhibitors: A1, no background; A2, 50 g/L glucose; A3, 30 g/L cellobiose; A4, 80 g/L xylose; I, no background.

Fig. 9.

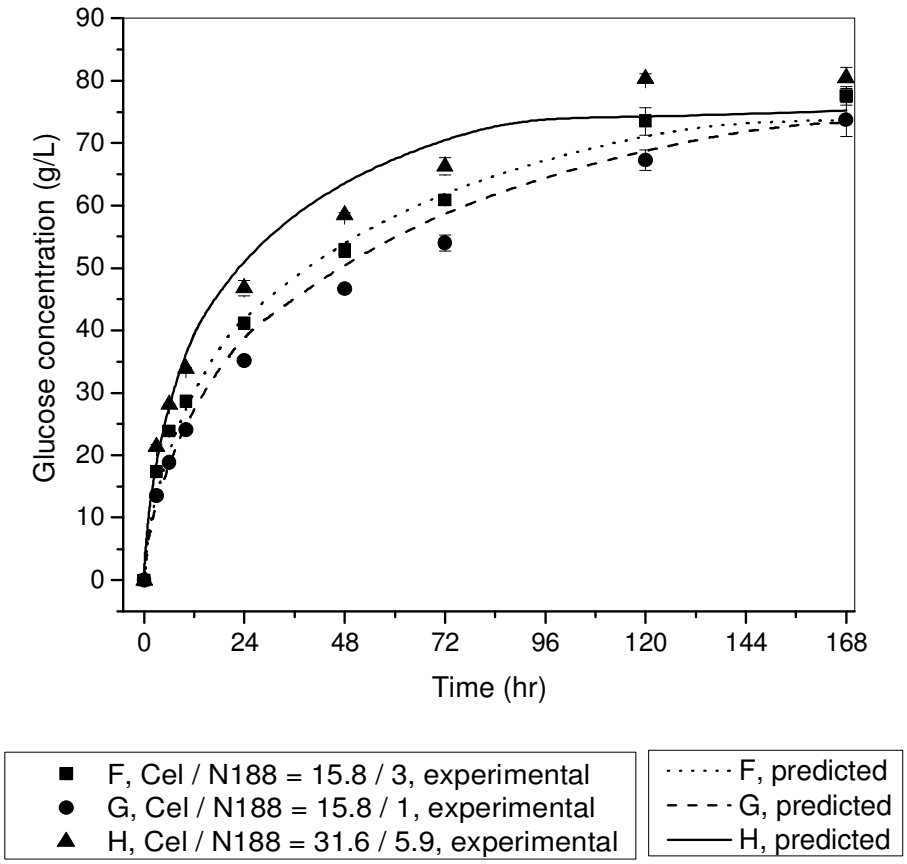

Fig. 9. Validation of Model 2 ($G_{cr,tetr}$=75) by enzymatic hydrolysis of 100 g/L Avicel under different enzyme loading and combination. F, Cel/N188 = 15.8/3 mg-protein/g-substrate; G, Cel/N188 = 15.8/1 mg-protein/g-substrate; H, Cel/N188 = 31.6/5.9 mg-protein/g-substrate. Background inhibitor is 40 g/L xylose.

Fig. 10.

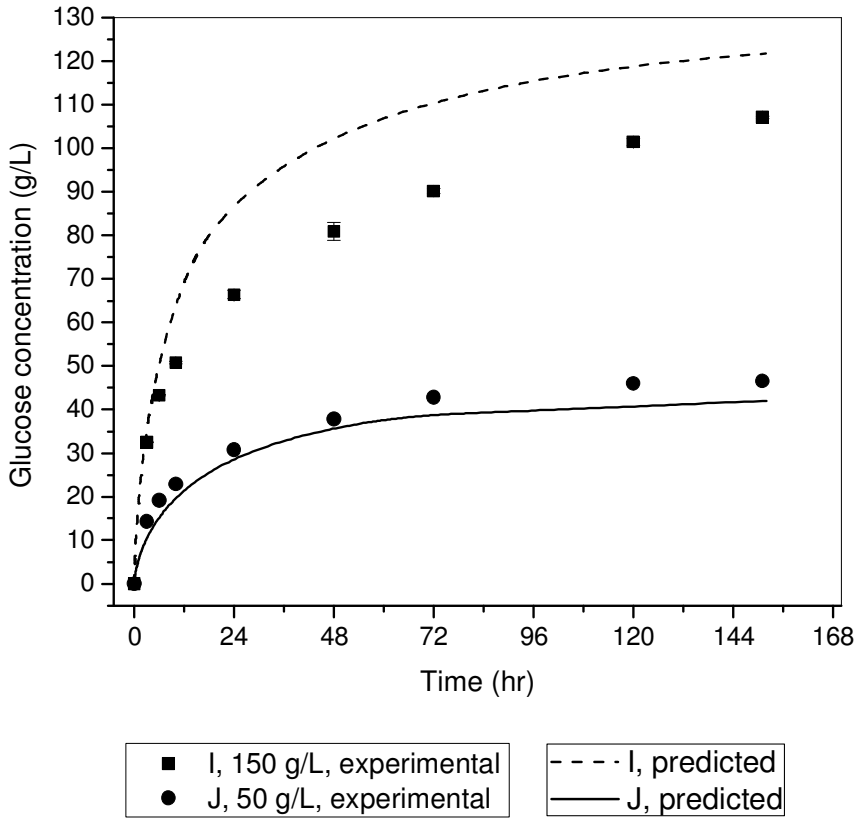

Fig. 10. Validation of Model 2 ($G_{cr,tetr}$=75) by enzymatic hydrolysis of different Avicel concentration by Cel (15.8 mg-protein/g-substrate) and N188 (5.9 mg-protein/g-substrate). I, 150 g/L; J, 50 g/L.

Table 1

Experimental conditions of hydrolysis for the development and validation of kinetic model

Substrate (g/L)	Enzyme / Substrate * (mg-protein/g-substrate)	Case no.	Initial Inhibitor	Inhibitor concentration (g/L)
Avicel (100)	Cel + N188 (15.8 + 5.9)	A1	No	-
		A2	Glucose	50
		A3	Cellobiose	30
		A4	Xylose	80
	Cel (10.5)	B1	No	-
		B2, B3	Glucose	25 and 50
		B4, B5	Cellobiose	15 and 30
		B6, B7	Xylose	40 and 80
	Cel (21.1)	C1	No	-
		C2, C3	Glucose	25 and 50
		C4, C5	Cellobiose	15 and 30
		C6, C7	Xylose	40 and 80
Cellobiose (37.5)	N188 (1.95)	D1	No	-
		D2, D3	Glucose	25 and 50
		D4, D5	Xylose	40 and 80
	N188 (3.9)	E1	No	-
		E2, E3	Glucose	25 and 50
		E4, E5	Xylose	40 and 80
Avicel (100)	Cel + N188 (15.8 + 3)	F	Xylose	40
	Cel + N188 (15.8 + 1)	G	Xylose	40
	Cel + N188 (31.6 + 5.9)	H	Xylose	40
Avicel (150)	Cel + N188 (15.8 + 5.9)	I	No	-
Avicel (50)	Cel + N188 (15.8 + 5.9)	J	No	-
Avicel (100)	Cel + Xbg (15.8 + 1)	K	Xylose	40
Cellobiose (37.5)	Xbg (3.9)	L	No	-
		M	Glucose	50
Barley straw (90)	Cel + N188 (15.8 + 5.9)	N	No	-
		O	Glucose	50
		P	Cellobiose	30
		Q	Xylose	80

* Enzyme loading: “Cel + N188 (15.8 + 5.9)” in No. A1~A5 means the enzyme/substrate in the reaction is 15.8 mg-Cel protein/g Avicel + 5.9 mg-N188 protein/g Avicel

Table 2

Summary of the models proposed in this research

	Model 1	Model 2 ($G_{cr,Tetra}$ = 75 or 80)	Model 3 ($G_{cr,Tetra}$ = 75 or 80)
r_3	$r_3 = \frac{k_{3r}E_{2F}G_2}{K_{3M}(1+\frac{G}{K_{3IG}}+\frac{X}{K_{3IX}})+G_2}$ Transglycosylation for cellotriose production: 3G $\rightleftarrows$ $G_3 + 2H_2O$ $r_{Tri} = r_{Tri+} - r_{Tri-} = k_{G3+}\left[\frac{1}{1+e^{(G_{cr,Tri}-G)}}\right]G - k_{G3-}\left[\frac{1}{1+e^{(G_{cr,Tri}-G)}}\right]G_3$ ($G_{cr,Tri}$ = 40) Data E1~E5 are used for parameter estimation		
r_1 and r_2	$r_1 = \frac{k_{1r}E_{1B}R_S S}{1+\frac{G_2}{K_{1IG2}}+\frac{G}{K_{1IG}}+\frac{X}{K_{1IX}}}$ $r_2 = \frac{k_{2r}(E_{1B}+E_{2B})R_S S}{1+\frac{G_2}{K_{2IG2}}+\frac{G}{K_{2IG}}+\frac{X}{K_{2IX}}}$ [Strategy 1] Data B1~B7 were used for parameter estimation [Strategy 2] Data A1~A4 were used for parameter estimation	$r_1 = \frac{k_{1r}E_{1B}R_S S}{1+\frac{G_2}{K_{1IG2}}+\frac{G}{K_{1IG}}+\frac{X}{K_{1IX}}}$ $r_2 = \frac{k_{2r}(E_{1B}+E_{2B})R_S S}{1+\frac{G_2}{K_{2IG2}}+\frac{G}{K_{2IG}}+\frac{X}{K_{2IX}}}$ Transglycosylation for cellotetraose production $G + G_3 \rightleftarrows G_4 + H_2O$ $r_{Tetra} = r_{Tetra+} - r_{Tetra-} = k_{G4+}\left[\frac{1}{1+e^{(G_{cr,Tetra}-G)}}\right]G - k_{G4-}\left[\frac{1}{1+e^{(G_{cr,Tetra}-G)}}\right]G_4$ ($G_{cr,Tetra}$ = 75 or 80) Data A1~A4 were used for parameter estimation	$r_1 = \frac{k_{1r}E_{1B}R_S S}{K_{1M}(1+\frac{G_2}{K_{1IG2}}+\frac{G}{K_{1IG}}+\frac{X}{K_{1IX}})+S}$ $r_2 = \frac{k_{2r}(E_{1B}+E_{2B})R_S S}{K_{2M}(1+\frac{G_2}{K_{2IG2}}+\frac{G}{K_{2IG}}+\frac{X}{K_{2IX}})+S}$ Transglycosylation for cellotetraose production $G + G_3 \rightleftarrows G_4 + H_2O$ $r_{Tetra} = r_{Tetra+} - r_{Tetra-} = k_{G4+}\left[\frac{1}{1+e^{(G_{cr,Tetra}-G)}}\right]G - k_{G4-}\left[\frac{1}{1+e^{(G_{cr,Tetra}-G)}}\right]G_4$ ($G_{cr,Tetra}$ = 75 or 80) Data A1~A4 and I were used for parameter estimation.

Table 3

Parameters of the Langmuir adsorption and substrate reactivity.

Parameters	Value
Avicel	
K_{1ad} (L/g protein)	1.238
K_{2ad} (L/g protein)	1.865
E_{1max} (g protein/g substrate)	0.03257
E_{2max} (g protein/g substrate)	0.00102
Pretreated barley straw	
K_{1ad} (L/g protein)	18.98
K_{2ad} (L/g protein)	21.71
E_{1max} (g protein/g substrate)	0.02255
E_{2max} (g protein/g substrate)	0.00517
α	1

Table 4

Hydrolysis kinetic parameters derived from model simulation and standard assay.

		Model 1 (strategy 1)	Model 1 (strategy 2)	Model 2 ($G_{cr,tetr}$=75)	Model 2 ($G_{cr,tetr}$=80)	Model 3 ($G_{cr,tetr}$=75)	Model 3 ($G_{cr,tetr}$=80)	Kadam's value	N188, standard assay	Xbg, standard assay
1	k_{1r}	18.86	24.19	16.73	16.45	23.28	24.16	22.3		
2	K_{1IG2}	0.0042	0.0040	0.0089	0.0058	0.0465	0.0498	0.015		
3	K_{1IG}	0.0947	0.2041	0.2773	0.3720	0.4284	0.6635	0.1		
4	K_{1IX}	0.0859	0.0463	0.0558	0.0998	0.4613	0.2608	0.1		
5	K_{1M}	-	-	-	-	6.7546	6.4797	-		
6	k_{2r}	7.926	7.077	6.593	3.101	7.449	6.768	7.18		
7	K_{2IG2}	147.87	3467.78	118.68	1328.59	129.39	128.97	132.0		
8	K_{2IG}	0.01509	0.0199	0.0286	0.0059	0.0496	0.0323	0.04		
9	K_{2IX}	0.0097	1.2023	1.6950	1.2514	288.9385	39.6367	0.2		
10	K_{2M}	-	-	-	-	6.5795	6.8987	-		
11	K_{3r}			228.264				285.5	91690	815497
12	K_{3M}			3.1740				24.3	0.5814	1.4924
13	K_{3IG}			0.9617				3.9	0.6600	1.4061
14	K_{3IX}			12.614				201.0	12.007	9.1762
15	k_{G3+}			0.0075						
16	k_{G3-}			0.1197						
17	k_{G4+}	-	-	0.0083	0.0070	0.0079	0.0102			
18	k_{G4-}	-	-	0.0754	0.0523	0.1249	0.0785			

The order of the calculations are as following: 1) k_{3r}, K_3M, K_{3IG}, k_{+G3}, k_{-G3}, 2) K_{3IX}, 3) k_{1r}, K_{1IG2}, $K_{1IG,}$ K_{1IX}, K_{1M}, k_{2r}, K_{2IG2}, $K_{2IG,}$ K_{2IX}, K_{2M}, k_{+G4}, k_{-G4}, *4)* K_{1IX}, K_{2IX}

Table 5

WSSE analysis of the performance of the models.

	Model 1 Strategy 1	**Model 1 Strategy 2**	**Model 2 ($G_{cr,\ Tetra}$=75)**	**Model 2 ($G_{cr,\ Tetra}$=80)**	**Model 3 ($G_{cr,\ Tetra}$=75)**	**Model 3 ($G_{cr,\ Tetra}$=80)**
A	1696	2874	1081	1190	1502	1300
B	622	2417	4085	1533	1253	921
C	1835	5254	6981	1811	4556	2230
D	336	336	336	336	336	336
E	263	263	263	263	263	263
F	446	68	64	203	273	530
G	350	34	70	167	101	236
H	193	103	165	183	164	261
I	1138	3928	2397	1518	314	647
J	550	217	139	260	667	412
K[a]	-	-	-	-	-	-
N	331	407	372	567	339	262
O	169	363	50	72	136	25
P	385	368	126	507	389	131
Q	337	398	411	428	285	273
WSSE sum	**8650**	**17032**	**16540**	**9039**	**10579**	**7827**

[a] Data set K involved XBg, not evaluated by WSSE analysis.

Appendix 5.1. Evaluation of model for cellobiose-to-glucose reaction

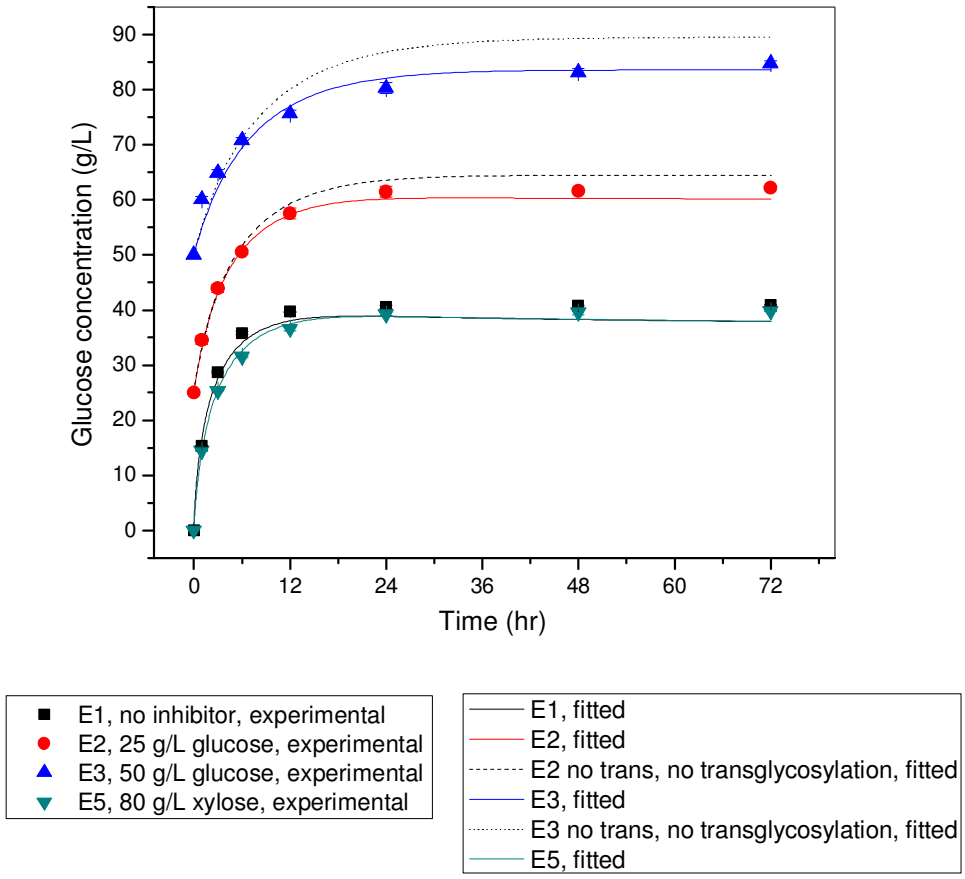

Fig. A1. Parameter estimation of cellobiose hydrolysis reaction. 37.5 g/L cellobiose hydrolyzed by N188 (3.9 mg-protein/g-substrate) with different initial inhibitor background. Background with 40 g/L xylose (E4) is not shown. Fiiting curves without the incorporation of transglycosylation reaction are also shown.

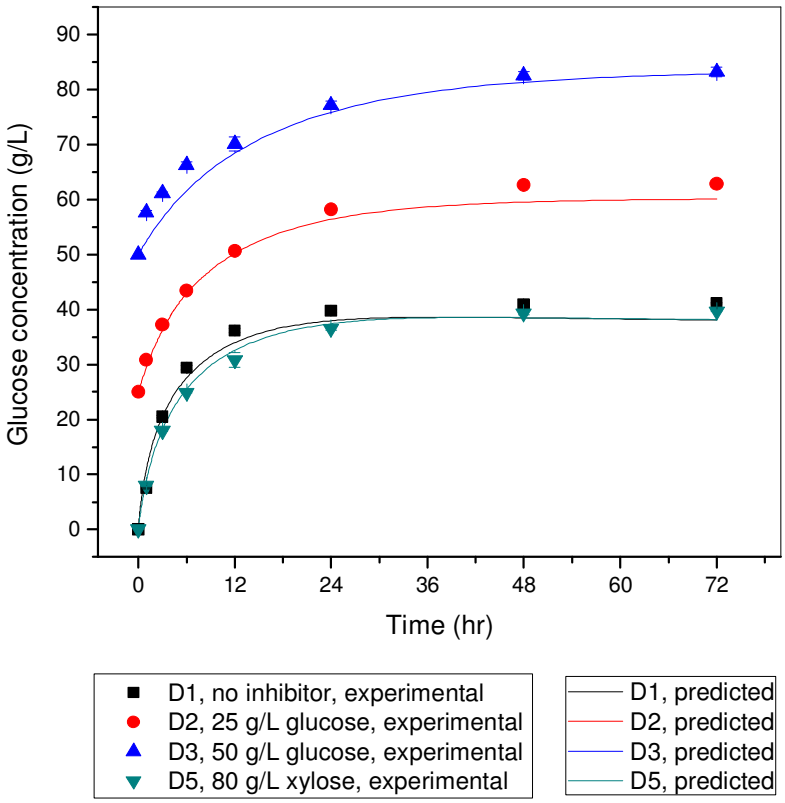

Fig. A2. Validation of cellobiose hydrolysis reaction. 37.5 g/L cellobiose hydrolyzed by N188 (1.95 mg-protein/g-substrate) with different initial inhibitor background. Background with 40 g/L xylose (D4) is not shown.

Appendix 5.2. Evaluation of Model 1 (Strategy 1)

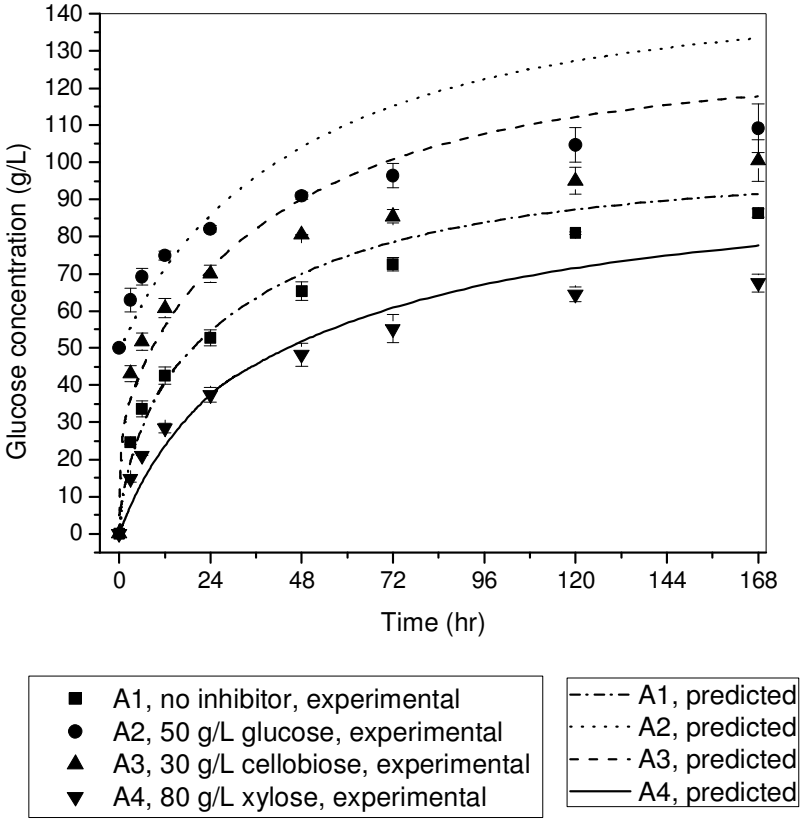

Fig. A3. Validation of Model 1 (strategy 1). 100 g/L Avicel hydrolyzed by Celluclast (15.8 mg-protein/g-substrate) + N188 (5.9 mg-protein/g-substrate) with different initial inhibitor background.

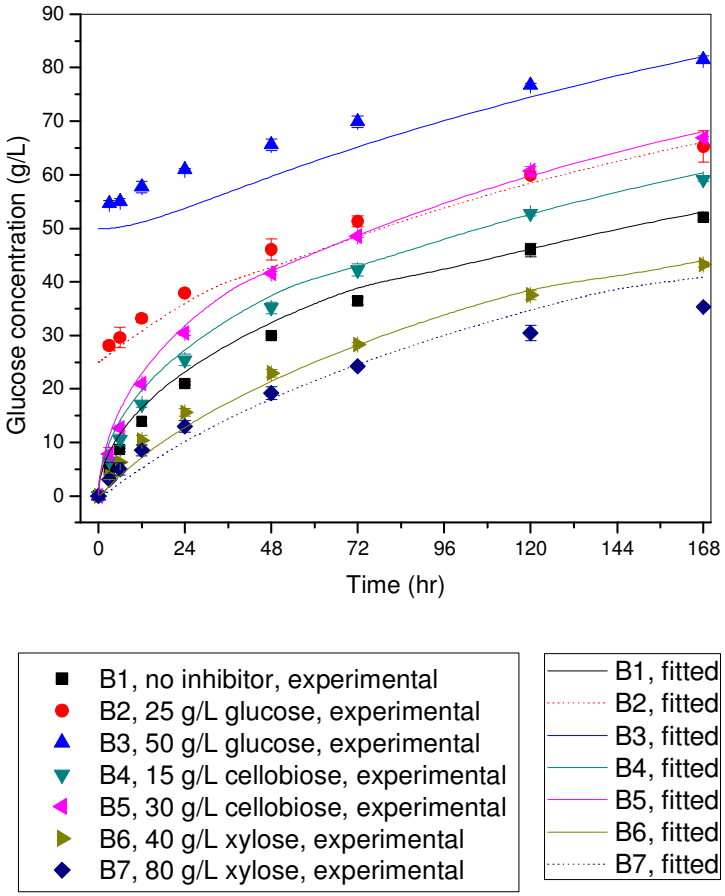

Fig. A4. Parameter estimation of Model 1 (strategy 1). 100 g/L Avicel hydrolyzed by Celluclast (10.5 mg-protein/g-substrate) with different initial inhibitor background.

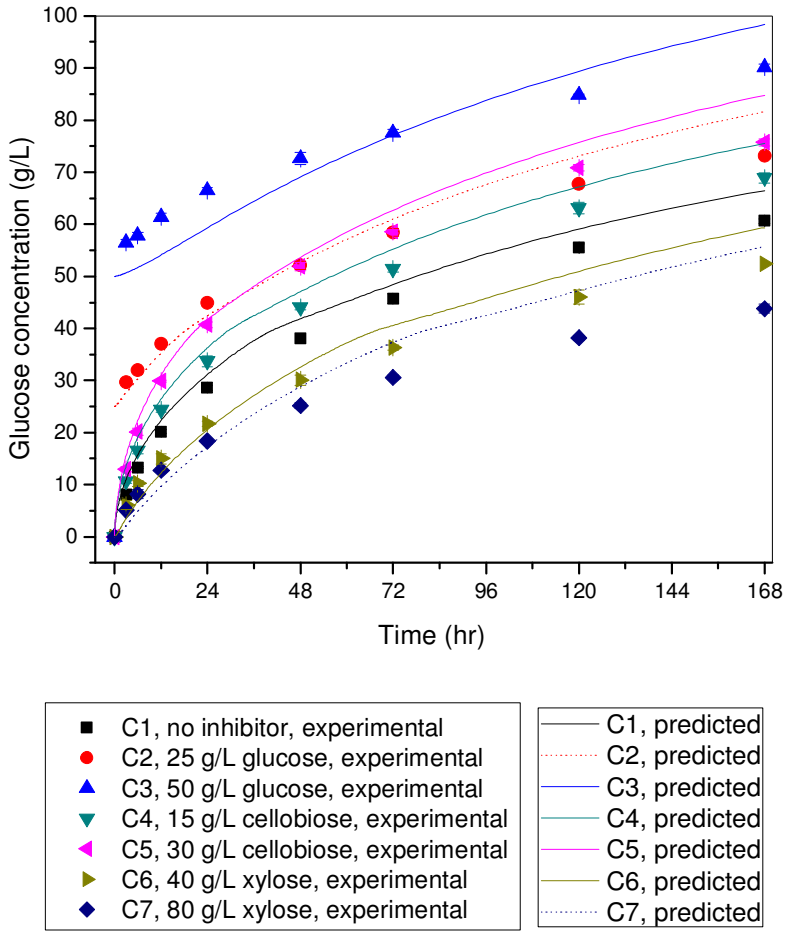

Fig. A5. Validation of Model 1 (strategy 1). 100 g/L Avicel hydrolyzed by Celluclast (21.1 mg-protein/g-substrate) with different initial inhibitor background.

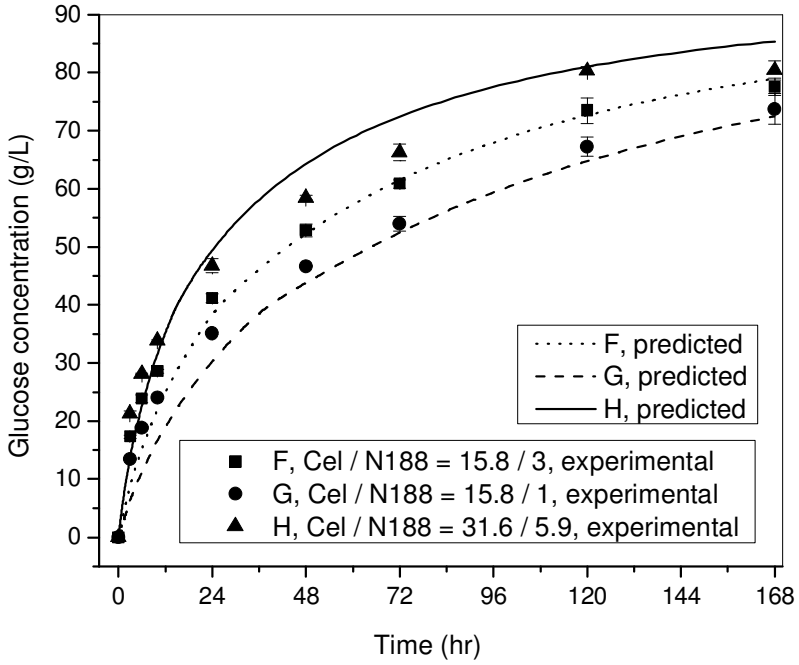

Fig. A6. Validation of Model 1 (strategy 1). 100 g/L Avicel hydrolyzed by different ratio of Celluclast/N188 loading with initial 40 g/L xylose background.

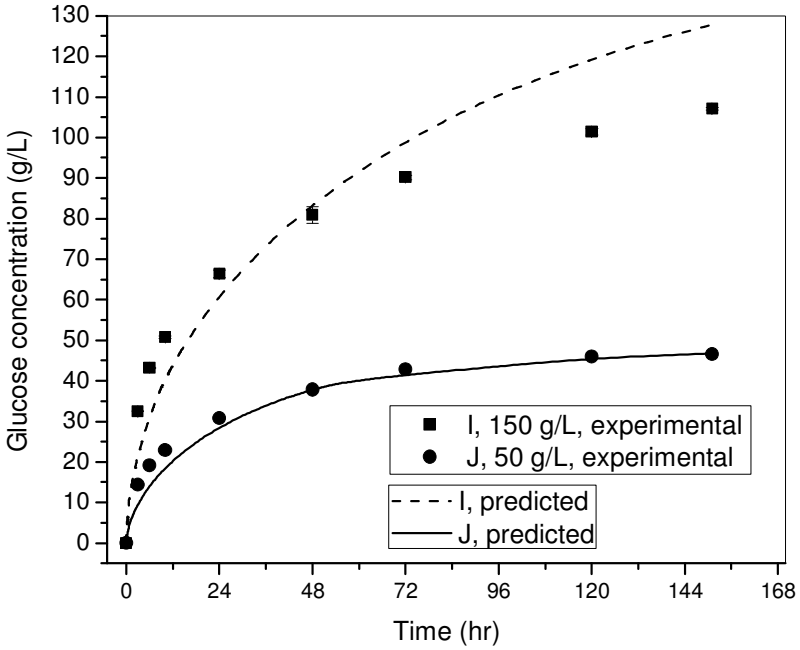

Fig. A7. Validation of Model 1 (strategy 1). 50 and 150 g/L Avicel hydrolyzed by Celluclast (15.8 mg-protein/g-substrate) + N188 (5.9 mg-protein/g-substrate).

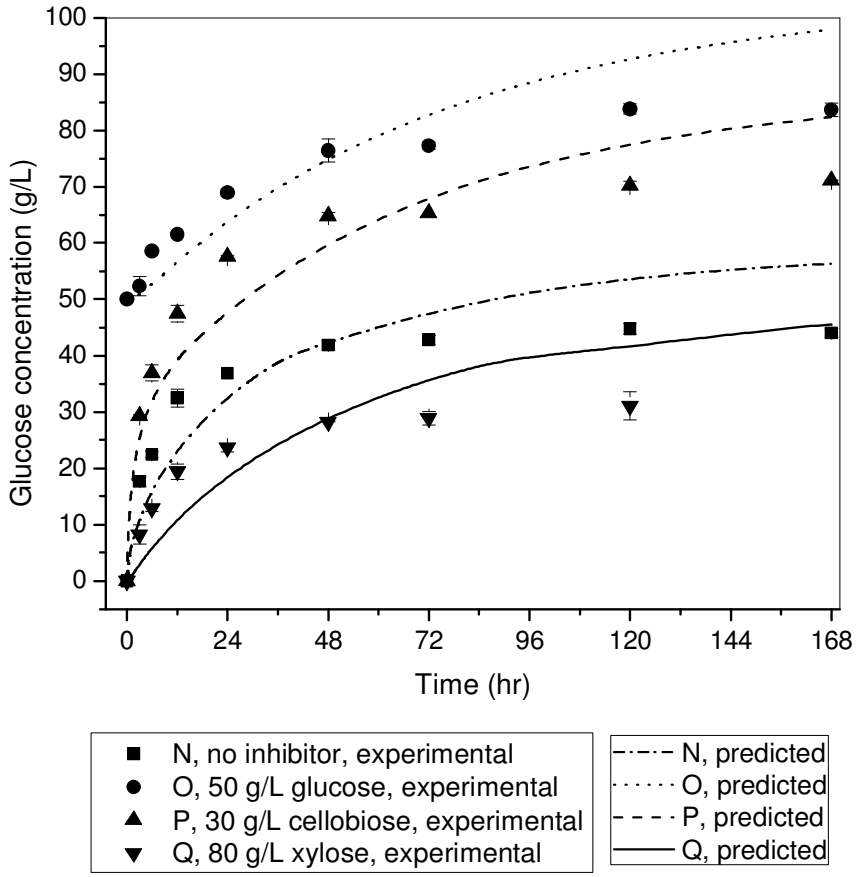

Fig. A8. Validation of Model 1 (strategy 1). 90 g/L Barley straw hydrolyzed by Celluclast (15.8 mg-protein/g-substrate) + N188 (5.9 mg-protein/g-substrate) with different initial inhibitor background.

Appendix 5.3. Evaluation of Model 1 (Strategy 2)

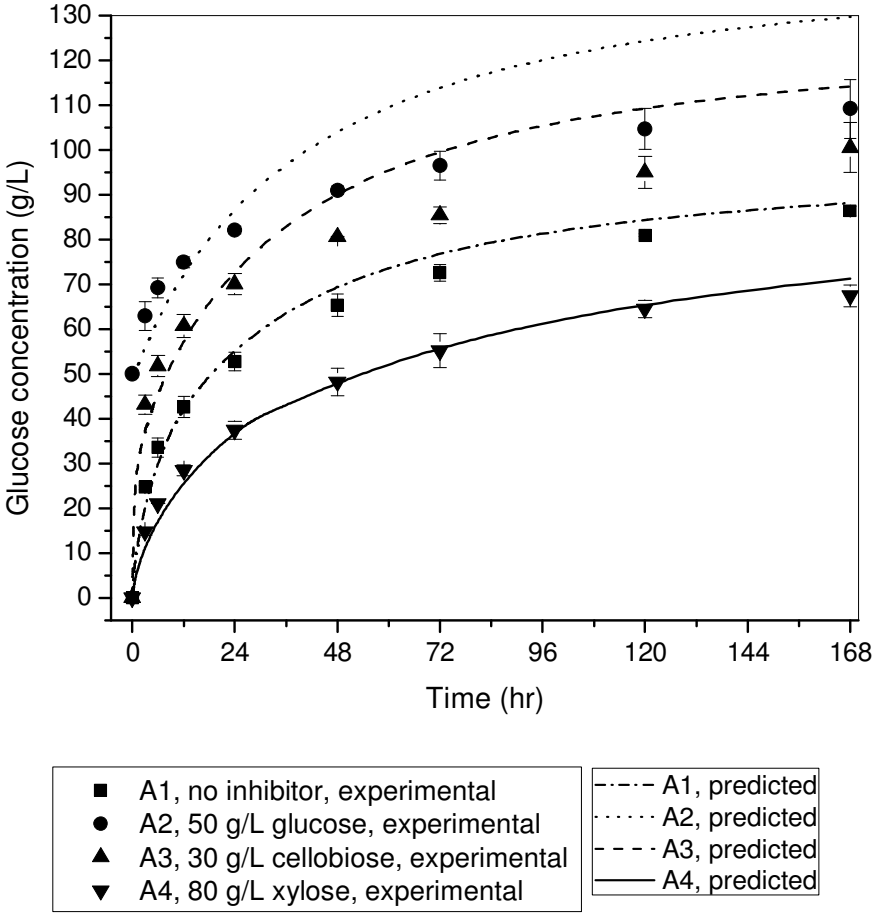

Fig. A9. Parameter estimation of Model 1 (strategy 2). 100 g/L Avicel hydrolyzed by Celluclast (15.8 mg-protein/g-substrate) + N188 (5.9 mg-protein/g-substrate) with different initial inhibitor background.

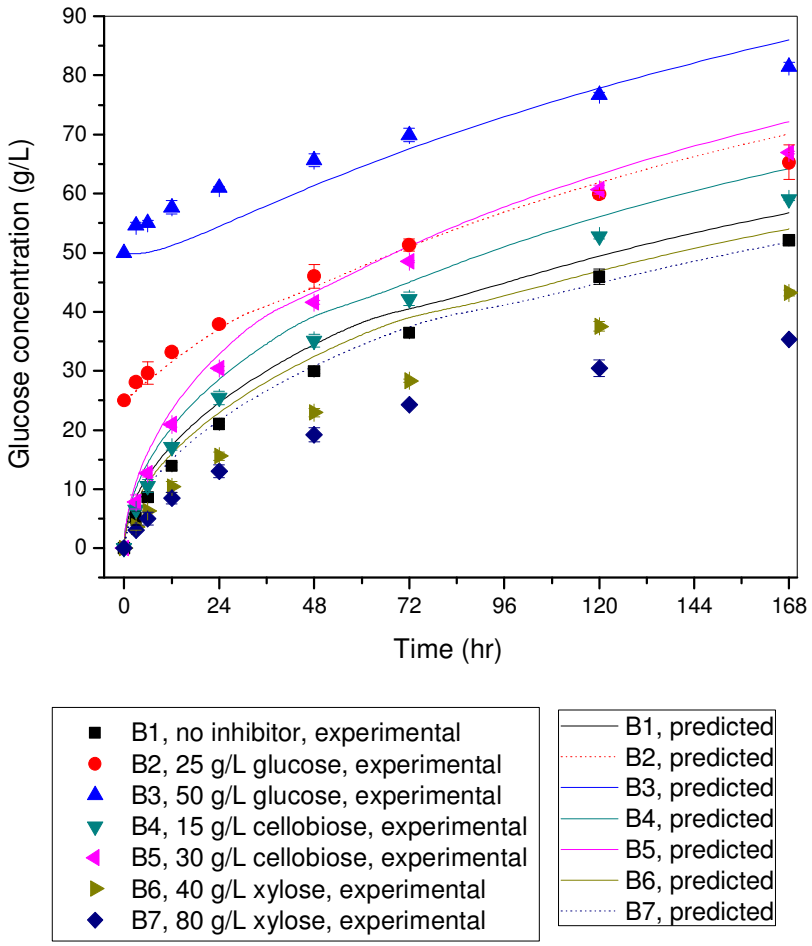

Fig. A10. Validation of Model 1 (strategy 2). 100 g/L Avicel hydrolyzed by Celluclast (10.5 mg-protein/g-substrate) with different initial inhibitor background.

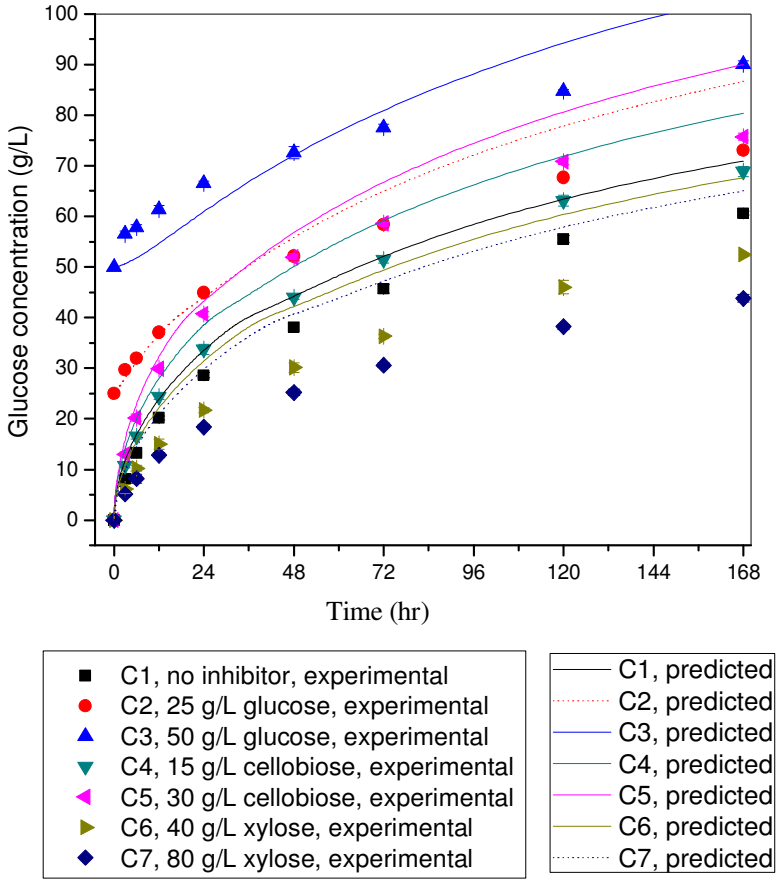

Fig. A11. Validation of Model 1 (strategy 2). 100 g/L Avicel hydrolyzed by Celluclast (21.1 mg-protein/g-substrate) with different initial inhibitor background.

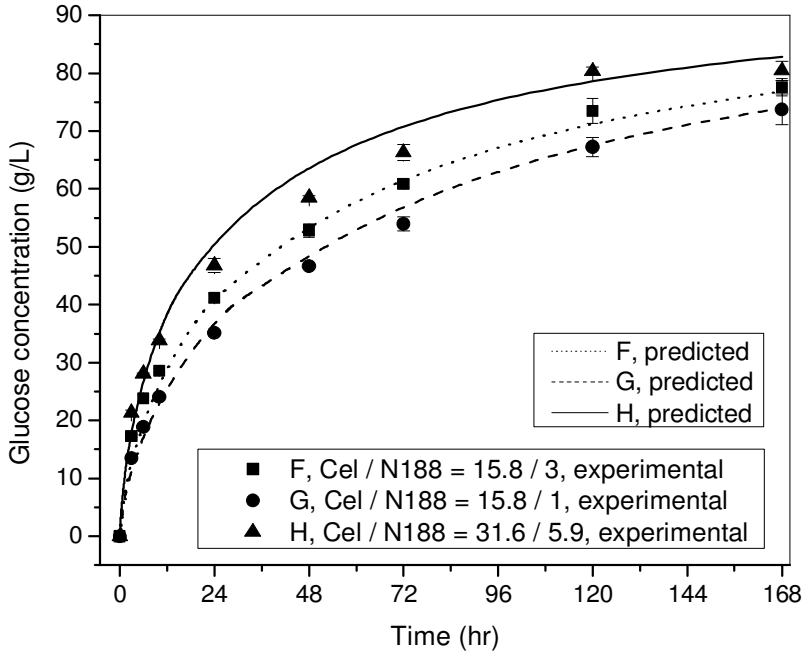

Fig. A12. Validation of Model 1 (strategy 2). 100 g/L Avicel hydrolyzed by different ratio of Celluclast/N188 loading with initial 40 g/L xylose background.

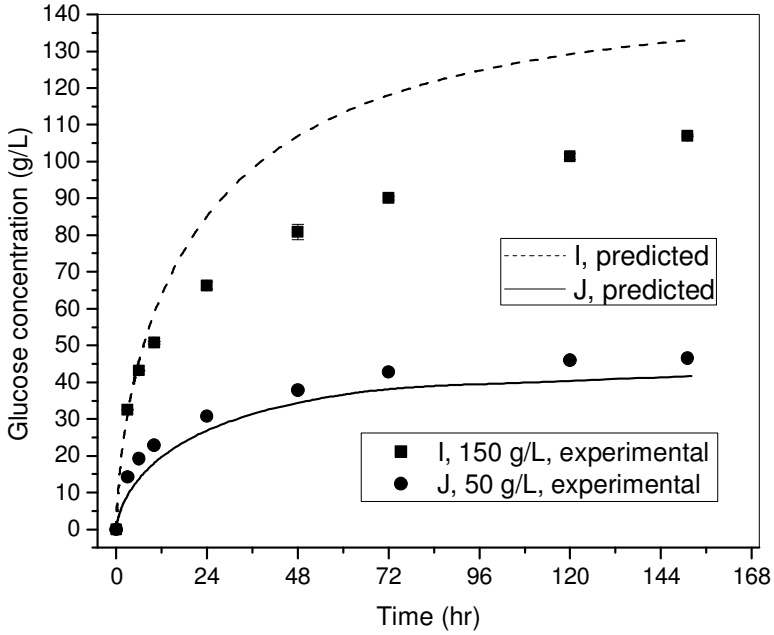

Fig. A13. Validation of Model 1 (strategy 2). 50 and 150 g/L Avicel hydrolyzed by Celluclast (15.8 mg-protein/g-substrate) + N188 (5.9 mg-protein/g-substrate).

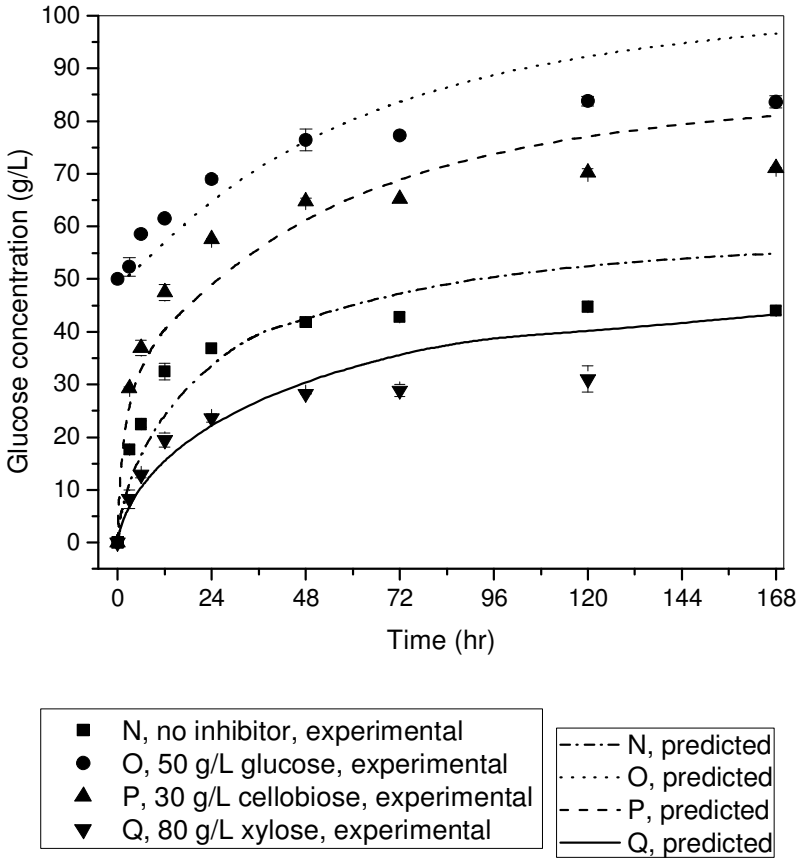

Fig. A14. Validation of Model 1 (strategy 2). 90 g/L Barley straw hydrolyzed by Celluclast (15.8 mg-protein/g-substrate) + N188 (5.9 mg-protein/g-substrate) with different initial inhibitor background.

Appendix 5.4. Evaluation of Model 2 ($G_{cr,tetra}$ = 75 g/L)

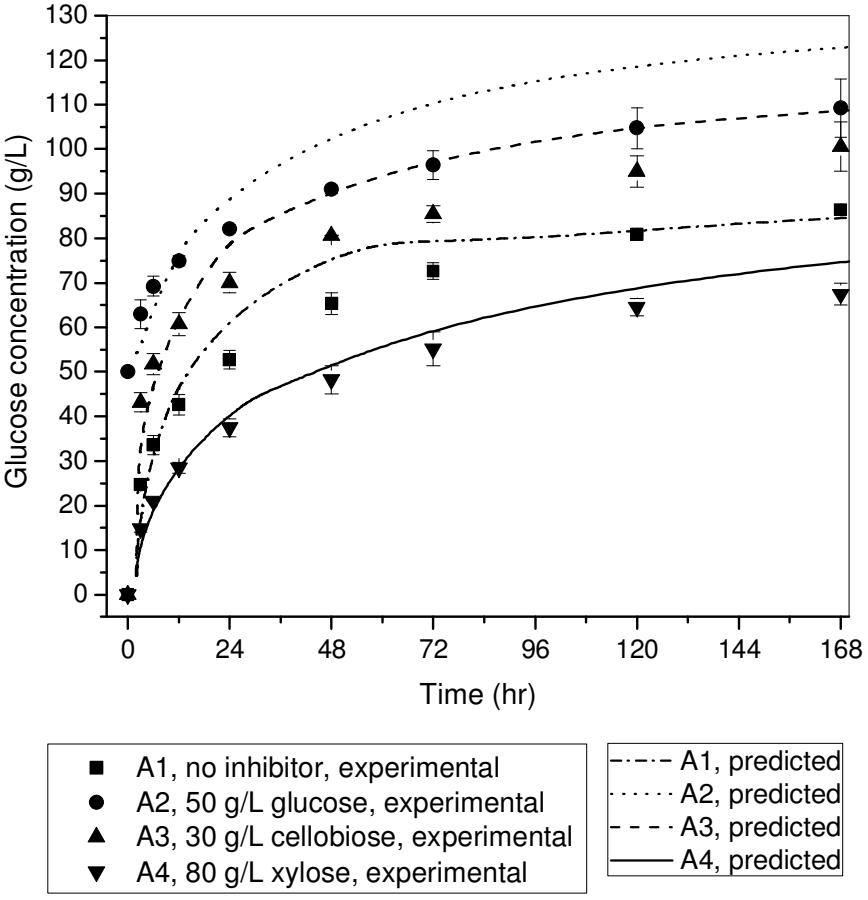

Fig. A15. Parameter estimation of Model 2 ($G_{cr,tetra}$ = 75 g/L). 100 g/L Avicel hydrolyzed by Celluclast (15.8 mg-protein/g-substrate) + N188 (5.9 mg-protein/g-substrate) with different initial inhibitor background.

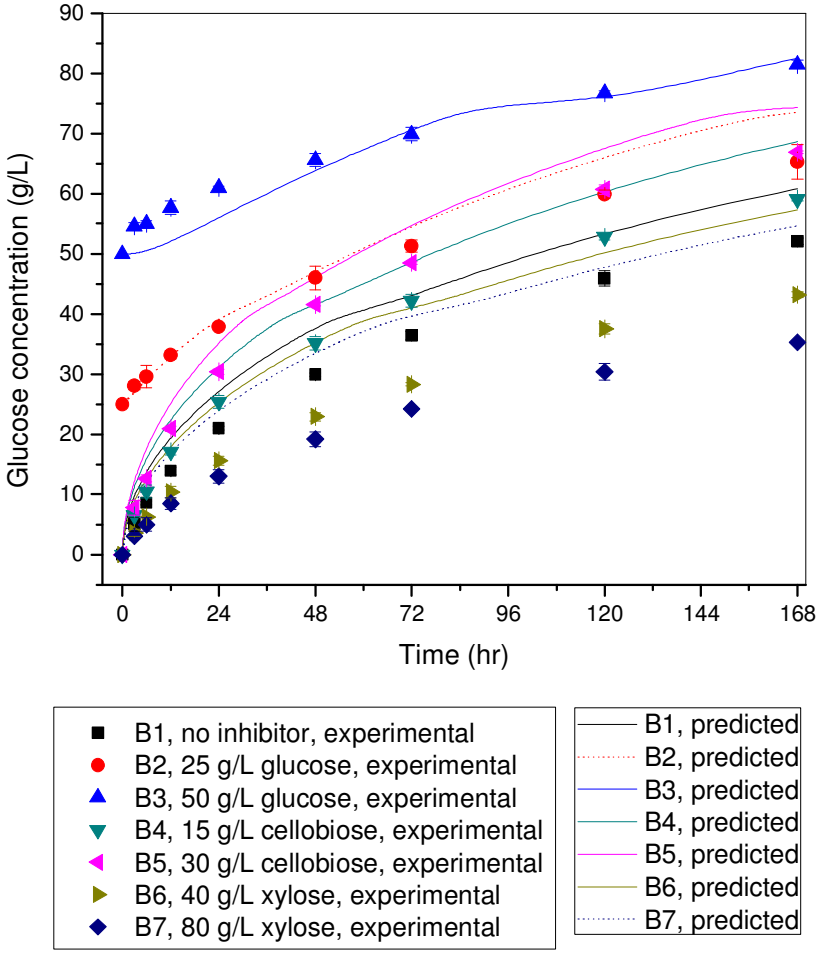

Fig. A16. Validation of Model 2 ($G_{cr,tetra}$ = 75 g/L). 100 g/L Avicel hydrolyzed by Celluclast (10.5 mg-protein/g-substrate) with different initial inhibitor background.

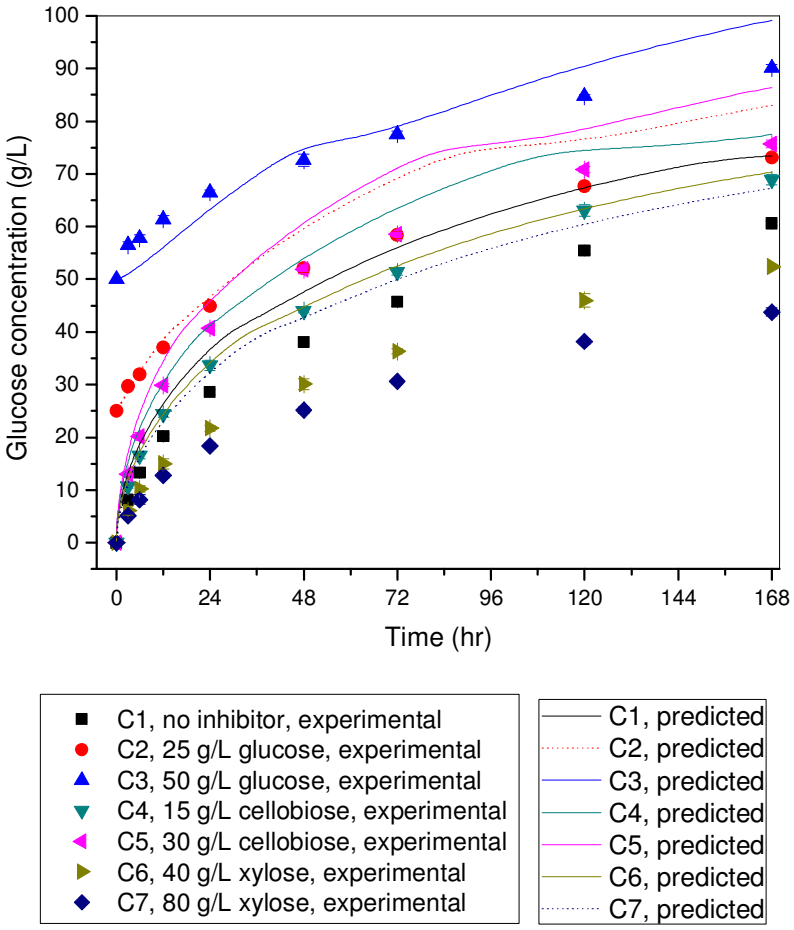

Fig. A17. Validation of Model 2 ($G_{cr,tetra}$ = 75 g/L). 100 g/L Avicel hydrolyzed by Celluclast (21.1 mg-protein/g-substrate) with different initial inhibitor background.

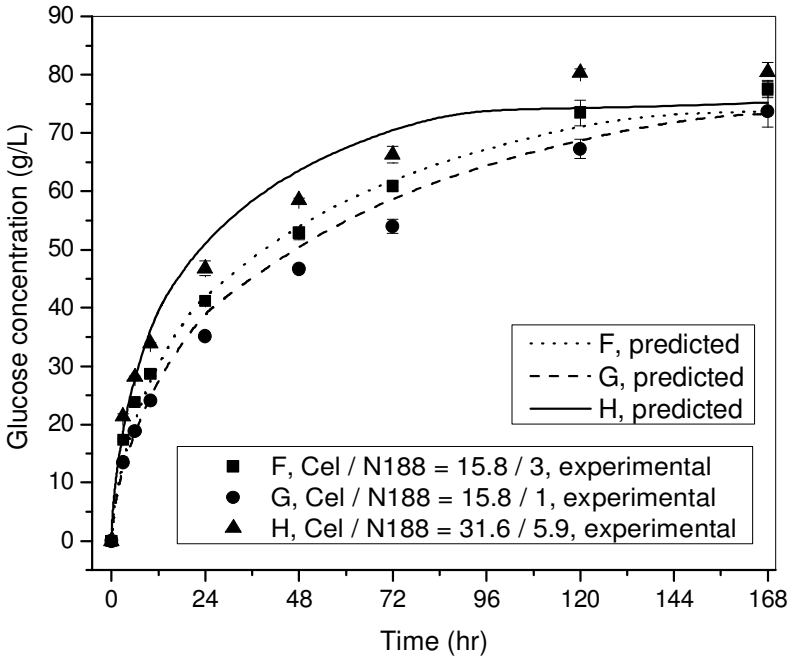

Fig. A18. Validation of Model 2 ($G_{cr,tetra}$ = 75 g/L). 100 g/L Avicel hydrolyzed by different ratio of Celluclast/N188 loading with initial 40 g/L xylose background.

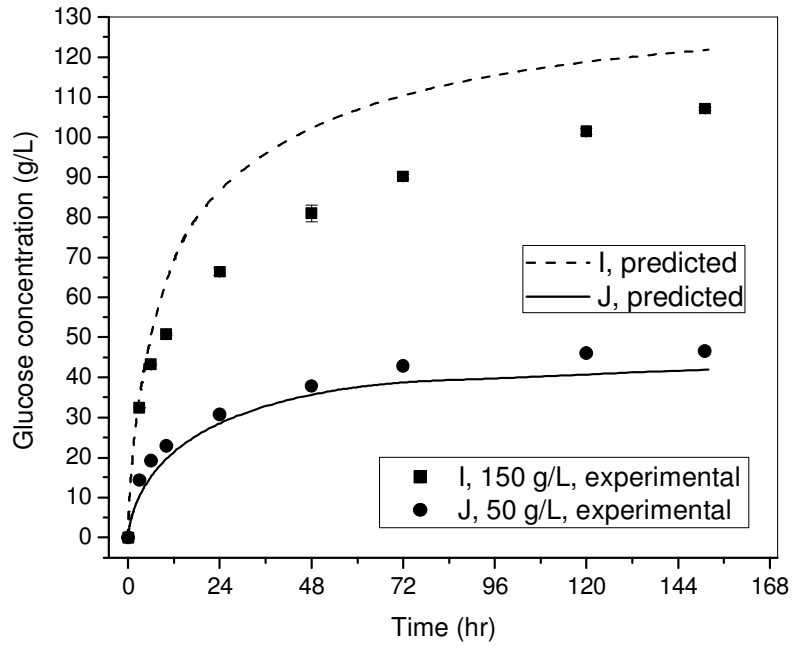

Fig. A19. Validation of Model 2 ($G_{cr,tetra}$ = 75 g/L). 50 and 150 g/L Avicel hydrolyzed by Celluclast (15.8 mg-protein/g-substrate) + N188 (5.9 mg-protein/g-substrate).

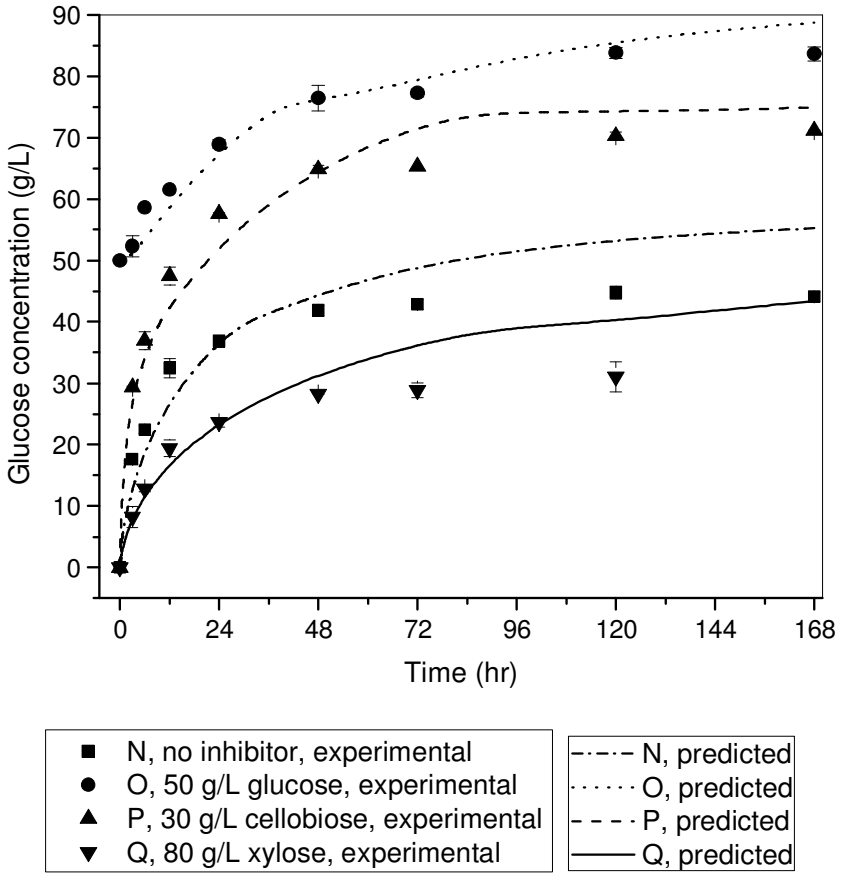

Fig. A20. Validation of Model 2 ($G_{cr,tetra}$ = 75 g/L). 90 g/L Barley straw hydrolyzed by Celluclast (15.8 mg-protein/g-substrate) + N188 (5.9 mg-protein/g-substrate) with different initial inhibitor background.

Appendix 5.5. Evaluation of Model 2 ($G_{cr,tetra}$ = 80 g/L)

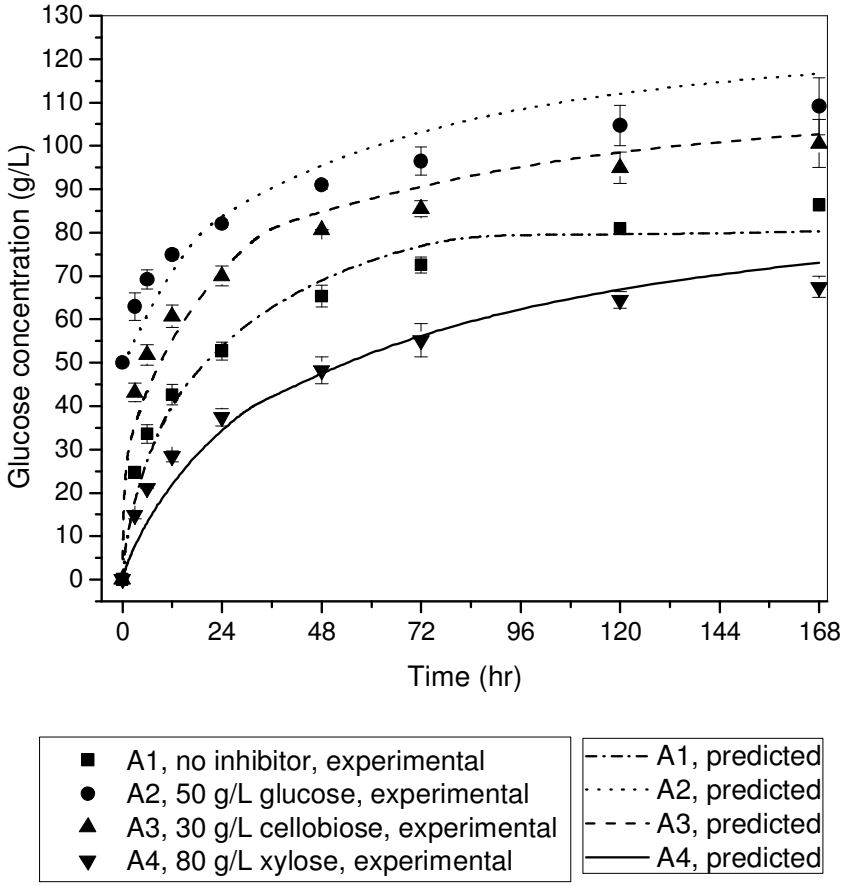

Fig. A21. Parameter estimation of Model 2 ($G_{cr,tetra}$ = 80 g/L). 100 g/L Avicel hydrolyzed by Celluclast (15.8 mg-protein/g-substrate) + N188 (5.9 mg-protein/g-substrate) with different initial inhibitor background.

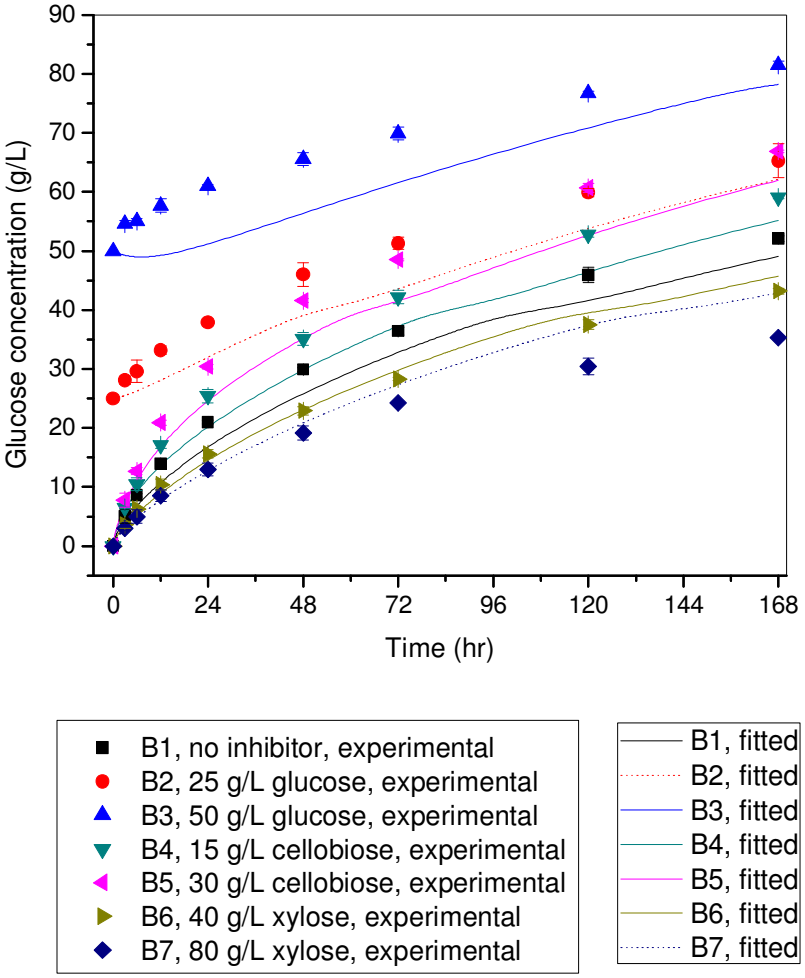

Fig. A22. Validation of Model 2 ($G_{cr,tetra}$ = 80 g/L). 100 g/L Avicel hydrolyzed by Celluclast (10.5 mg-protein/g-substrate) with different initial inhibitor background.

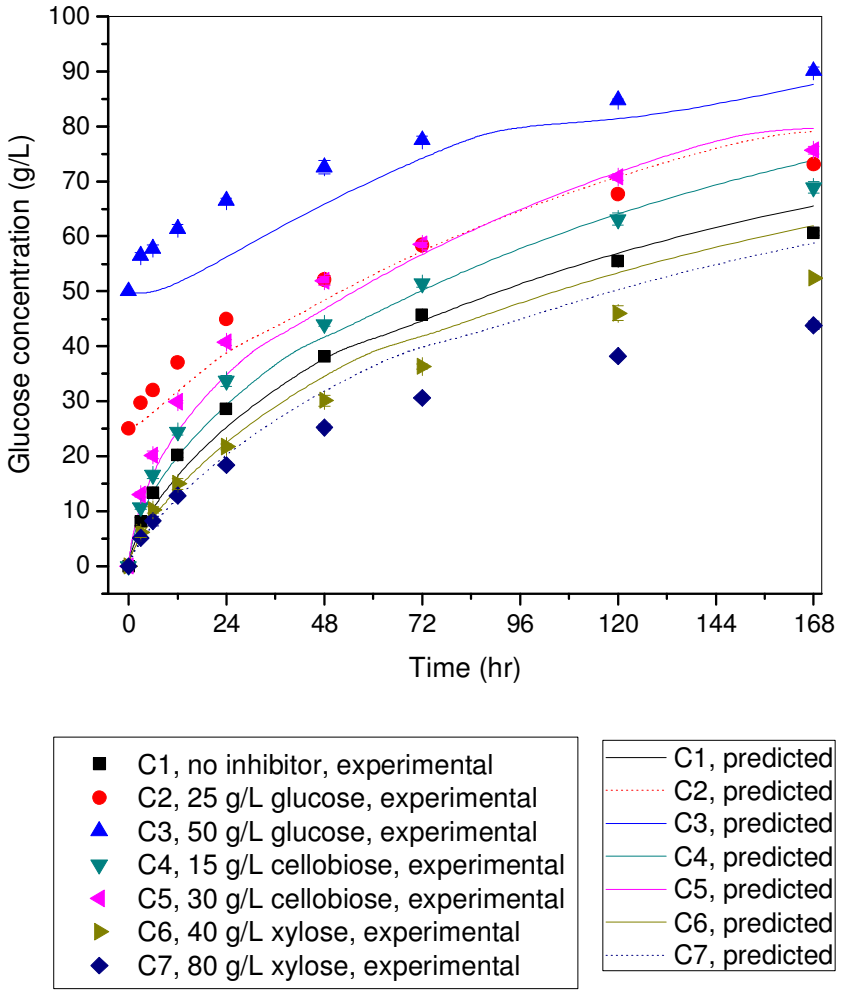

Fig. A23. Validation of Model 2 ($G_{cr,tetra}$ = 80 g/L). 100 g/L Avicel hydrolyzed by Celluclast (21.1 mg-protein/g-substrate) with different initial inhibitor background.

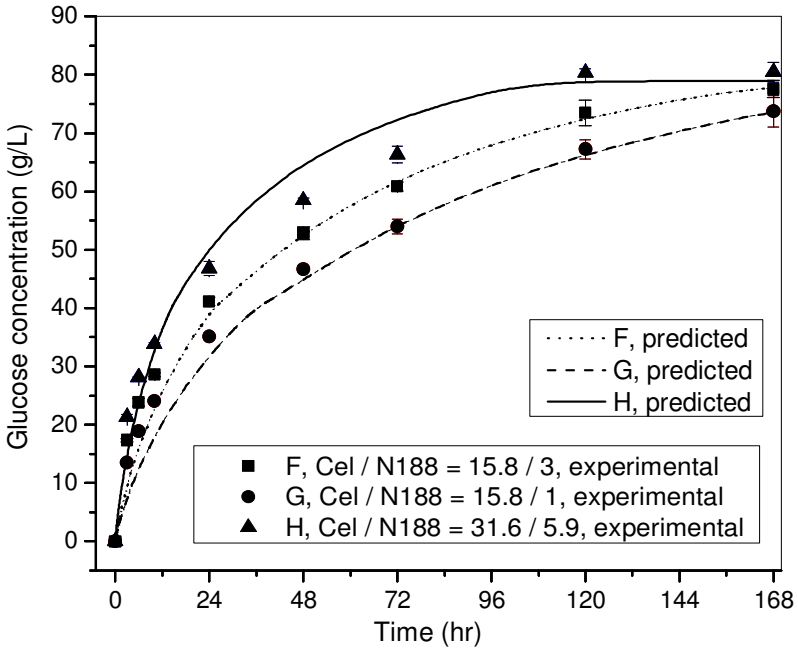

Fig. A24. Validation of Model 2 ($G_{cr,tetra}$ = 80 g/L). 100 g/L Avicel hydrolyzed by different ratio of Celluclast/N188 loading with initial 40 g/L xylose background.

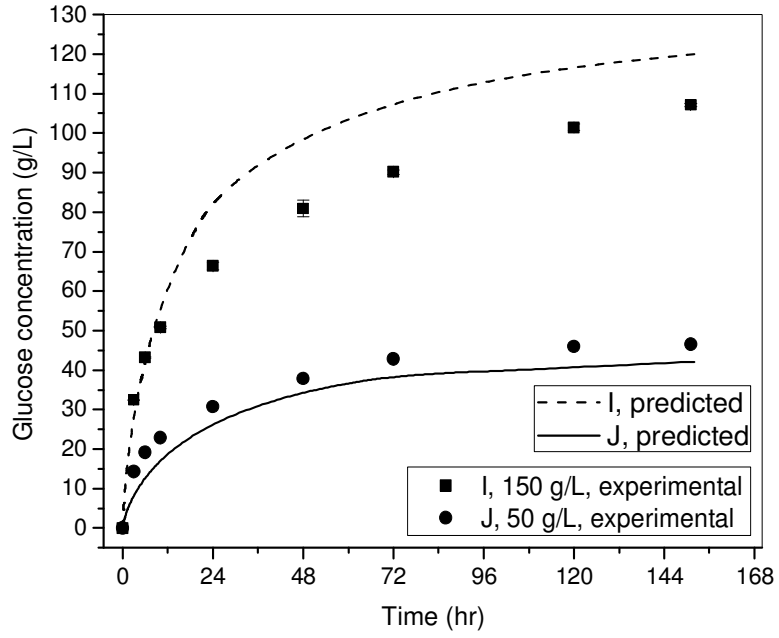

Fig. A25. Validation of Model 2 ($G_{cr,tetra}$ = 80 g/L). 50 and 150 g/L Avicel hydrolyzed by Celluclast (15.8 mg-protein/g-substrate) + N188 (5.9 mg-protein/g-substrate).

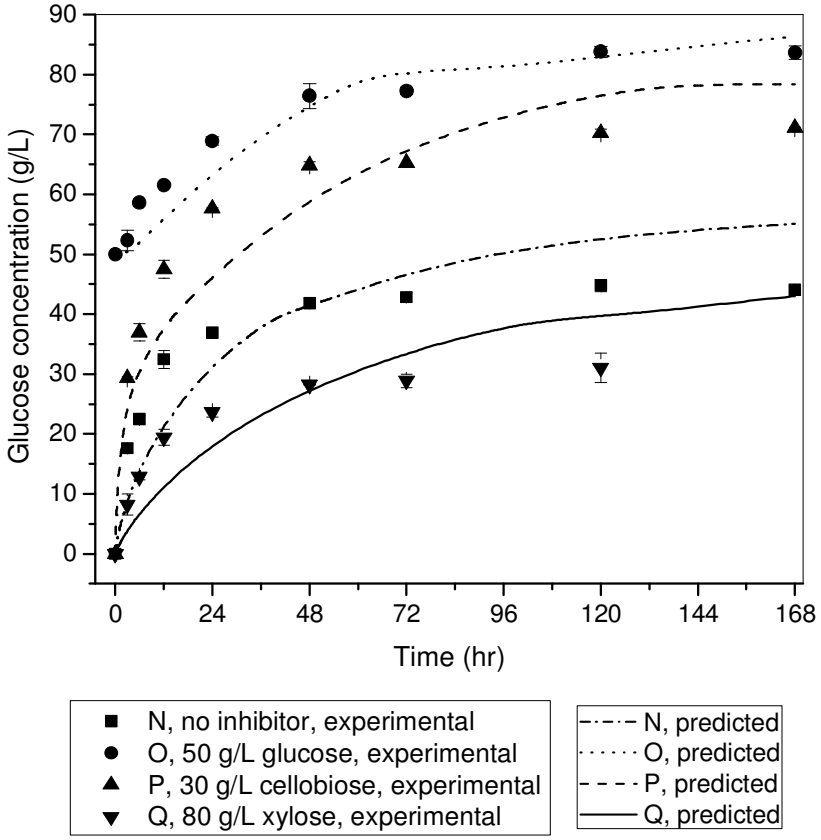

Fig. A26. Parameter estimation of Model 2 ($G_{cr,tetra}$ = 80 g/L). 100 g/L Avicel hydrolyzed by Celluclast (15.8 mg-protein/g-substrate) + N188 (5.9 mg-protein/g-substrate) with different initial inhibitor background.

Appendix 5.6. Evaluation of Model 3 ($G_{cr,tetra}$ = 75 g/L)

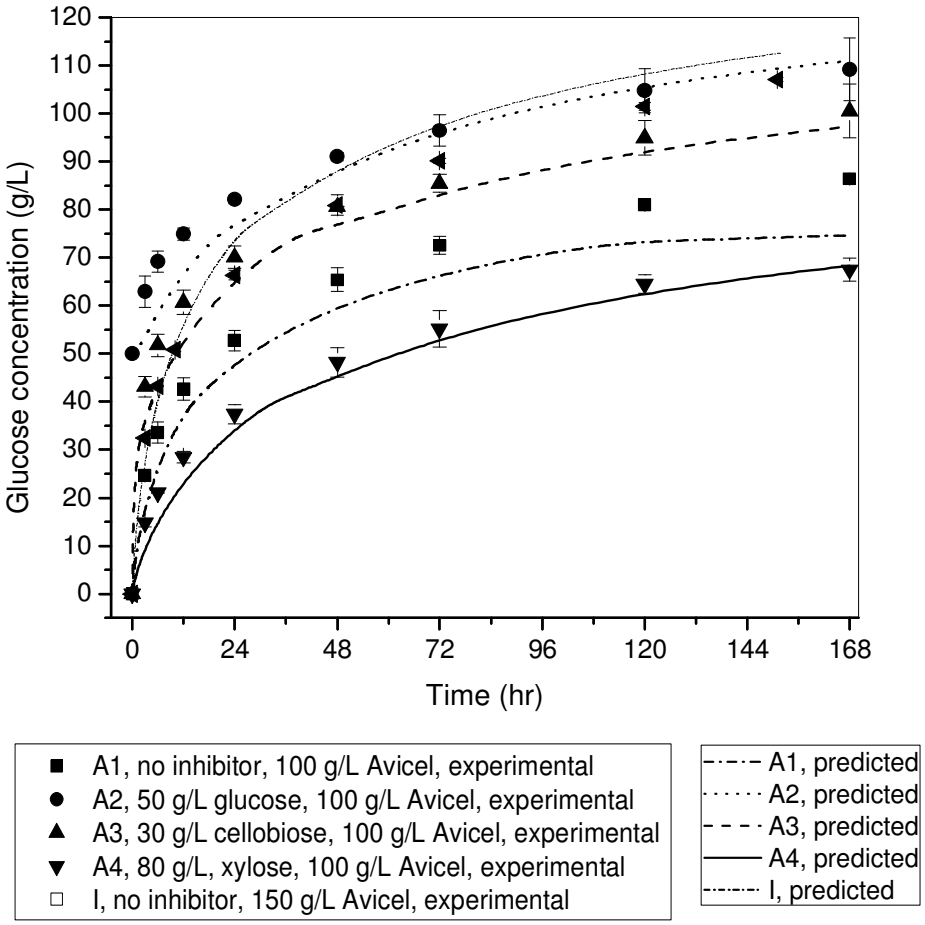

Fig. A27. Parameter estimation of Model 3 ($G_{cr,tetra}$ = 75 g/L). 100 and 150 g/L Avicel hydrolyzed by Celluclast (15.8 mg-protein/g-substrate) + N188 (5.9 mg-protein/g-substrate) with different initial inhibitor background.

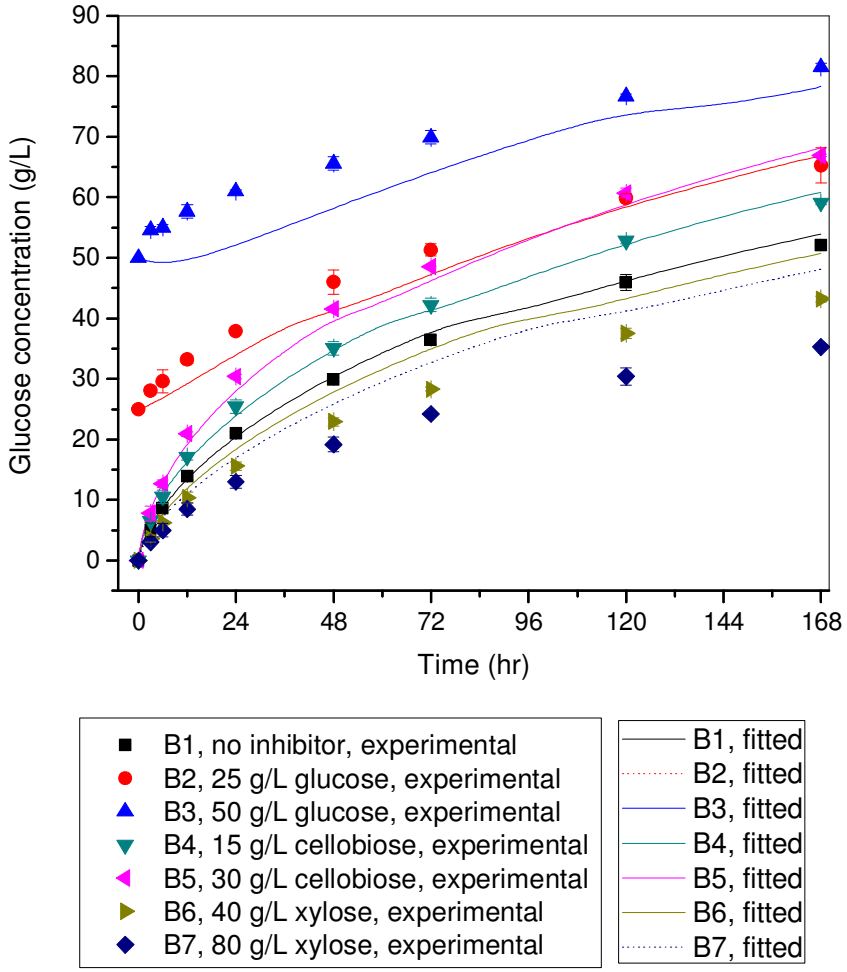

Fig. A28. Validation of Model 3 ($G_{cr,tetra}$ = 75 g/L). 100 g/L Avicel hydrolyzed by Celluclast (10.5 mg-protein/g-substrate) with different initial inhibitor background.

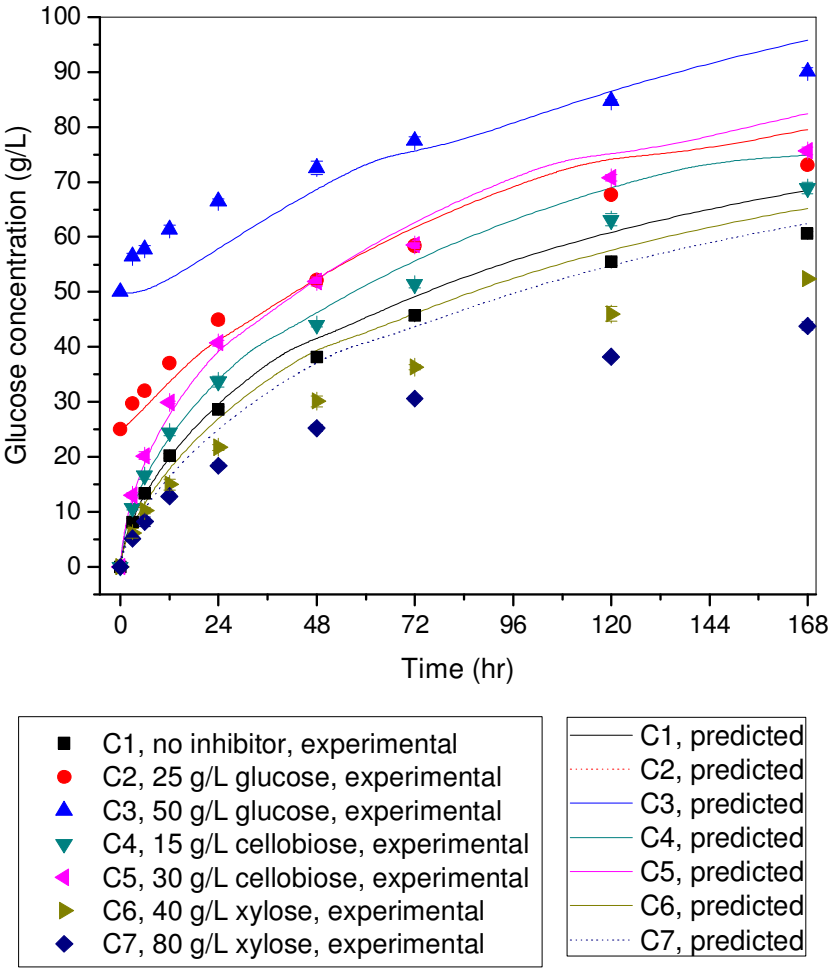

Fig. A29. Validation of Model 3 ($G_{cr,tetra}$ = 75 g/L). 100 g/L Avicel hydrolyzed by Celluclast (21.1 mg-protein/g-substrate) with different initial inhibitor background.

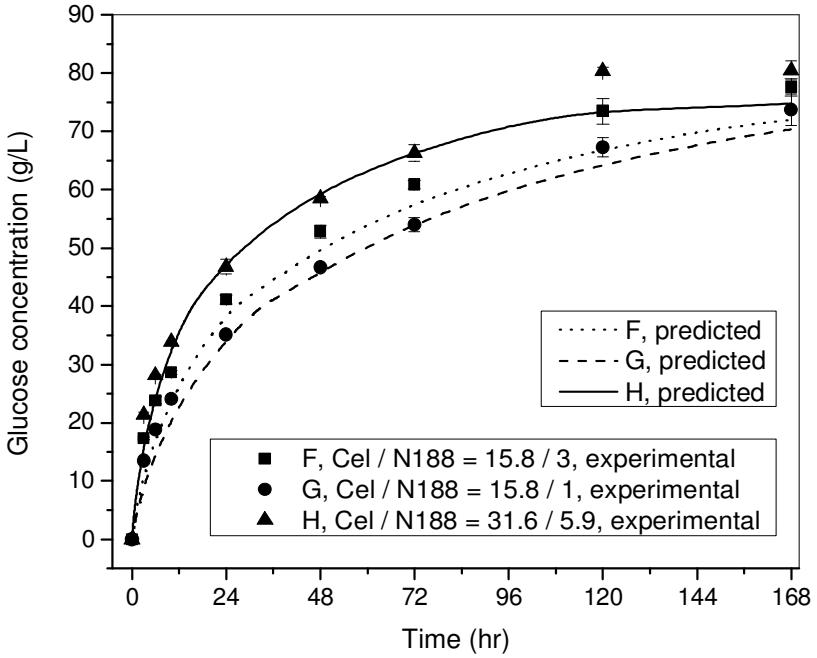

Fig. A30. Validation of Model 3 ($G_{cr,tetra}$ = 75 g/L). 100 g/L Avicel hydrolyzed by different ratio of Celluclast/N188 loading with initial 40 g/L xylose background.

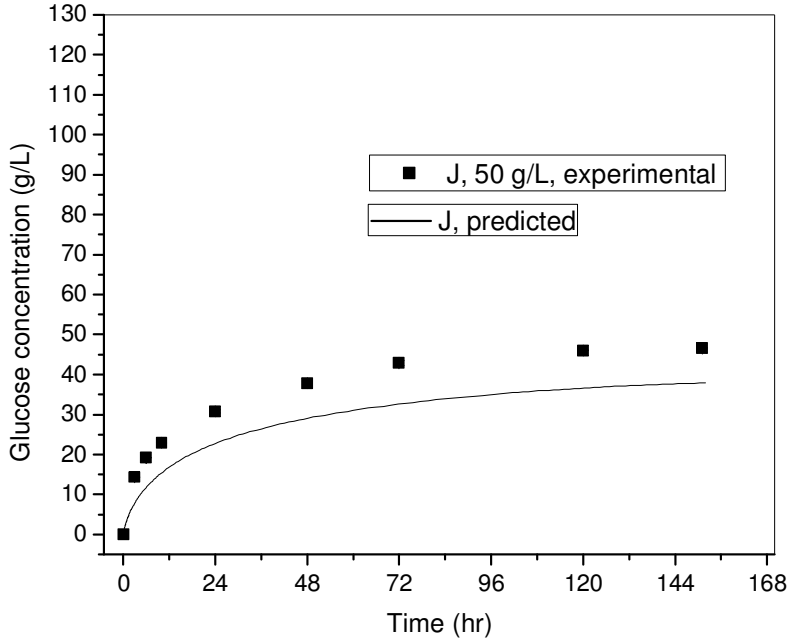

Fig. A31. Validation of Model 3 ($G_{cr,tetra}$ = 75 g/L). 50 g/L Avicel hydrolyzed by Celluclast (15.8 mg-protein/g-substrate) + N188 (5.9 mg-protein/g-substrate).

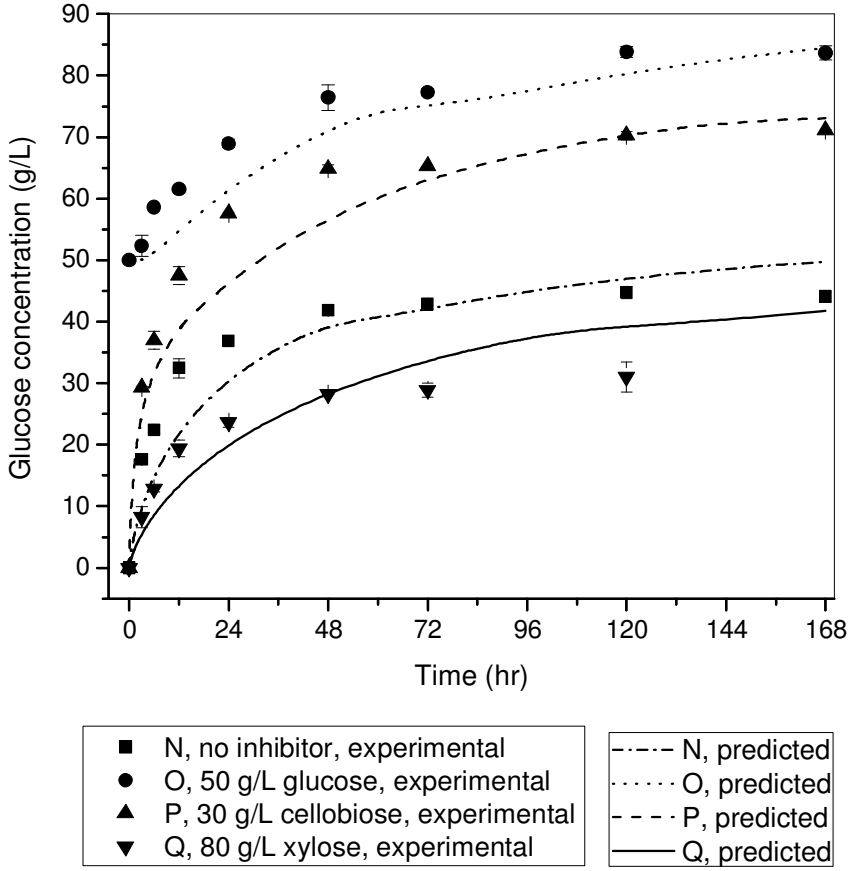

Fig. A32. Parameter estimation of Model 3 ($G_{cr,tetra}$ = 75 g/L). 100 g/L Avicel hydrolyzed by Celluclast (15.8 mg-protein/g-substrate) + N188 (5.9 mg-protein/g-substrate) with different initial inhibitor background.

Appendix 5.7. Evaluation of Model 3 ($G_{cr,tetra}$ = 80 g/L)

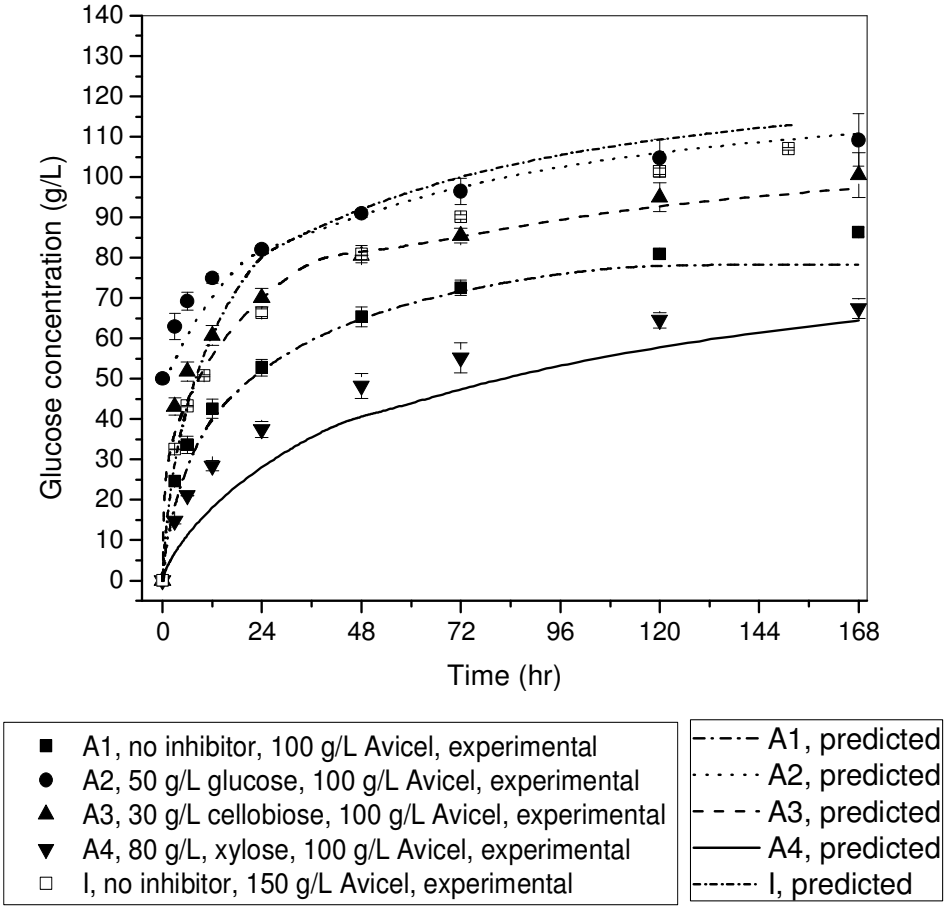

Fig. A33. Parameter estimation of Model 3 ($G_{cr,tetra}$ = 80 g/L). 100 and 150 g/L Avicel hydrolyzed by Celluclast (15.8 mg-protein/g-substrate) + N188 (5.9 mg-protein/g-substrate) with different initial inhibitor background.

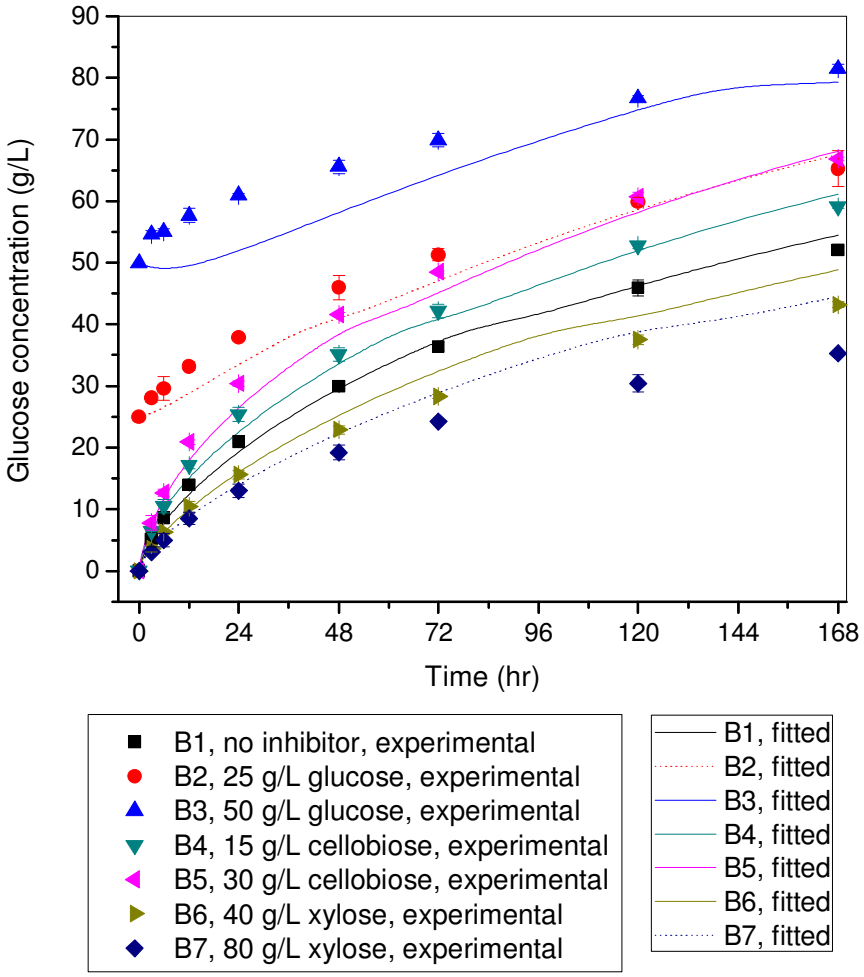

Fig. A34. Validation of Model 3 ($G_{cr,tetra}$ = 80 g/L). 100 g/L Avicel hydrolyzed by Celluclast (10.5 mg-protein/g-substrate) with different initial inhibitor background.

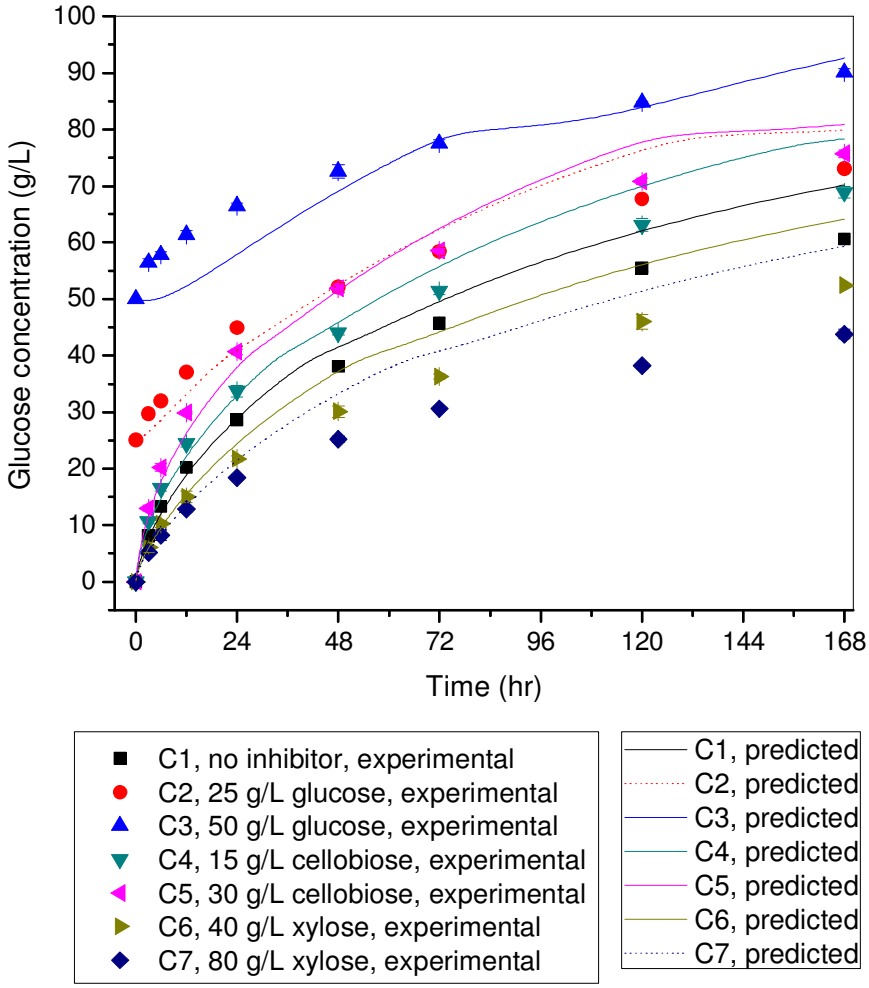

Fig. A35. Validation of Model 3 ($G_{cr,tetra}$ = 80 g/L). 100 g/L Avicel hydrolyzed by Celluclast (21.1 mg-protein/g-substrate) with different initial inhibitor background.

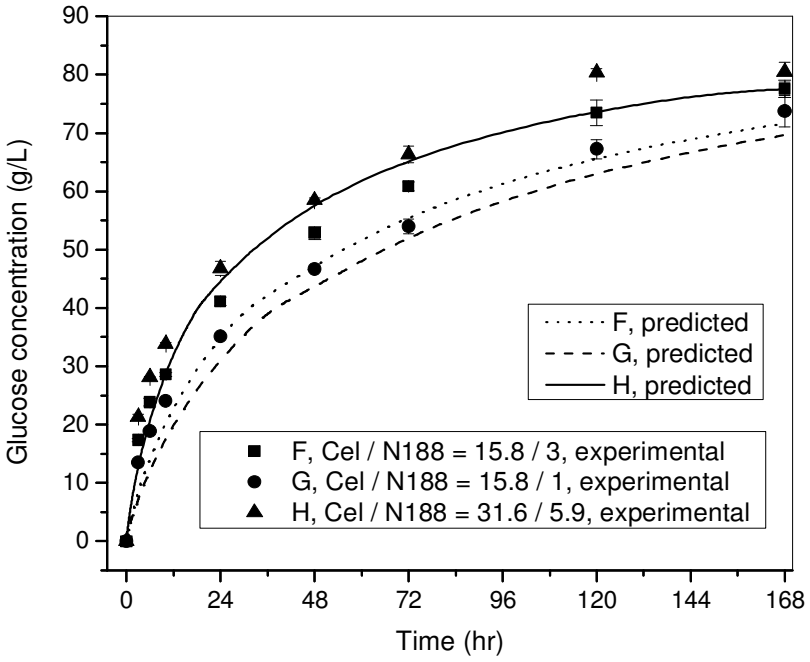

Fig. A36. Validation of Model 3 ($G_{cr,tetra}$ = 80 g/L). 100 g/L Avicel hydrolyzed by different ratio of Celluclast/N188 loading with initial 40 g/L xylose background.

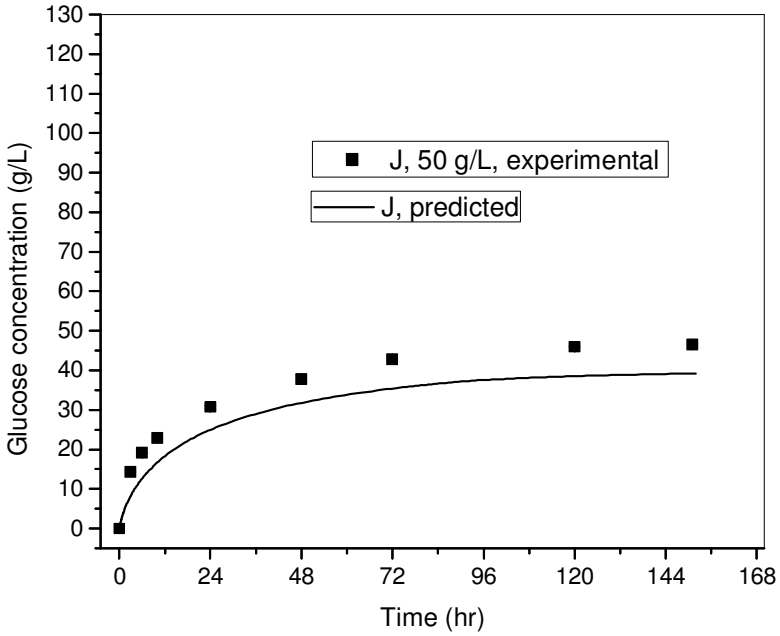

Fig. A37. Validation of Model 3 ($G_{cr,tetra}$ = 80 g/L). 50 g/L Avicel hydrolyzed by Celluclast (15.8 mg-protein/g-substrate) + N188 (5.9 mg-protein/g-substrate).

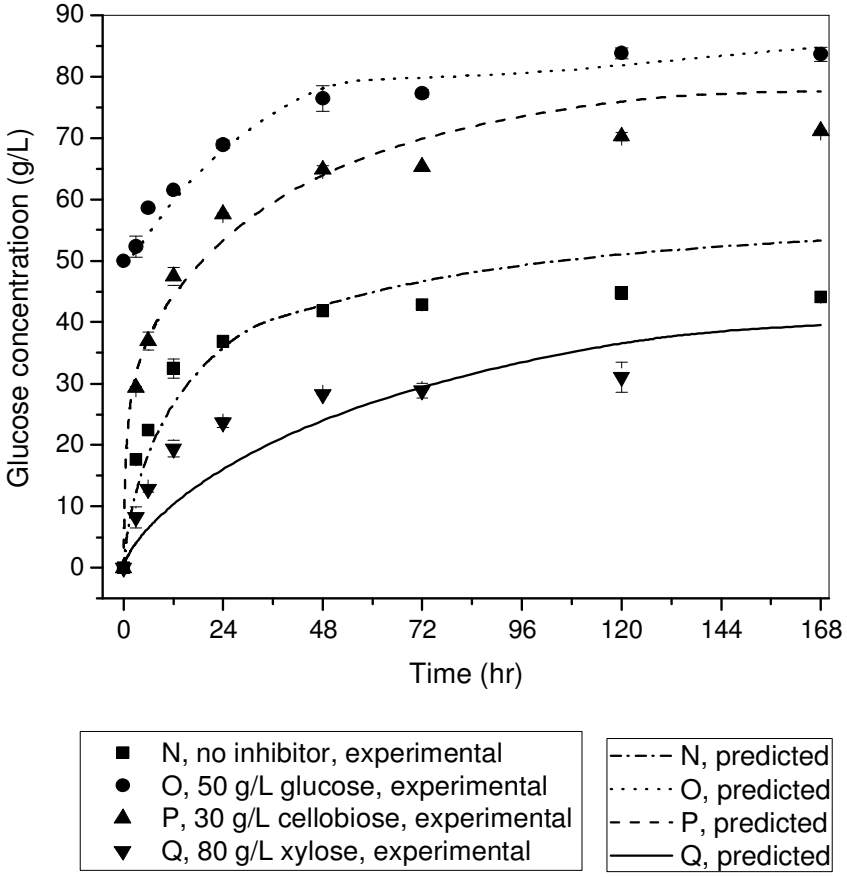

Fig. A38. Parameter estimation of Model 3 ($G_{cr,tetra}$ = 80 g/L). 100 g/L Avicel hydrolyzed by Celluclast (15.8 mg-protein/g-substrate) + N188 (5.9 mg-protein/g-substrate) with different initial inhibitor background.

Appendix 5.8. Comparison of hydrolysis kinetics of Avicel by N188 and Xbg

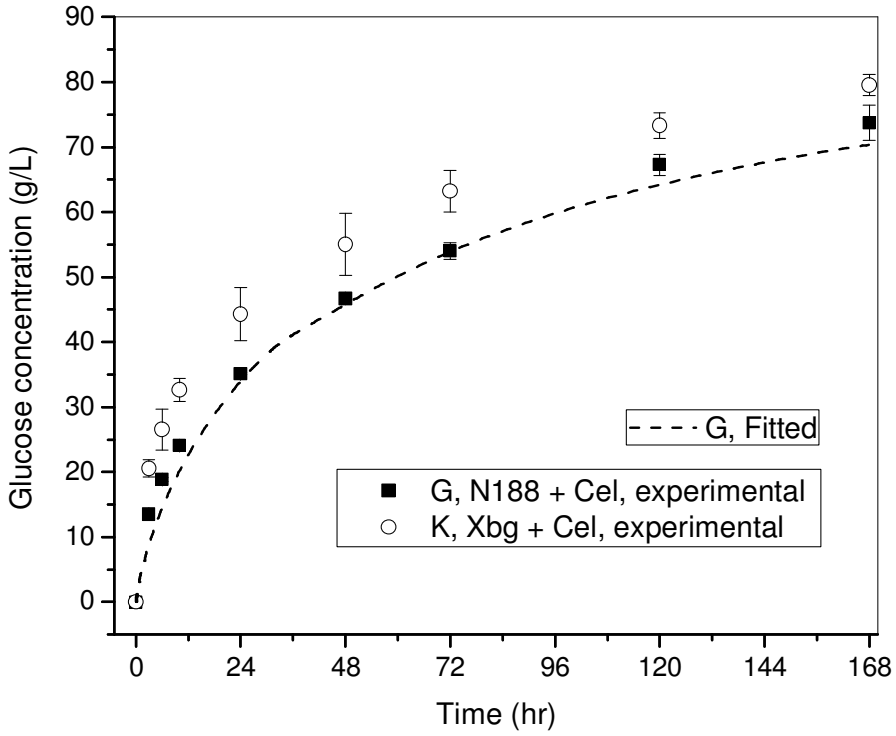

Fig. A39. 100 g/L Avicel hydrolyzed by Celluclast (15.8 mg-protein/g-substrate) + BG (N188 or Xbg, 1 mg-protein/g-substrate) with initial 40 g/L xylose background. The dashed line is prediction of data set G by Model 2 ($G_{cr,tetra}$ = 75 g/L).

Appendix 5.9.Transglycosylation reaction induced by Celluclast, N188 and Xbg

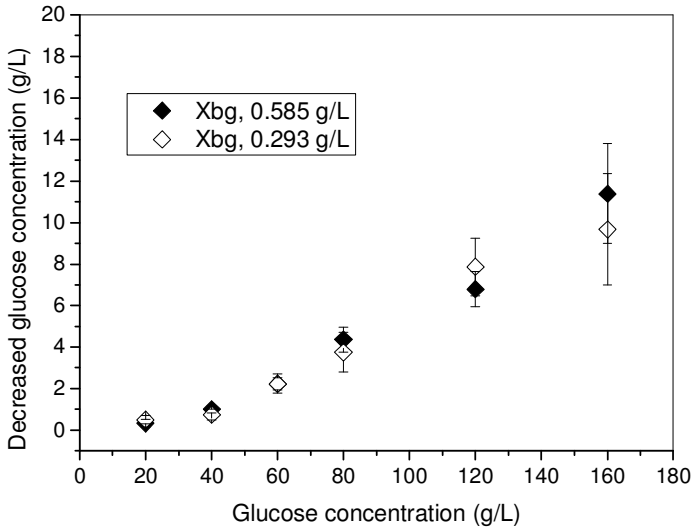

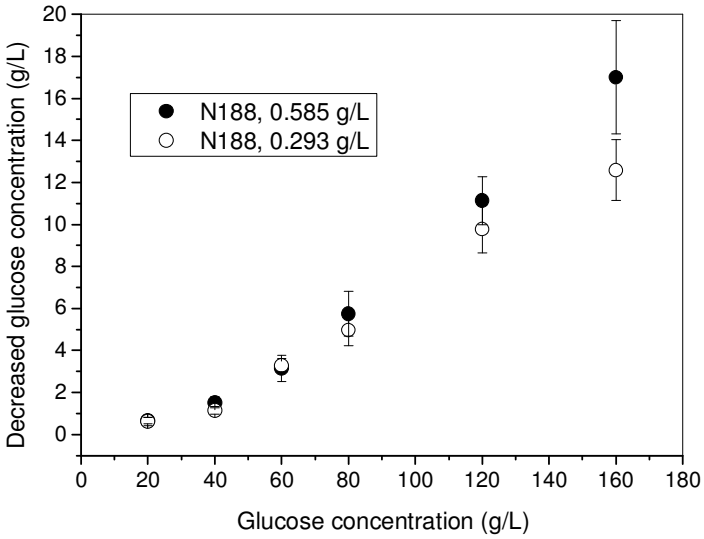

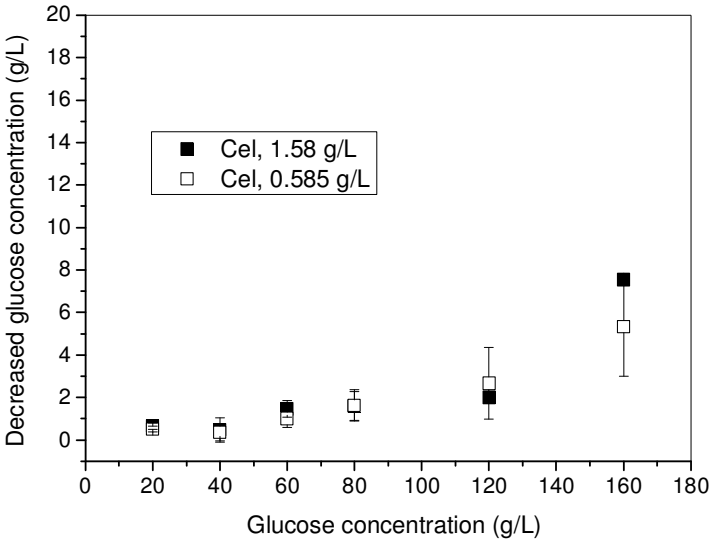

Chapter 6
Conclusions and Future Works

In the first part, ionic liquid pretreatment, the parameters investigated here were substrate concentration, temperature and time. The optimized condition is 150°C around 55-60 minutes and barley straw concentration is 8-10%. However, considered the amount of consumed ionic liquid, barley straw concentration can be upto 20%. It was also proved that at 150°C, [EMIM]Ac causes degradation of cellulose, release some oligosaccharide or glucose. These soluble small molecules can not be precipitated and recovered by regeneration. Their chemical structures were also changed by [EMIM]Ac.

It should be noticed that as far as we know, all previous researches including this study, the biomass were pretreated by ILs without mechanical agitation. This means the dissolution process only depends on diffusion. First, ILs dissolute outer part of the biomass particle, form a "jelly-like" layer. Then the other IL molecules penetrate through the jelly-like layer into the inner part of the particle (Figure 6.1). Due to the viscose layer, the penetration/diffusion process is very slow. Therefore, higher temperature and longer time is needed for elevating the energy of the molecules. With mild mechanical shear force, most jelly-like layers can be scraped from the particle, expose the inner part of raw biomass to free ILs molecules (Figure 6.2). Thus, the pretreatment time can be reduced.

The biomass-IL mixture is difficult to be mixed efficiently by typical impeller, owning to it extremely high viscosity. In order to expose raw biomass to IL molecules, device such as extruder in plastic process can be utilized (Fig 6.3). With this continuous process, temperature or period of pretreatment can be reduced by proper mixing. Energy and degradation reaction can be reduced. The influence of device design and its operation conditions on the ionic liquid pretreatment need further investigation.

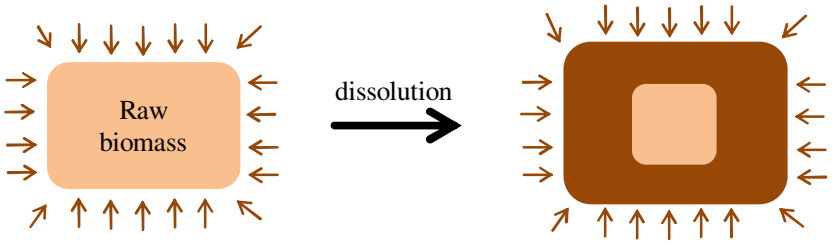

Figure 6.1 Process of dissolution of biomass by ILs without any mechanical force. Light brown: raw biomass; dark brown: dissolved biomass; dark brown arrow: diffusion direction s of free ILs molecules.

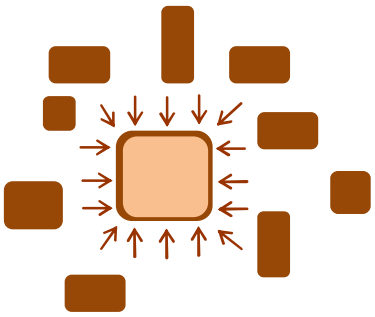

Figure 6.2 Process of dissolution of biomass by ILs with mechanical shear force. Light brown: raw biomass; dark brown: dissolved biomass; dark brown arrow: diffusion direction s of free ILs molecules.

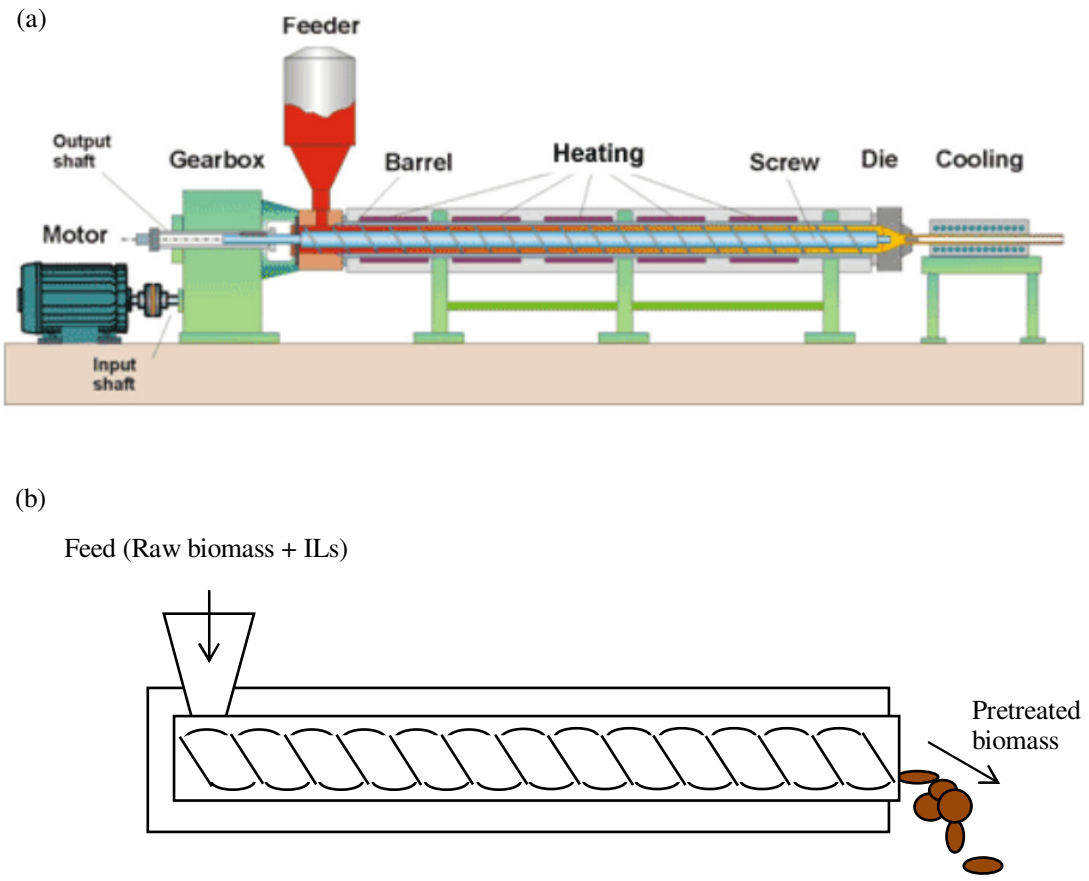

Figure 6.3 Extruder. (a) A typical extrusion equipment and process in plastic industry. (b) The application of extruder in ionic liquid pretreatment. From http://www.theadvancedteam.com/laser_extruder.php)

In the second part, immobilization of β-glucosidase, enzymes can be reused for up to 20 th times without significant loss of activity. Enzyme aggregates in a calcium alginate were visualized by confocal laser scanning microscope (CLSM). From activity analysis and CLAM images, it is revealed that more BG can be keeped in the matrix when the enzyme was cross-linked by higher glutaraldehyde/enzyme ratio. This is a promising system to recycle the enzyme for reducing the cost. However in indusry, several technical problems still need to be solved. The first is the difussion of cellobiose into the inner part of calcium aginate bead is slow. The diameters of the beads in this research are around 3~5 mm, which is large. Therefore the diffusion rate can be increased by reducing the size of the beads. The concnetration of

sodium alginate for preparing the beads is 3.75%. The high viscosity lead to difficulties and time consuming for preparing smaller beads by dropping the gel into calcium chloride. According to the author's experience, it is too slow to prepare the beads. Extruding the gel in the form of fiber provide a faster way (Figure 6.4). Large amounts of immobilized enzyme can be prepared within shorter time.

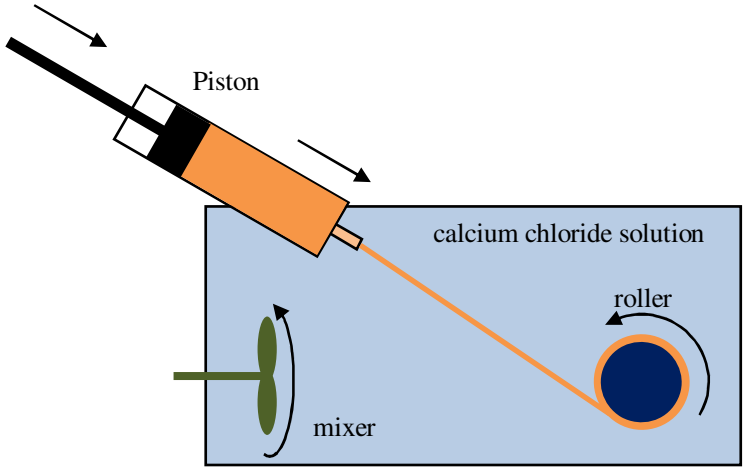

Figure 6.4 Illustration of producing fiber-shaped immobilized enzyme. Sodium alginate-enzyme mixture gel is extruded from the piston to calcium chloride solution. The fiber is collected by a roller. The diameter of the fiber can be controlled by the size of the aperture and extrusion speed.

Another practical problem is to get higher glucose concentration higher lignocellulose dry matter in the hydrolysis reaction is preferred. However pretreated lignocellulose tends to absorb large amount of water, so the mixture containing DM 10% of lignocellulose is almost like solid state. This is unfavorable for immobilized enzyme. Immobilized BG is not able to work until the substrate is liquefied, since water is the medium for diffusion. In addition, calcium alginate beads need water to keep their shape. The volume of immobilized enzyme should not be too large so the enzyme can be immersed in liquid as early as possible. That means the activity per unit of volume should be high enough. The enzyme density in calcium alginate bead of "experiment A" shown in Figure 4.3 is 0.88 mg/mL. This is very dilute and means collision probability between cellobiose and BG is low (Figure 6.5).

According to above discussion, we can say in order to increase the efficiency of immobilized BG for industry, the specific area of the immobilized enzyme should be large enough, and enzyme density in

calcium alginate should be high. The optimized combination of these two factors and their effects on reaction with high lignocellulose loading should be further investigated. Another topic to be investigated is how to apply the immobilized enzyme in the reactor system. Andric (2010) made an intensive review of researches for decreasing product inhibition. Applications of immobilized BG to reduce product inhibition were also included, which are shown in Figure 6.6. In this PhD study we intended to apply immobilized BG to packed bed and membrane system, however due to the limitation of the instruments, the circulation of substrate slurry in the system did not go well; clogging in the system is serious. Suitable instrument is needed for further investigation.

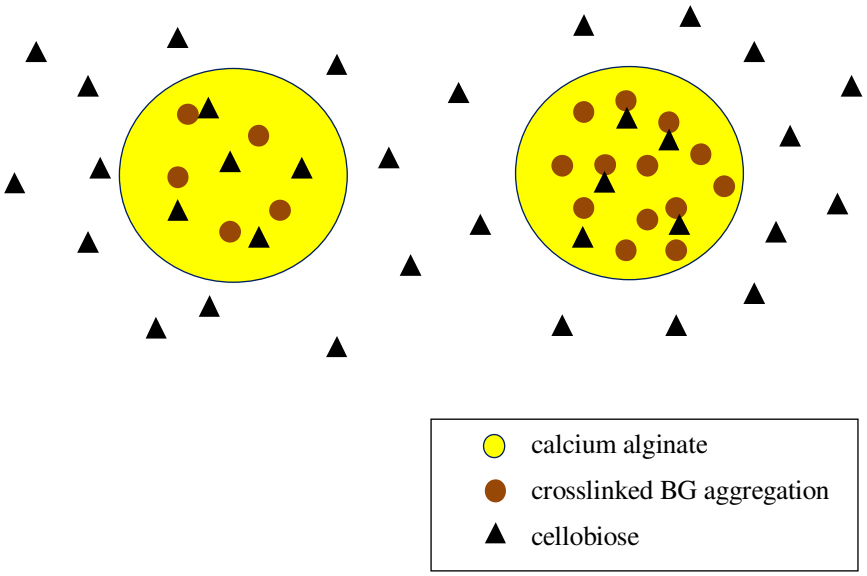

Figure 6.5 Collision probabilities between cellobiose and immobilized BG in calcium alginate with low or high BG densities. Left: low BG density; Right: high BG density.

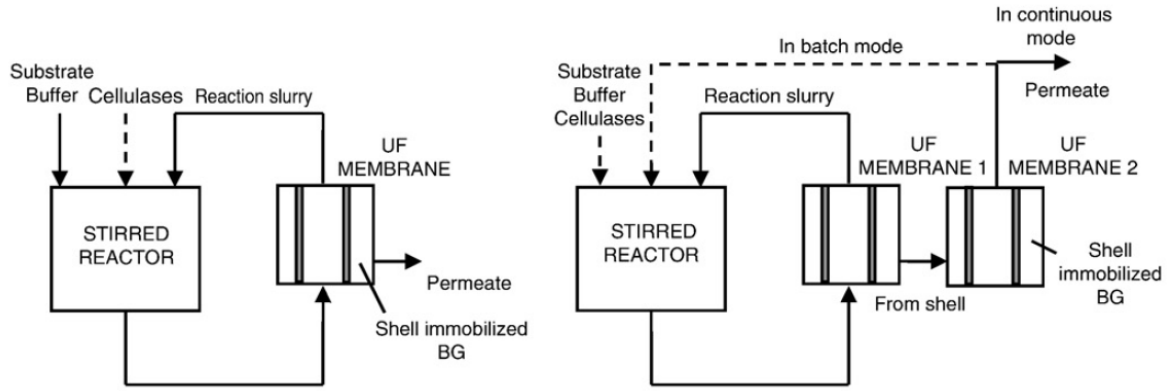

Figure 6.6 Application of immobilized BG in the reactors. (From Andric 2010)

In the last part, hydrolysis kinetic models, a model proposed by Kadam was systematically validated and modified by a step by step analysis. Transglycosylation was investigated and incorporated into the model to calibrate the deviation of predictioin under high glucose level. The parameters were shown not universal, depend on estimation strategy and substrate but the model still can be used over a broad range of substrate and enzyme loading. Therefore, we can see the model not only based on enzyme kinetics theory, but also rely on mathametical fitting. The parameters were estimated from the hydrolysis of 100 g/L Avicel. Although the model can predict hydrolysis of 50 g/L Avicel well, it failed to predict the kinetics when substrate is up to 150 g/L. This may be attributed to that the level of transglycosylation is also depends on enzyme concentration, which was not included in the mathematical equations. The relation between enzyme concentration and transglycosylation needs further investigation.

In industrial process, more than 15% DM of lignocellulose is prefered to get higher glucose concentration. However, due to the water adsorbing capability of lignocellulose, extremely high viscosity make the experiment difficult to be conducted. Although most properties of this model is clarified in this research, as the structure and composition of Avicel is still different from lignocellulose, the model should

be evaluated intensively under the hydrolysis of lignocellulose; especially to understand the influence of lignin on this model. Further investigation should be done in the future.

Production of lignocellulosic bioethanol involves several steps. Each step is not independent but highly connected. Pretreatment and the type/style of enzyme can change the hydrolysis kinetics. This PhD study includes pretreatment, enzyme immobilization and kinetic modeling. We can see the hydrolysis kinetic of barley straw pretreated by [EMIM]Ac and hot water extraction are very different. The reaction rates of free enzyme and immobilized enzyme are also different. Therefore these observations can help us set up a suitable model for reactor and process design without misusing the model.